

# Lawrence Berkeley National Laboratory

## Recent Work

### Title

ROTATIONAL PERTURBATIONS AND LOW-LYING ELECTRONIC STATES OF CaO.

### Permalink

<https://escholarship.org/uc/item/5pd432p6>

### Author

Johansen, Helen.

### Publication Date

1970-08-01

ROTATIONAL PERTURBATIONS AND LOW-LYING  
ELECTRONIC STATES OF CaO

Helen Johansen  
(Ph. D. Thesis)

August 1970

AEC Contract No. W-7405-eng-48

RECEIVED  
LAWRENCE  
RADIATION LABORATORY

001 - 7 1970

LIBRARY AND  
DOCUMENTS SECTION

TWO-WEEK LOAN COPY

*This is a Library Circulating Copy  
which may be borrowed for two weeks.  
For a personal retention copy, call  
Tech. Info. Division, Ext. 5545*

LAWRENCE RADIATION LABORATORY  
UNIVERSITY of CALIFORNIA BERKELEY

34

## **DISCLAIMER**

This document was prepared as an account of work sponsored by the United States Government. While this document is believed to contain correct information, neither the United States Government nor any agency thereof, nor the Regents of the University of California, nor any of their employees, makes any warranty, express or implied, or assumes any legal responsibility for the accuracy, completeness, or usefulness of any information, apparatus, product, or process disclosed, or represents that its use would not infringe privately owned rights. Reference herein to any specific commercial product, process, or service by its trade name, trademark, manufacturer, or otherwise, does not necessarily constitute or imply its endorsement, recommendation, or favoring by the United States Government or any agency thereof, or the Regents of the University of California. The views and opinions of authors expressed herein do not necessarily state or reflect those of the United States Government or any agency thereof or the Regents of the University of California.

Contents

Abstract	
I Introduction	1
II Experimental	5
III Results: CaO <sup>18</sup>	8
A. Analysis	
B. Rotational Constants	
C. Vibrational Constants	
D. Perturbations	
IV Comparison of CaO <sup>16</sup> and CaO <sup>18</sup>	46
V Conclusion	61
Appendix A Comparison of CaO <sup>16</sup> and CaO <sup>18</sup>	63
Appendix B Computer Programs	66
Acknowledgments	107
References	108

ROTATIONAL PERTURBATIONS AND LOW-LYING ELECTRONIC STATES OF CaO

Helen Johansen

Department of Chemistry, University of California,  
and  
Inorganic Materials Research Division,  
Lawrence Radiation Laboratory,  
Berkeley, California 94720

ABSTRACT

Sixteen bands of the  $A^1\Sigma - X^1\Sigma$  transition of  $\text{CaO}^{18}$  were analyzed. They are the (6,3), (5,2), (5,3), (4,1), (4,2), (3,0), (3,1), (3,2), (2,0), (2,1), (2,3), (1,0), (1,1), (1,2), (0,0), and (0,1) bands. The spectroscopic constants found are:

$X^1\Sigma$	$A^1\Sigma$
$\omega_e = 702.18$	$\omega_e = \sim 686.5$
$\omega_e x_e = 4.29$	$\omega_e x_e = \sim 1.5$
$B_e = .4093$	$B_e = .3733$
$\alpha_e = .003$	$\alpha_e = .0009$
$D_e = \sim 5.24 \times 10^{-7}$	$D_e \cong 4.58 \times 10^{-7}$
$\beta_e = \sim 5.9 \times 10^{-8}$	

$$V_{0,0} = 11548.6$$

Thirty-seven perturbations were found in the upper state. They are due to six electronic states or substates. A comparison of these perturbations with those found in  $\text{CaO}^{16}$  (Hultin and Lagerqvist, 1950) indicates that four of these perturbing states lie below the  $X^1\Sigma$ , one is at  $\sim 8080 \text{ cm}^{-1}$  and one is the  $X^1\Sigma$  state.

## I. INTRODUCTION

Previously analyzed spectra have shown four electronic states of CaO:  $X^1\Sigma(0.0)$ ,  $A^1\Sigma(\sim 11500 \text{ cm}^{-1})$ ,  $B^1\Pi(\sim 25900 \text{ cm}^{-1})$  and  $C^1\Sigma(\sim 28800 \text{ cm}^{-1})$ . (Lagerqvist, 1954; Hultin and Lagerqvist, 1950) However, a comparison of the electronic states of the eight-electron isoelectronic molecules and their trends in energy (Brewer, 1962), indicates low-lying  $^3\Pi$ ,  $^3\Sigma$ ,  $^1\Pi$  and  $^1\Delta$  states. There are also experimental indications that unanalyzed low-lying electronic states exist. First, the spectra of CaO contains several regions (5555 Å, 6100 Å) of very dense, complex structure which have so far resisted a complete analysis. (Gaydon, 1955; Kobajiehk and Sokolow, 1968) It is possible that they are due to triplet states of CaO. Other possibilities include  $\text{Ca}_2\text{O}_2$ , CaOH and  $\text{Ca}_2$ . Second, the Birge-Sponer extrapolation of the  $X^1\Sigma$  state gives 37 kcal for the dissociation energy. This value is at least 45 kcal lower than those obtained by other methods (Gaydon, 1968) which suggests that either  $X^1\Sigma$  is not the ground state or that the extrapolation is anomalous. Third, some 30 rotational perturbations have been found in the  $A^1\Sigma$  state of CaO. (Hultin and Lagerqvist, 1950). They have been explained as interactions between  $A^1\Sigma$  and six other states or substates. The absolute vibrational numbering of these perturbing states, and hence their origins, were not obtained since the  $v' = 0$  level of  $A^1\Sigma$  was perturbed. All that can be deduced from the  $\text{CaO}^{16}$  data is that at least 6 electronic states or substates lie below  $11500 \text{ cm}^{-1}$ .

It would be helpful to know the relative energies of these perturbing states especially since some of them are predicted to be triplets.

No triplet state has been directly analyzed in CaO and there is some controversy on whether the ground state is a singlet or a triplet. The statistical weight of the ground and low-lying electronic states is important in thermochemical calculations. For example in calculating the dissociation energy by a third law method ( $T = 2000^\circ\text{K}$ ), a difference of 7 kcal/mole is obtained depending on whether the ground state of CaO is  $^1\Sigma$  or  $^3\Pi$  (Gaydon, 1968).

Before we consider a way of determining these relative energies, a word is in order concerning rotational perturbations. A rotational perturbation is an interaction between rotational energy levels. Theoretically, it is a mixing of wavefunctions, the Hamiltonian being cross-terms not considered in the Born-Oppenheimer approximation. Experimentally it is seen as a shift of rotational energy levels away from their otherwise regular spacing. The following selection rules should hold in order for a rotational perturbation to occur:

(1) Both states must have the same total angular momentum,  $J$ , at approximately the same energy;  $\Delta J=0$ ,  $\Delta E \sim 0$ .

(2) Both states must have the multiplicity;  $\Delta S=0$ .

This rule holds only approximately (Ballik and Ramsey, 1962)

(3)  $\Delta\Lambda = 0, \pm 1$  for Hund's coupling cases (a) and (b)

$\Delta\Omega = 0, \pm 1$  for Hund's case (c)

(4) Both states must be positive, or both must be negative; +  $\leftrightarrow$  -

(5) For identical nuclei, both states must have the same symmetry in the nuclei; s  $\leftrightarrow$  a

(6) There must be sufficient overlap of the vibrational eigenfunctions.

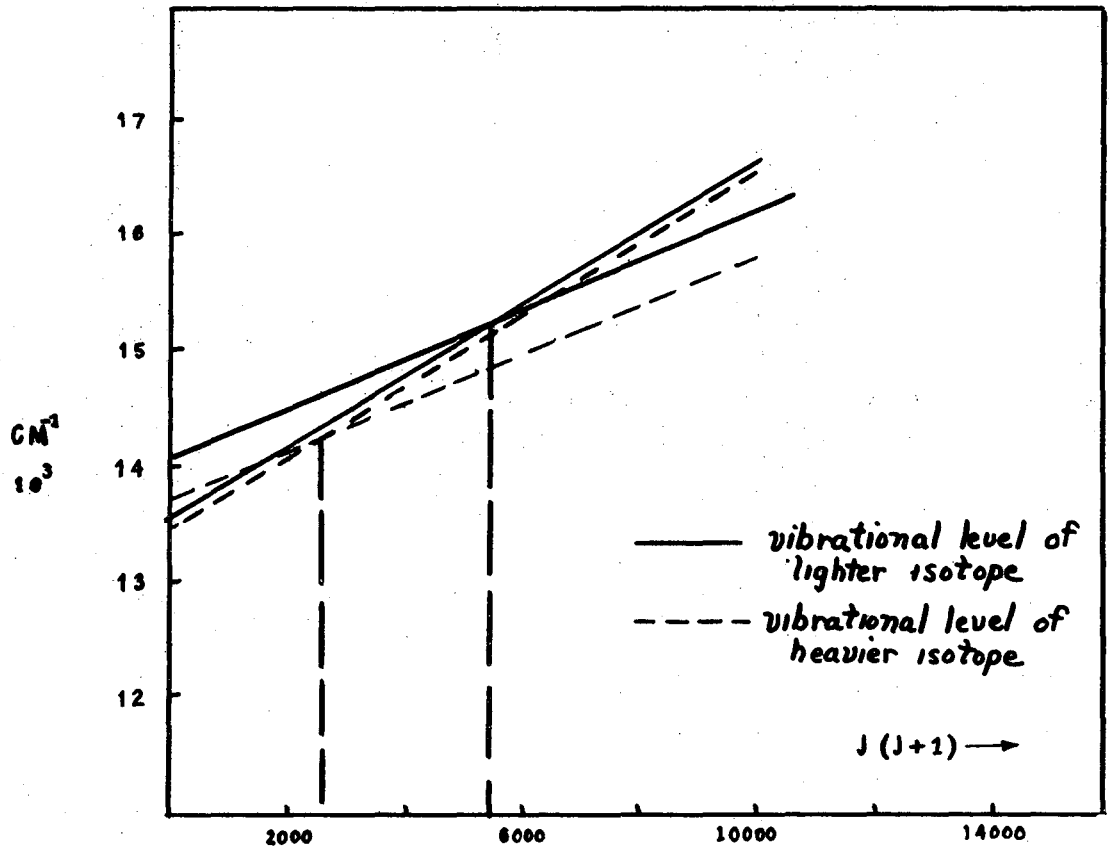
More thorough discussions of rotational perturbations can be found in Herzberg, Spectra of Diatomic Molecules, 1965, and Kovacs, Rotational Structure in the Spectra of Diatomic Molecules, 1969.

A standard method of assigning vibrational numbers,  $v$ , is to observe the isotopic shift of the vibrational levels according to formula (1):

$$\text{SHIFT} = \omega_e \left(v + \frac{1}{2}\right) - \omega_e x_e \left(v + \frac{1}{2}\right)^2 - \rho \omega_e \left(v + \frac{1}{2}\right) + \rho^2 \omega_2 x_e \left(v + \frac{1}{2}\right)^2 \quad (1)$$

where  $\rho = \sqrt{\mu/\mu_1}$ , and  $\mu$  is the reduced mass. The higher the  $v$ -number, the greater the shift, until the  $\omega_e x_e$  terms become dominant. A similar method can be used with the six states perturbing the  $A^1\Sigma$  state. A perturbation can occur when two (or more) vibrational levels (from different electronic states) have approximately the same energy at the same rotational quantum number,  $J(\Delta E \sim 0, \Delta J = 0)$ . Therefore on a plot of energy vs  $J(J+1)$ , a perturbation is possible where the lines representing the two vibrational levels cross (see Fig. 1). When a heavier isotope is used these levels shift downward in energy as indicated by formula (1) and intersect one another at a new energy and  $J$  value. (The isotopic-effect on the rotational constants is ignored in this example for simplicity. It would change the slope of the lines slightly.) The amount of the shift, and hence the position of the perturbation, is dependent upon which vibrational levels are involved. Thus a comparison of the perturbations in the  $A^1\Sigma$  state of  $\text{CaO}^{16}$  and  $\text{CaO}^{18}$  should help clarify the relative energies of the six perturbing states. With this end in mind the spectrum of  $\text{CaO}^{18}$  in the region of  $7200 \text{ \AA}$  to  $9400 \text{ \AA}$  ( $A^1\Sigma-X^1\Sigma$  system) was taken and analyzed.





XBL 706-1191

Fig. 1. Plot of energy vs  $J(J+1)$  showing how a rotational perturbation shifts with a change of isotope.

## II. EXPERIMENTAL

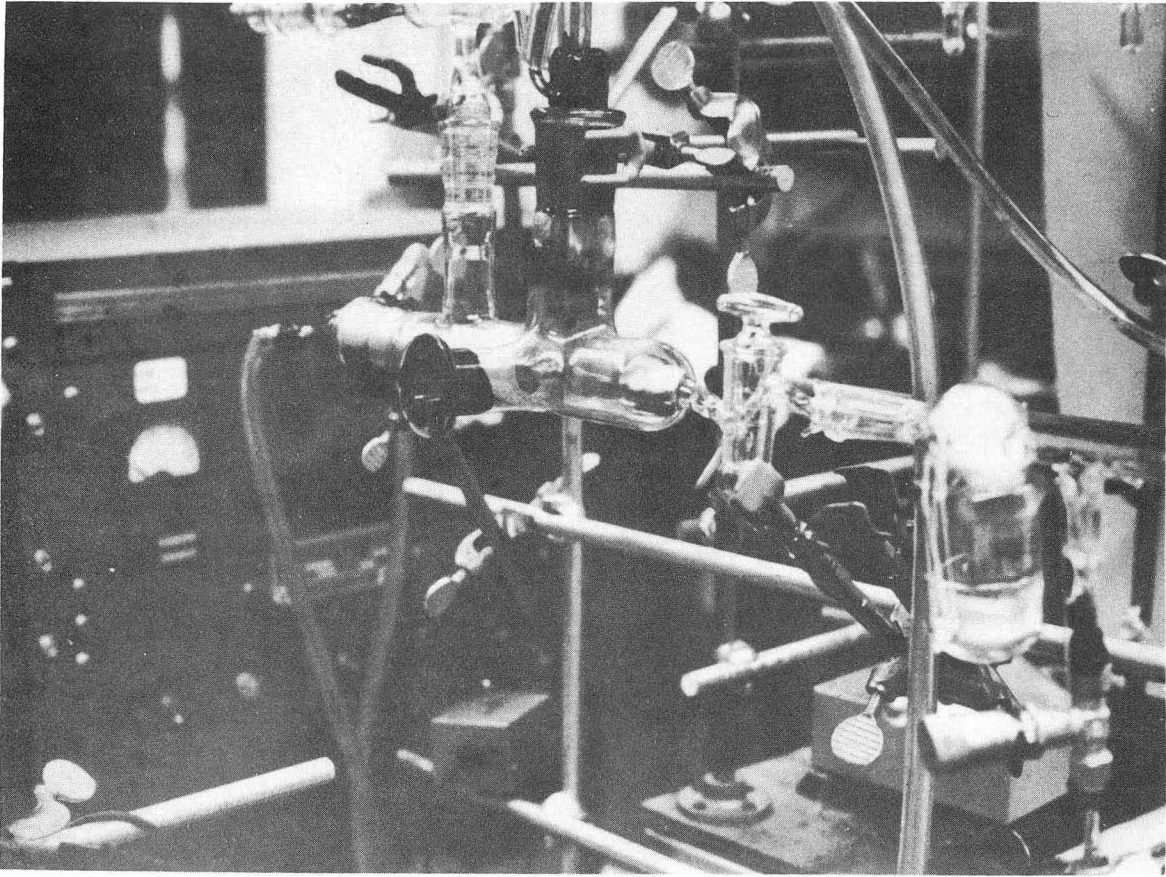
The light source used was a reduced pressure arc operated by a 300 volt d.c. power supply at a current of 1 amp (Hauge, 1965) (Figs. 2 and 3). The electrode-holders were water-cooled and held calcium rods one-fourth inch in diameter. The arc was initiated with a Tesla coil and run at a pressure of 1 torr of He gas and  $\sim 0.3$  torr of  $O_2^{18}$ . Oxygen was added to the system as it was used up at regular intervals. A  $P_2O_5$  trap was used to absorb water vapor. Before new electrodes were used, their tips were first scraped clear of CaO.

The spectrograms were taken in the first order of a 1.5 meter. Jarell Ash grating spectrograph(1180 grooves/mm). Exposure times ran from 15 min to 1 hr. Eastman Kodak IN and IM plates were used; the IM plates were hypersensitized first with ammonia.\* A Kodak Wratten gelatin filter No. 89B was also used. The dispersion was  $4.4 \text{ \AA}/\text{mm}$ ; resolution approximately  $0.1 \text{ cm}^{-1}$ . A thorium electrodeless discharge tube generated the standard lines. (A neon Osram lamp was used in the  $9000 \text{ \AA}$ - $9400 \text{ \AA}$  region to identify the Th lines.)

---

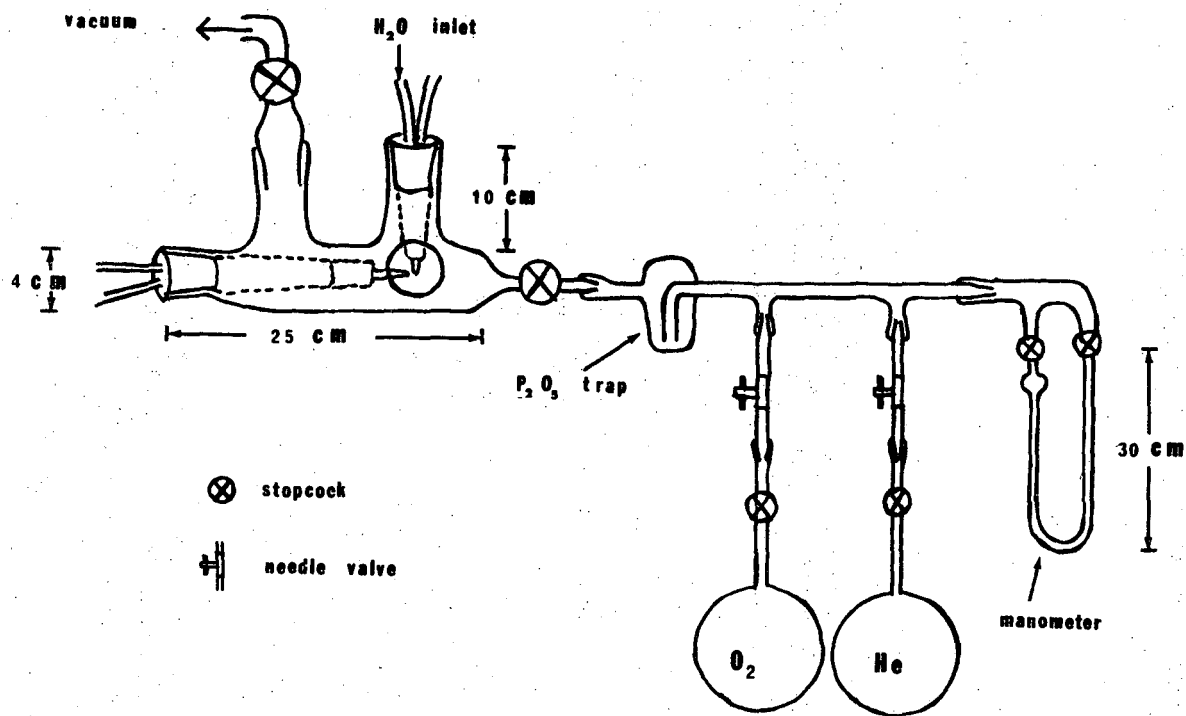
\* The hypersensitizing procedure was obtained from Dr. Sumner Davis and is as follows:

- (1) Four minutes in a solution of 6% ammonium hydroxide at  $40^\circ\text{F}$
- (2) One minute in a solution of one part isopropyl alcohol, two parts distilled water, and one cc of glacial acetic acid per one hundred cc of solution.
- (3) Four minutes in a solution of two parts isopropyl alcohol and one part distilled water by volume.
- (4) Dry the plate before storage or use. The plate should be stored in the freezer and used within two weeks.



XBB 706-2709

Fig. 2. Photograph of arc.



XBL 706-1163

Fig. 3. Schematic of vacuum system.

### III. RESULTS

#### A. Analysis

Five red-degraded sequences appeared in the CaO spectrum at approximately 7300, 7700, 8150, 8650, and 9200 Å. Analysis has shown them to be respectively the (3,0), (2,0), (1,0), (0,0), and (0,1) sequences of the  $A^1\Sigma-X^1\Sigma$  transition of  $CaO^{18}$ . There was no problem with contamination by  $O_2^{16}$ . However strong atomic lines blotted out part of the (2,0) and (0,0) sequences. Weak exposures were taken in these regions to pick up as many  $CaO^{18}$  lines as possible (see Figs. 4, 5, 6, 7).

Sixteen bands were analyzed: (0,0), (0,1), (1,0), (1,1), (1,2), (2,0), (2,1), (2,3), (3,0), (3,1), (3,2), (4,1), (4,2), (5,2), (5,3), and (6,3). Perturbations have been found in the upper level of each of these bands. See Table 2 for a listing of the assigned lines. Two columns are given for both the R- and P- branches. A shift from one column to the other indicates a perturbation. M's stand for missing lines, A's for lines that have been obscured by an atomic line, and H's for lines obscured by band heads.

The analysis itself was accomplished by calculating the combination differences,  $\Delta_2 F''(J)$ , of the  $X^1\Sigma$  vibrational levels using  $\rho$  and the spectroscopic constants of  $CaO^{16}$  (Hultin and Lagerqvist, 1950). The spectrum was then scanned by computer for sets of lines which satisfied these combination differences and the results were plotted out (Kopp, et al. 1965).

$$\Delta_2 F''(J) = R(J-1) - P(J+1) = F_v''(J+1) - F_v''(J-1) \quad (2)$$

$R(J)$  and  $P(J)$  refer to the indicated  $J$  lines in the R and P branches and  $F_v''(J)$  is the energy of the  $J$ -rotational level of the lower

vibrational state. A more detailed explanation and a listing of the computer program is found in Appendix B.

### B. Determination of Rotational Constants

The rotational constants of the unperturbed  $X^1\Sigma$  vibrational levels were determined by plotting  $\Delta_2 F''(J)/4(J+\frac{1}{2})^2$  vs  $(J+\frac{1}{2})^2$  where

$$\Delta_2 F''(J) = R(J-1) - P(J+1) = 4B_V''(J+\frac{1}{2}) - 8D_V''(J+\frac{1}{2})^3 \quad (3)$$

A sample plot is found in Appendix B and the rotational constants,  $B_V''$  and  $D_V''$  in Table 3.

The corresponding plot for the upper-state levels (i.e.  $\Delta_2 F'(J) = R(J) - P(J)$ ) fluctuated greatly due to the perturbations and could only give very approximate B-values. However, for such strongly perturbed levels it is meaningless to speak of a fixed B-value since every rotational level has a B-value which is a mixture of the  $B_V$ -values of the perturbed and perturbing states. One can however obtain a good approximation to the "unperturbed"  $B_V$  values by plotting  $T/4J$  vs  $J^2$  where:

$$\frac{T}{4J} = \frac{R(J-2) - R(J-1) + P(J) - P(J+1)}{4J} = B'' - B' + 6D'' - 2J^2(D'' - D') \quad (4)$$

This gives  $(B_V'' - B_V')$  as the intercept at  $J=0$ . Using the  $B_V''$  values found with Eq. (3), the  $B_V'$  values are easily calculated. The  $D_V'$  constants were obtained from the unperturbed sections of a plot of  $\Delta_2 F'(J)/4(J+\frac{1}{2})^2$ . Their average is found in Table 4.

The calculated B-values in Table 3 are from the equations:

$$B_V'' = 0.4093 - 0.003(V+\frac{1}{2}) \quad (5)$$

$$B_V' = 0.3733 - 0.0009(V+\frac{1}{2})$$

C. Determination of Vibrational Constants

The band origins,  $\nu_0$ , were determined in two ways. The first was the usual plot of  $[(R(J-1) + P(J))/2]$  vs  $J^2$

$$R(J-1) + P(J) = 2\nu_0 + 2(B' - B'')J^2 \quad (6)$$

The second method was to plot the left-hand side of Eq. (7) vs  $J$ .

$$B_v'' - \frac{1}{4} \{J(J+1)[P(J)+R(J-2)] - (J-1)[P(J+1)+R(J-1)]\} = \nu_0 \quad (7)$$

Both of these methods however could only give approximate values of  $\nu_0$  since the upper state is highly perturbed. For example, the  $V' = 1$  level is shifted  $\sim 8 \text{ cm}^{-1}$ .

In order to calculate the vibrational constants of the unperturbed lower state, the influence of the upper state was subtracted out as follows (Hultin and Lagerqvist, 1950). Equation (6) was written for the two bands with the same upper level but with different lower levels a and b.

$$[R(J-1) + P(J)]_{v', v_a''} = 2\nu_0(v', v_a'') + 2(B'_a - B''_a)J^2 \quad (8)$$

$$[R(J-1) + P(J)]_{v', v_b''} = 2\nu_0(v', v_b'') + 2(B'_b - B''_b)J^2 \quad (9)$$

The difference between Eqs. (8) and (9),  $A$ , is

$$\begin{aligned} A &= 2[\nu_0(v', v_a'') - \nu_0(v', v_b'') + 2(B''_b - B''_a)J^2] \\ &= 2[G''(v_b'') - G''(v_a'')] + 2(B''_b - B''_a)J^2 \end{aligned} \quad (10)$$

where  $G''(v_a'')$  is the energy of the  $v_a''$  vibrational level of the lower state at  $J=0$ . The quantity  $A/2$  is plotted vs  $J^2$  to obtain  $[G''(v_b'') - G''(v_a'')]$  as intercept and  $[B''_b - B''_a]$  as slope. The values obtained were very

close to those calculated for  $\text{CaO}^{18}$  from the  $\text{CaO}^{16}$  spectroscopic constants given by Hultin and Lagerqvist (1950). The  $\omega_e$  and  $\omega_e x_e$  constants calculated from the  $[G''(v_b'') - G''(v_a'')]$  values are found in Table 4.

Using these  $[G''(v_b'') - G''(v_a'')]$  differences, a consistent set of band origins were picked out of the results of Eqs. (6) and (7). They are given in the Deslandre's Table of Table 1. These origins and the calculated intercepts at  $J=0$  of the lower state vibrational level were used to calculate the energies of the upper state vibrational levels and the average values of these energies were in turn used to obtain the upper state vibrational constants (Table 3).

#### D. Perturbations in $\text{CaO}^{18}$

The 37 perturbations found in the  $A^1\Sigma$  state of  $\text{CaO}^{18}$  are listed in Table 5. They can be assigned to six perturbing states:  $Z^{18}$ ,  $Q^{18}$ ,  $Y^{18}$ ,  $W^{18}$ ,  $X^{18}$ , and  $B^{18}$ . On the plot of energy vs  $J(J+1)$  in Fig. 14, the solid lines represent the first seven vibrational levels of the  $A^1\Sigma$  state and the squares show the perturbations. The circles indicate the end of the analysis for that particular level and in all probability another perturbation. The dashed lines connect perturbations arising from the same perturbing state. In Table 5 the relative vibrational numbering for the perturbing states is given in column  $v_p$ , with the lowest levels of each state called X, Y, Z, Q, W, and B respectively.

In order to determine the  $B_v$  values of the perturbing levels, plots (Figs. 8-13) were made of  $T/4J$  vs  $J$  (see Eq. (4)) for all the analyzed bands. (Gerö, 1935; Kovacs, 1937; Hultin and Lagerqvist, 1950) For the unperturbed regions an almost horizontal line is obtained, while at a perturbation, two  $T/4J$  curves,  $F_1$  and  $F_2$ , rise to a peak. Equations



(11) and (12) are applicable for these plots:

$$B_{\nu}^P = 2B_{\nu}'' - B_{\nu}' - 2S \quad (11)$$

$$J_0 \sim J^* - \frac{1}{2} \quad (12)$$

where  $S$  is the value of  $T/4J$  at which the curves  $F_1$  and  $F_2$  cross and  $J^*$  is the  $J$  value at this point,  $J_0$  is the  $J$  value at which the perturbation culminates,  $B_{\nu}^P$  is the  $B$  value of the perturbing state,  $B_{\nu}'$  the  $B$  values of the  $A^1\Sigma$  state, and  $B_{\nu}''$  the  $B$  value of the  $X^1\Sigma$  state. A proof of these equations is found in Kovacs (1937). The  $B_{\nu}^P$  values are listed in Table 5. They compare quite well with the expected values calculated from Eq. (13)

$$B_{\nu}^i = \rho^2 B_{\nu} \quad (13)$$

where

$$\rho^2 = 0.9204$$

$$B_{\nu}^i = B_{\nu} \text{ for CaO}^{18}$$

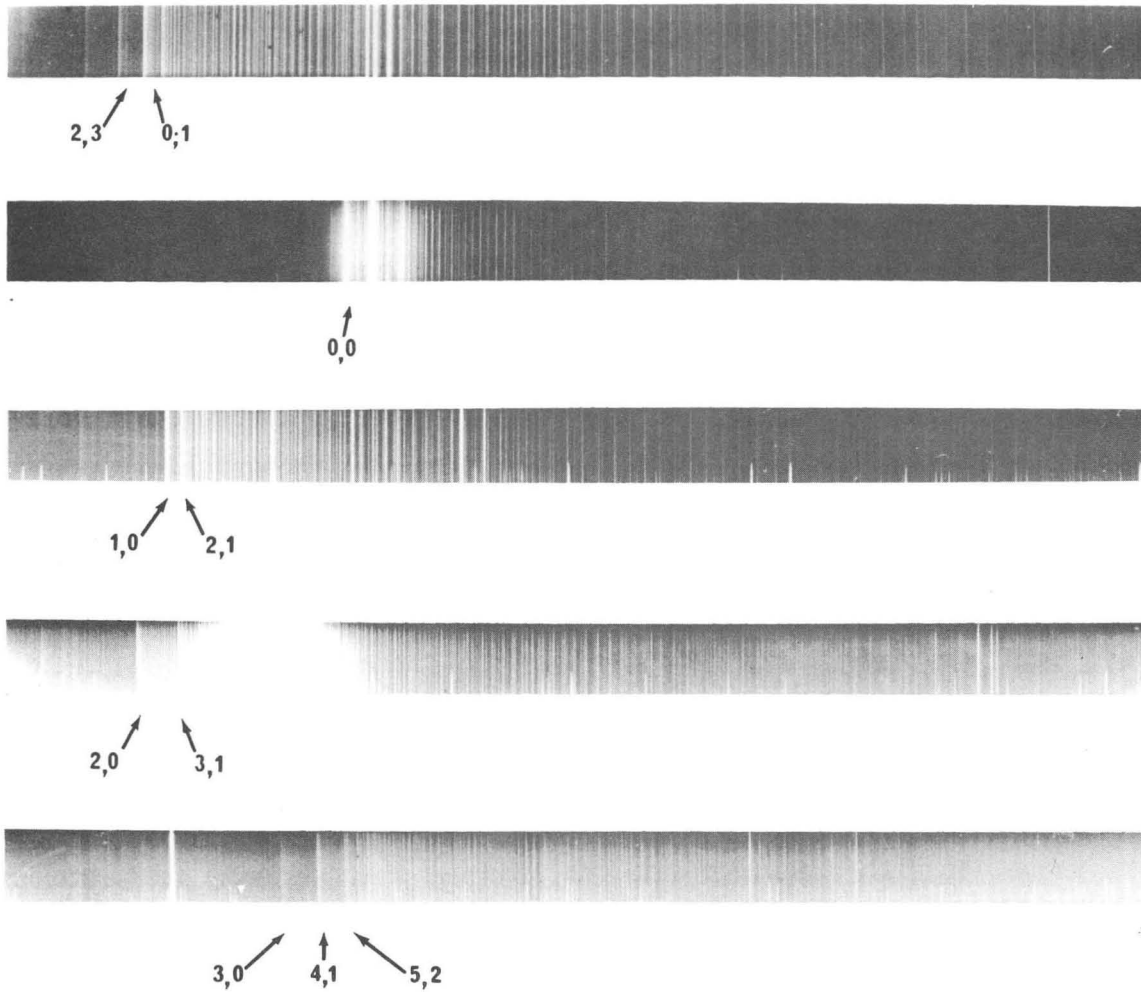
$$B_{\nu}^i = B_{\nu} \text{ for CaO}^{16}$$

Lagerqvist and Hultin obtained  $B_{\nu} \sim 0.33$  for the  $X^{16}$ ,  $Y^{16}$ ,  $Z^{16}$  and  $Q^{16}$  states of  $\text{CaO}^{16}$  and  $\sim 0.38$  for the  $B^{16}$  state. For  $\text{CaO}^{18}$ ,  $B_{\nu} \sim 0.308$  for the  $X^{18}$ ,  $Y^{18}$ ,  $Q^{18}$  and  $Z^{18}$  states and  $\sim 0.35$  for  $B^{18}$ .

The error in the  $B_{\nu}^P$  values found by the above method depends on the number of comparison lines found at each perturbation, the quality of these lines (i.e. overlapped, well-defined), the number of bands in which the perturbation is found, whether or not there are nearby perturbations to distort the  $B_{\nu}$  values of the perturbed level, etc. Because of the difficulty in estimating this error, the  $G(\nu)$  values

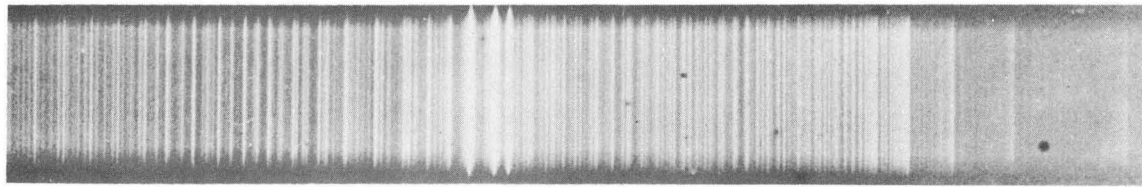
(where  $G(v)$  is the energy of the  $v$ -vibrational level at  $J=0$ ) were obtained by a simple graphical procedure. Consider the  $(Y+1)$  level of  $Y^{18}$  as an example. As shown in Table 5, the  $(Y+1)$  level of  $Y^{18}$  interacts with  $A^1\Sigma$  at two points,  $v_{A^1\Sigma} = 0, J_0 = 93.50$  and  $v_{A^1\Sigma} = 1, J_0 = 27.0$ . If  $D_v$  is assumed to be small (or, since both isotopic states are treated in the same way, the effect of  $D_v$  should cancel), the  $(Y+1)$  vibrational level can be represented as a straight line on a graph of energy vs  $J(J+1)$  (Fig. 14). That straight line is determined by the two points of perturbation mentioned above. The slope of the line is equal to the  $B_v$  value for that level and is listed in Table 5 under  $B_v^P(\text{slope})$ . In both  $\text{CaO}^{16}$  and  $\text{CaO}^{18}$  the  $B_v^P(\text{slope})$  values are  $\sim 0.02$  lower than the  $B_v^P$  values.

Since the  $B_v$  values of the other vibrational levels of  $Y^{18}$  would be expected to be similar to that of the  $(Y+1)$  level, the  $Y^{18}$  state can be shown as a series of lines parallel to  $(Y+1)$  and cutting through the other  $Y^{18}$  perturbations. The dashed lines in Fig. 14 represent the  $Y^{18}$  state; the solid lines the  $A^1\Sigma$  state. This was done for all the perturbing states of  $\text{CaO}^{18}$  and  $\text{CaO}^{16}$ . The perturbations of  $\text{CaO}^{16}$  were first replotted using the bottom of the potential curve of the  $X^1\Sigma$  state as the zero of energy. This was done so that the  $\text{CaO}^{16}$  and  $\text{CaO}^{18}$  levels would have the same reference point and could be compared. The  $G(v)$  results are given in Table 6 and the vibrational levels are graphed in Figs. 17 to 20. For the  $Z^{18}$  and  $Q^{18}$  states, the dashed lines in Fig. 14 connecting the perturbations coming from the same state were extended and the points of probable perturbation found used in graphing.

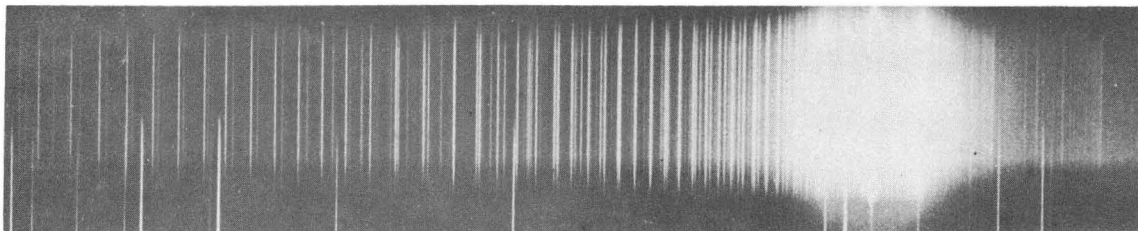


XBB 706-2706

Fig. 4. Spectrograms of the  $(0,0)$ ,  $(0,1)$ ,  $(1,0)$ ,  $(2,0)$ , and  $(3,0)$  sequences of the  $A'\Sigma - X'\Sigma$  transition of  $\text{CaO}^{16}$ .



(0,1) (2,3)

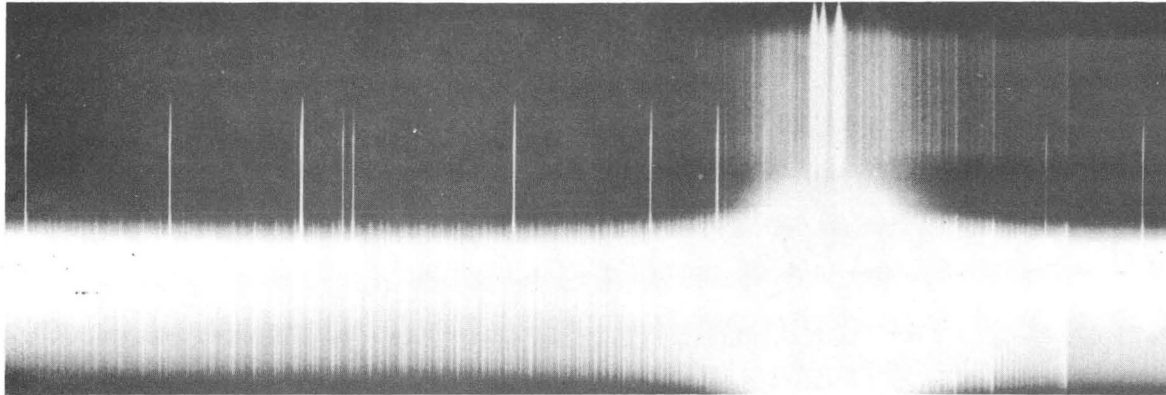


(0,0)

CaO<sup>18</sup>

XBB 706-2705

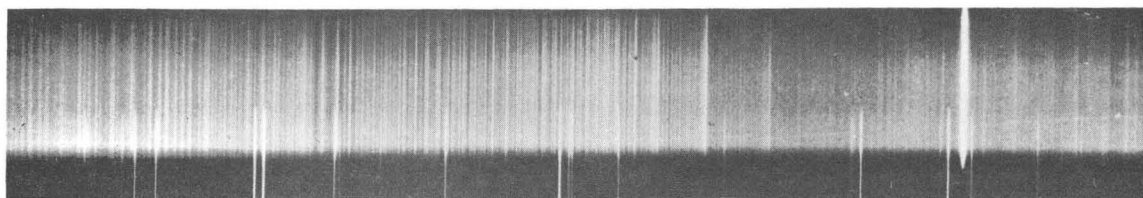
Fig. 5. Reproduction of the (0,0) and (0,1) sequences.



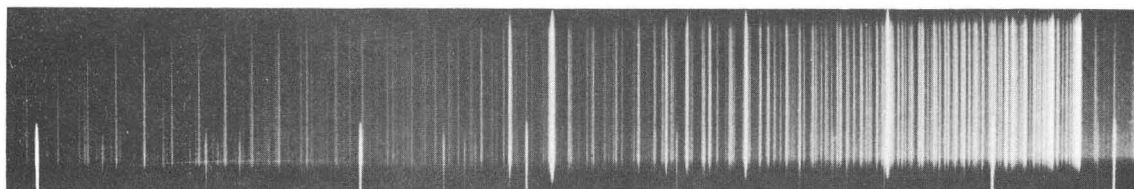
(4,2) (3,1) (2,0)

XBB 706-2708

Fig. 6. Reproduction of the (2,0) sequence.



(5,2) (4,1) (3,0)



(2,1) (1,0)

Ca O<sup>18</sup>

XBB 706-2707

Fig. 7. Reproductions of the (1,0) and (3,0) sequences.

Table 1. Deslandres Tables - Band Origins:  $\text{CaO}^{18}$

6						13548.6
5					13558.8	677.1 12881.7
4			13571.7	685.5		672.6 12886.2
3	13589.7	691.7	12898.	685.7		673.7 674.9 12212.3
2	676.9 12912.8	693.2	678.4 12219.6			10858.6
1	674.8 12238.5	689.1	679.2 11540.4	682.8		10857.6
↑ V'	689.9 11548.6	695.8	687.6 10852.8			
	V'' →	0	1	2	3	

Table 2. Listing of assigned lines in CaO<sup>18</sup>

V'V''	0.	0.	0.	1.0
J	P(J)	R(J)	P(J)	R(J)
1			10850.59	
2			10849.64	
3			10843.52	
4			10847.69	
5			10845.03	
6			10845.49	
7			10844.28	
8			10842.82	
9			10841.52	
10			10840.07	
11			10839.60	
12			10837.05	
13			10835.39	
14			10833.74	
15			10832.04	
16			10830.14	10856.38
17			10828.30	10855.95
18			10826.33	10855.50
19		11547.90	10824.39	10855.01
20		11547.23	10822.31	10854.45
21	11514.52	11546.58	10820.24	10853.78
22	11512.25	11545.87	10818.10	10853.13
23	11509.95	11545.00	10815.79	10852.27
24	11507.60	11544.10	10813.53	10851.52
25	11505.11	11543.06	10811.16	10850.59
26	11502.65	A	10808.69	10849.68
27	11499.93	A	10806.21	10848.62
28	11497.26	11539.78	10803.62	10847.43
29	11494.54	11538.41	10800.97	10846.20
30	11491.72	11536.94	10798.23	10844.92
31	11488.79	11535.51	10795.36	10843.49
32	11485.78	11533.86	10792.47	10841.86
33	11482.64	11532.04	10789.44	10840.07
34	11479.40	11530.06	10786.20	10837.93
35	11475.99	11527.79	10782.96	10835.39
36	11472.39	11524.93	10779.52	10832.54
37	11468.50	11521.45	10777.52	10847.26
38	11464.06	11516.73	10774.86	10843.14
39	11459.94	11475.98	10770.55	10840.07
40	11452.75	11463.92	10765.15	10837.05
41		11463.26	10773.52	10834.59
42		11458.47	10774.86	10834.59
43		11454.08	10770.30	10832.17
44		11449.88	10766.19	10830.14
45		11445.83	10762.24	10827.77
46		11441.72	10758.33	10825.54
47		11437.61	10754.64	10823.25
48		11433.47	10750.75	10820.79
49		11429.08	10746.86	10818.96
50	11425.38	11499.95	10742.76	10816.34
51	11420.94	11496.97	10739.38	10813.90
52	11416.52	11493.84	10735.29	10811.16
53	11411.96	11490.43	10731.17	10808.50
54	11407.30	11486.43	10726.91	10805.43
55	11402.29	11481.14	10722.50	10801.79
56	11396.72	11473.88	10717.92	10796.78
57	11389.67	11471.38	10712.65	10808.50
58	11381.10	11467.16	10708.00	10802.13
59		11472.92	10717.89	10797.67
60		11458.52	10710.67	10793.74
61		11453.43	10703.92	A
			10698.41	10785.94
			10692.95	10781.12



Table 2, continued.

V'V''		0.		0.		1.0	
J	P(J)	R(J)	R(J)	P(J)	P(J)	R(J)	R(J)
62		11369.21	11473.31	11457.93		10687.23	10775.84
63		11362.65	11467.78	11450.57		10681.04	10769.02
64	11370.93	11355.25	11461.88	11441.72		10673.99	10762.45
65	11362.65	11346.65	11457.66		10683.41	10660.03	10778.38
66	11356.40	11338.26	11452.75		10677.42	10658.29	10773.86
67	11350.48		11445.33	11458.47	10672.13		10767.45
68	11344.09			11452.83	10666.93		10772.93
69	11335.41	11348.32		11447.64	10658.20	10668.76	10768.47
70		11340.73		11443.19		10661.91	10764.42
71		A		11438.84		10655.91	10760.45
72		11328.24		11434.58		10650.33	10756.62
73		11322.35		11430.31		10644.85	10752.76
74		11316.52		11426.04		10639.45	10748.95
75		11310.70		11421.75		10634.06	10745.18
76		11304.87		11417.43		10628.74	10741.23
77		11299.02		11412.94		10623.32	10737.30
78		11293.11		11408.51		10617.85	10733.28
79		11287.17		11403.92		10612.40	10729.21
80		11281.15		11399.30		10606.86	10725.03
81		11275.05		11394.52		10601.25	10720.75
82		11268.84		11389.67		10595.53	10716.29
83		11262.55		11384.43		10589.75	10711.61
84		11256.05		11378.94		10583.74	10706.05
85		11249.38		11372.39		10577.58	10701.06
86		11242.33	11382.64	11365.64		10571.07	10693.73
87		11234.75	11367.27	11356.40		10563.96	10685.73
88	11243.06	11226.03	11357.95			10555.21	
89	11226.03	11215.29	11346.65			10545.59	
90	11215.29	11239.90		11356.40			
91	11202.36	11221.43		11348.32			
92		11210.65	11355.98	11339.43			
93		11201.04	11344.09	11327.34			
94	11207.18	11190.66	11336.97				
95	11193.84	11177.03	11329.47				
96	11185.22			11327.34			
97	11176.16			11320.97			
98		11172.54		11314.41			
99		11164.62		11307.12			
100		11156.58	11317.54	11297.71			
101		11147.82	11307.12	11281.15			
102	11156.58	11136.92	11298.58				
103	11144.71	11118.46	11291.73				
104	11134.83		11285.29				
105	11126.39		11279.03				
106	11118.46		11272.92				
107	11110.71		11266.74				
108	11103.14		11260.62				
109	11095.53		11254.38				
110	11087.80		11248.03				
111	11080.17		11241.74				
112	11072.37		11234.75				
113	11064.39						
114	11056.26						
115	11047.73						
116							
117							
118							
119							
120							

V'V''		1.0		1.0		1.0		2.0	
J	P(J)	R(J)	P(J)	R(J)	P(J)	R(J)	P(J)	R(J)	
14			11523.92						
15			11523.50						
16			11524.16	11548.43				10864.45	
17			11521.93	11547.28				10864.13	
18			11519.68	11546.11			10836.86	10863.29	
19			11517.18	11545.91			10834.59	10862.46	
20			11514.75	11544.11			10832.04	10861.66	
21			11512.25	11543.09			10829.37	10860.96	
22			11509.36	A			10827.03	10859.36	
23			11507.03	A			10824.39	10858.47	
24			11504.37	11539.75			10821.68	10857.14	
25			11501.50	11538.41			10818.96	10855.95	
26			11498.62	11536.72			10816.41	10854.45	
27			11495.71		11533.82		10813.53	10856.38	
28			11492.17		11537.42		10810.04	10855.01	
29				11492.69	11536.04			10853.78	
30				11489.56	11534.24		10810.43	10852.27	
31				11486.43	11532.62		10807.51	10851.09	
32				11483.36	11530.77		10804.87	10849.68	
33				11480.11	11528.92		10801.93	10847.69	
34				11475.78	11526.95		10798.85	10846.20	
35				11473.31	11525.82		A	10844.92	
36				11469.92	11523.68		10792.47	10843.14	
37				11466.30	11520.63		A	10840.90	
38		12213.91	11462.78	11524.16	11516.16		10786.56	10836.65	
39		12210.43	11458.47	11520.47			10783.18	10844.28	
40	12149.50	12207.83	11463.48	11452.63	11518.77		10779.52	10841.25	
41	12144.40	12204.83	11455.31	11515.50			10781.12	10839.52	
42	12140.50	12199.38	11451.51	11510.42	11527.47		10776.72	10836.86	
43	12135.95	12189.95	11446.86	11506.62	11517.96		10773.24	10832.17	
44	12129.82	12137.11	11440.75	11450.57	11515.50		10759.02	10830.49	
45	12117.63	12132.68	11429.08	11445.83	11512.25		10752.74	10823.04	
46		12128.02	11441.77	11441.77	11509.95		10770.55	10835.39	
47		12123.45	11437.61	11437.61	11507.03		10766.84	10833.00	
48		12118.99	11433.47	11433.47	11505.15		10762.74	10830.48	
49		12114.29	11429.08	11429.08	11502.01		10758.71	10828.30	
50		12109.68	11425.38	11425.38	11499.32		10754.54	10825.64	
51		12105.09	11420.74	11420.74	11495.25		10750.75	10823.25	
52		12100.39	11415.52	11415.52	11493.10		10746.76	10820.79	
53		12095.65	11411.96	11411.96	11490.43		10742.76	10818.10	
54		12090.83	11407.30	11407.30	11487.40		10738.57	10815.67	
55		12085.88	11402.95	11402.95	11483.93		10734.58	10812.87	
56		12080.76	11398.36	11398.36			10730.33	10810.04	
57		12075.30	11393.43	11393.43			10726.08	10806.98	
58	12075.51	12159.66					10721.60	10803.62	
59	12069.43	12156.36					10716.95	10799.79	
60	12063.77	12151.95					10711.32	10801.93	
61	12058.30	12148.31					10706.92	10798.58	
							10707.44	A	
							10702.73	10792.52	
62	12052.68	12144.40							
63	12047.49	12140.50					10698.00	A	
64	12042.01	12136.36					10693.42	10736.20	
65	12036.45	12132.12					10688.58	10731.18	
66	12030.77	12127.70					10683.85	10727.52	
67	12024.99	12122.98					10679.23	10723.84	
68	12018.97	12117.83					10673.99	10721.42	
69	12012.67						10669.09	10718.25	
70	12005.99						10663.31	10715.74	
71							10658.20		
							10651.87		

Table 2, continued.

V'V''		3.0		1.0		3.0		2.0	
J	P(J)	R(J)	P(J)	R(J)	P(J)	R(J)	P(J)	R(J)	
16									
17		13590.88							
18		13590.23							
19	13561.09	13589.54							
20	13558.38	13588.72							
21	13556.43	13588.04							12213.91
22	13553.61	13586.96							12212.98
23	13551.22	13585.96							12212.47
24	13548.73	13584.91							12211.56
25	13546.32	13583.66							12210.91
26	13543.89	13582.42							12209.87
27	13540.86	13581.01							12209.57
28	13538.01	13579.69	12849.44	12899.88					12207.66
29	13534.81	13578.18	12846.84	12898.78					12206.76
30	13531.46	13576.46	12843.64	12887.19					12205.28
31	13528.47	13574.80	12841.05	12885.80					12204.59
32	13525.43	13572.67	12838.10	12884.35					12203.33
33	13522.10	13570.36	12835.04	12882.39					12201.88
34	13518.18	13567.40	13571.99	12828.34					12200.08
35	13514.32		13568.48						12198.31
36	13509.27	13514.32	13566.25						12196.37
37		13509.27	13563.86						12194.27
38		13505.44	13561.53						12192.24
39		13501.28	13558.38						12189.85
40		13497.48	13556.43						12188.02
41		13493.20	13559.70						12187.52
42		13489.11	13555.49						12187.52
43	13490.09	13482.32	13553.04						12185.31
44	13484.98		13550.03						12184.29
45	13480.74		13547.16						12182.76
46	13476.28		13543.89						
47	13471.63		13540.86						
48	13466.78		13537.21						
49	13462.12		13532.23	13540.86					
50	13456.98		13535.14						
51	13450.53	13459.08	13531.46						
52		13452.03	13527.88						
53		13446.58	13524.66						
54		13441.29	13520.93						
55		13436.42	13518.18						
56		13431.46	13514.57						
57		13426.95	13510.99						
58		13421.85	13507.27						
59		13416.50	13503.33						
60		13411.23	13500.04						
61		13406.09	13495.99						
62		13400.68	13492.11						
63		13395.20	13488.30						
64		13389.80	13484.26						
65		13384.19	13479.93						
66		13378.62							
67		13372.98							
68									
69									
70									
71									
72									

Table 2, continued.

Table 2, continued.

V'V''					
	4.0	1.0		4.0	2.0
J	P(J)	R(J)		P(J)	R(J)
15	13551.86	13574.80			
16	13550.03	13574.34			
17	13547.97	13573.91			
18	13545.99	13573.29			
19	13543.89	13572.67			
20	13541.66	13571.95			
21	13539.58	13571.16			
22	13537.21	13570.36			
23	13534.81	13569.50			
24	13532.23	13568.48		12849.45	
25	13529.91	13567.40		12847.29	12884.59
26	13527.19	13566.25		12844.76	12883.85
27	13524.66	13565.05		12842.25	12882.31
28	13522.10	13563.86		12839.63	12881.56
29	13519.08	13562.47		12836.99	12880.43
30	13516.18	13561.09		12834.41	12879.20
31	13513.37	13559.70		12831.72	12877.87
32	13510.30	13558.22		12828.84	12876.63
33	13507.27	13556.43		12825.97	12875.14
34	13503.93	13554.75		12822.86	12873.78
35	13500.66	13553.04		12819.96	12872.41
36	13497.48	13551.22		12816.83	12870.31
37	13494.18	13549.22		12813.80	12868.66
38	13490.65	13547.16		12810.47	12867.14
39	13487.26	13545.25		12807.09	A
40	13483.61	13543.25		12803.94	A
41	13479.93	13540.36		12800.59	A
42	13476.28	13538.76		12797.04	A
43	13472.53	13536.32		12793.57	A
44	13468.67	13533.00	13540.86	12789.92	12854.33
45	13464.70	13226.97	13533.00	12786.29	12848.56
46	13459.72	13467.62	13529.01	12781.49	
47	13452.03	13458.29	13526.49	12774.71	12850.86
48		13452.67	13523.76		12848.56
49		13448.36	13520.93	12775.07	12846.12
50		13444.21	13518.18	12771.14	12843.64
51		13439.84	13515.19	12767.13	12841.05
52		13435.52	13514.57	12763.17	12838.58
53		13430.97	13509.27	12759.05	12838.11
54	13428.53	13422.60	13506.15	12754.92	12833.40
55	13421.85		13503.21	12752.90	12830.36
56	13417.13		13500.04	12746.49	12827.45
57	13412.47		13496.55	12742.04	12825.07
58	13407.87		13493.20	12737.72	12821.79
59	13402.34		13489.62	12733.50	12818.80
60	13397.87		13484.54	12728.79	12814.99
61	13392.87	13477.65	13484.26	12724.05	12810.49
				12718.83	12803.94
					12811.56
62	13386.03		13478.98	12712.68	12806.05
63	13377.63	13384.19	13475.15	12704.65	12712.01
64		13377.63	13471.63		12705.57
65		13372.32	13467.98		12700.63
66		13367.01	13463.84		12695.44
67		13361.50	13459.72		12690.66
68		13355.01	13455.77		12685.36
69		13350.14	13452.03		12680.61
70		13344.81			12675.59
71		13339.43			12670.68
72					

V'V''			5.0			3.0			6.0			3.0		
J	P(J)	R(J)	J	P(J)	R(J)	J	P(J)	R(J)	J	P(J)	R(J)	J	P(J)	R(J)
25														13547.16
26														13546.32
27										13504.88				13545.25
28										13502.49				13543.89
29										13500.04				13543.25
30										13497.43				13542.27
31		13547.97			12875.14					13494.86				13540.86
32		13546.32			12873.78					13492.11				13539.58
33	13495.88	13544.86		12823.36	12872.41					13489.11				13533.01
34	13492.86	13543.25		12820.60	12871.44					13486.24				13536.32
35	13489.62	13541.66		12817.41	12869.61					13483.12				13534.09
36	13486.41	13539.58		12814.50	12867.86					13479.93				13533.00
37	13483.12	13538.01		12811.54	12866.31					13476.28				13531.46
38	13479.93	13536.32		12808.51	A					13473.52				13529.91
39	13476.28	13534.09		12805.19	A					13470.16				13527.88
40	13472.86	13532.10		12801.88	A					13467.25				13525.43
41	13469.41	13529.91		12798.59	A					13463.84				13523.26
42	13465.80	13527.88		12795.43	A					13459.72				13520.93
43	13462.12	13525.62		12792.01	12855.35					13455.77	13473.52			13526.91
44	13458.29	13523.26		12788.45	12853.13					13452.03	13463.31			13524.66
45	13454.44	13520.93		12784.78	12851.15						13456.40			13522.56
46	13450.53	13518.18		12780.92	12848.56						13452.67			13520.38
47	13446.58	13514.32		12777.40	12844.78						13449.04			13518.18
48	13442.22	13515.89		12773.60	12840.23	12846.84					13445.24			13515.89
49	13436.92	13512.24		12768.21		12843.64					13441.29			13513.37
50	13436.92	13509.27		12761.88	12768.64	12841.01					13437.51			13510.99
51	13431.46	13506.15			12763.65	12838.53					13433.53			13508.43
52	13426.95	13503.33			12759.39	12835.95					13429.37			13505.44
53	13422.60	13500.28			12755.29	12833.37					13425.46	13512.73		13501.23
54	13418.11	13497.48			12751.09	12830.54					13420.86	13506.15		13494.18
55	13413.61	13494.45			12746.97	M				13426.61	13415.25			13501.91
56	13409.19	13491.48			12742.90	12825.03				13418.57	13409.28	13499.14		
57	13404.50	13488.30			12738.44	12822.64				13412.62		13495.38		
58	13399.79	13484.98			12734.27	M				13408.28		13492.86		
59	13395.20	13481.68			12730.25	12816.85				13403.68		13488.30		
60	13390.39	13478.51			12725.83	12813.76				13399.14				
61	13385.54	13475.15			12721.52	12811.01				13392.87				
62	13380.72	13471.63			12717.47	12808.51								
63	13375.75	13467.98			12712.68	12805.00								
64	13370.72	13464.30			12708.18	12801.93								
65	13365.67	13460.82			12703.57	12799.62								
66	13360.52	13456.98			12698.33	12795.47								
67	13355.31	13453.40			12594.41	12792.46								
68	13350.14	13449.45			12589.42	12789.05								
69	13344.81	13445.60			12584.82	M								
70	13339.46	13441.76			12679.97	12732.59								
71	13334.08				12674.94									
72	13328.56				12670.15									
73														

Table 2., continued



Table 2, continued.

V'V''	2.0	0.	2.0	1.0	2.0	3.0	
J	P(J)	R(J)	P(J)	R(J)	P(J)	R(J)	
62		12729.27	12321.68		12046.88	12140.62	
63	12726.42		12316.33	12045.62		12136.36	10711.22
64	12719.44		12310.47	12039.10		12129.82	12141.75
65	12712.55		12799.75	12033.30		12120.33	12135.95
66	12705.23	12717.72	12811.54	12024.99	12037.10		12131.23
67	12692.65	12709.76	12806.05	12014.05	12029.68		12126.18
68		12702.79	12799.37		12023.24		12120.33
69		12695.36	12809.13		12016.60	12131.23	12113.17
70		12687.93	12799.75		12009.43	12120.33	12106.04
71	12695.86		12792.42	12018.47	12001.47	12113.66	12093.71
72	12684.32		12786.30	12006.43	11992.03	12108.24	
73	12675.96		12780.92	11998.02	11978.15	12103.23	
74	12668.23		12775.50	11991.04		12098.45	
75	12661.16		12770.37	11984.51		12093.71	
76	12654.28		12765.22	11978.15		12089.07	
77	12647.67		12760.24	11971.91		12084.48	
78	12641.02		12755.32	11965.74		12079.82	
79	12634.34		12750.00	11959.57		12074.98	
80	12628.03		12744.75	11953.31		12070.43	
81	12621.00		12739.42	11947.22		12065.65	
82	12614.29		12734.27	11940.97		12060.84	
83	12607.44		12728.74	11934.68		12055.92	
84	12600.36		12723.16	11928.30		12050.80	
85	12593.62		12717.72	11921.74		12045.63	
86	12586.45		12711.41	11915.22		12040.27	
87	12579.72		12705.53	11908.48		12034.36	
88	12571.84			11901.36		12028.33	12044.91
89	12564.38			11894.25			12036.05
90				11886.78	11903.04		12029.68
91					11892.86		12023.24
92					11884.92		12016.81
93					11877.25		12011.27
94					11869.64		
95					11862.10		
96							
97							
98							
99							

Table 3. Rotational Constants for the X' $\Sigma$  and A' $\Sigma$  States: CaO<sup>18</sup>

v	B''obs.	B''calc.	B'obs.	B'calc'.
0	.3732	.3728	.4078	.4078
1	.3725	.3720	.4049	.4048
2	.3706	.3710	.4017	.4018
3	.3698	.3702	.3988	.3988
4	.3693	.3692		
5	.3681	.3684		
6	.3678	.3674		



Table 4. Spectroscopic Constants:  $\text{CaO}^{18}$

	Constants for $X^1\Sigma$		Constants for $A^1\Sigma$	
	found	Cal from $\text{CaO}^{16}$	found	Cal from $\text{CaO}^{16}$
$v(0,0)$	0.0	0.0	11548.6	11548.80
$w_e$	702.18	702.40	~686.5	686.9
$w_{exe}$	4.29	4.43	~1.5	1.47
$B_e$	.4093	.4091	.3733	.3740
$\alpha_e$	.003	.00296	.0009	.0012
$D_e$	$\sim 5.24 \times 10^{-7}$	$5.56 \times 10^{-7}$	$\langle 4.58 \times 10^{-7} \rangle$	$4.57 \times 10^{-7}$
$\beta_e$	$\sim 5.9 \times 10^{-8}$	$2.4 \times 10^{-8}$		

Table 5. Summary of the Perturbations:  $\text{CaO}^{18}$

$V_P$	$V_{A^1\Sigma}$	$J_o$	$B_v^P$	$B_v^P$ (Slope)
Z	0	38.70	.304	
Q	0	48.50		
Y	0	56.20	.3088	
W	0	63.20	.328	
X	0	67.80		
Z + 1	0	87.80	.3018	
Q + 1	0	89.90	.2938	
Y + 1	0	93.50	.306	.284
W + 1	0	96.50		.281
X + 1	0	101.10	.311	
Z + 2	0	~114.00		.280
Y + 1	1	27.00		.284
W + 1	1	38.80		.281
X + 1	1	42.40	(.295)	
B	1	57.90	(.35)	
Z + 2	1	~70.70		.280
Z + 3	2	44.80	.269	
B + 1	2	53.	.35	
Q + 3	2	51.40		
Y + 3	2	61.40		
W + 3	2	64.90	.314	
X + 3	2	71.00	.3025	
Z + 4	2	~89.75		
Y + 4	3	35.00		
W + 4	3	42.00		
X + 4	3	50.00		

Table 5. Summary of the Perturbations:  $\text{CaO}^{18}$  (continued)

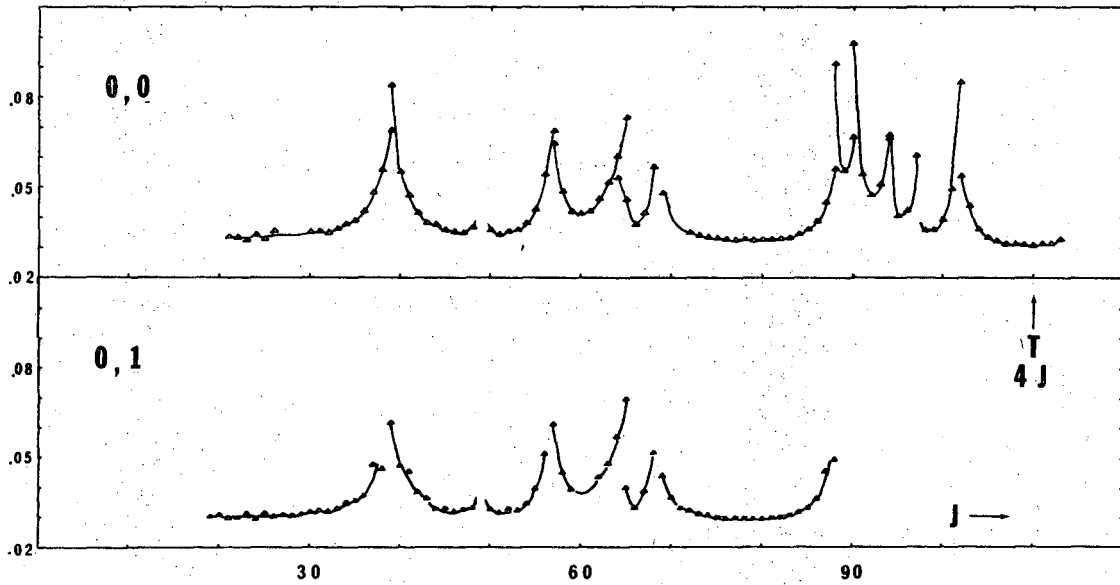
$V_P$	$V_{A^1\Sigma}$	$J_o$	$B_V^P$	$B_V^P$ (Slope)
Z + 5 Z + 6	3 4	~70.60 45.70		
Q + 6 Y + 6 (?)	4 4	52.70 61.70		
X + 6 Y + 7 (?)	4 5	~70.50 ~31.50		
X + 7 Z + 8	5 5	48.50 ~71.75		
Z + 9 Y	6 6	43.10 54.60	.3012	
	6	~60.60		

Table 6. Term Values of the Perturbing States at J=0 for CaO<sup>18</sup>

Z	12010	Q	12100	Y	12170	W	12270	X	12300
Z + 1	12480	Q + 1	12565	Y + 1	12650	W + 1	12720	X + 1	12730
Z + 2	12945	Q + 2	13035	Y + 2	13120	W + 2	(13190)	X + 2	(13210)
Z + 3	13405	Q + 3	13485	Y + 3	13595	W + 3	13645	X + 3	13705
Z + 4	(13880)	Q + 4	13940	Y + 4	14060	W + 4	14105	X + 4	14160
Z + 5	14300							X + 5	(14605)
Z + 6	14755			Y + 6 (?)	14940			X + 6	15010
Z + 7	(15200)	B	12650	Y + 7 (?)	15370			X + 6	15480
Z + 8	15640	B + 1	13322	Y + 8 (?)	16235				
Z + 9	16070								

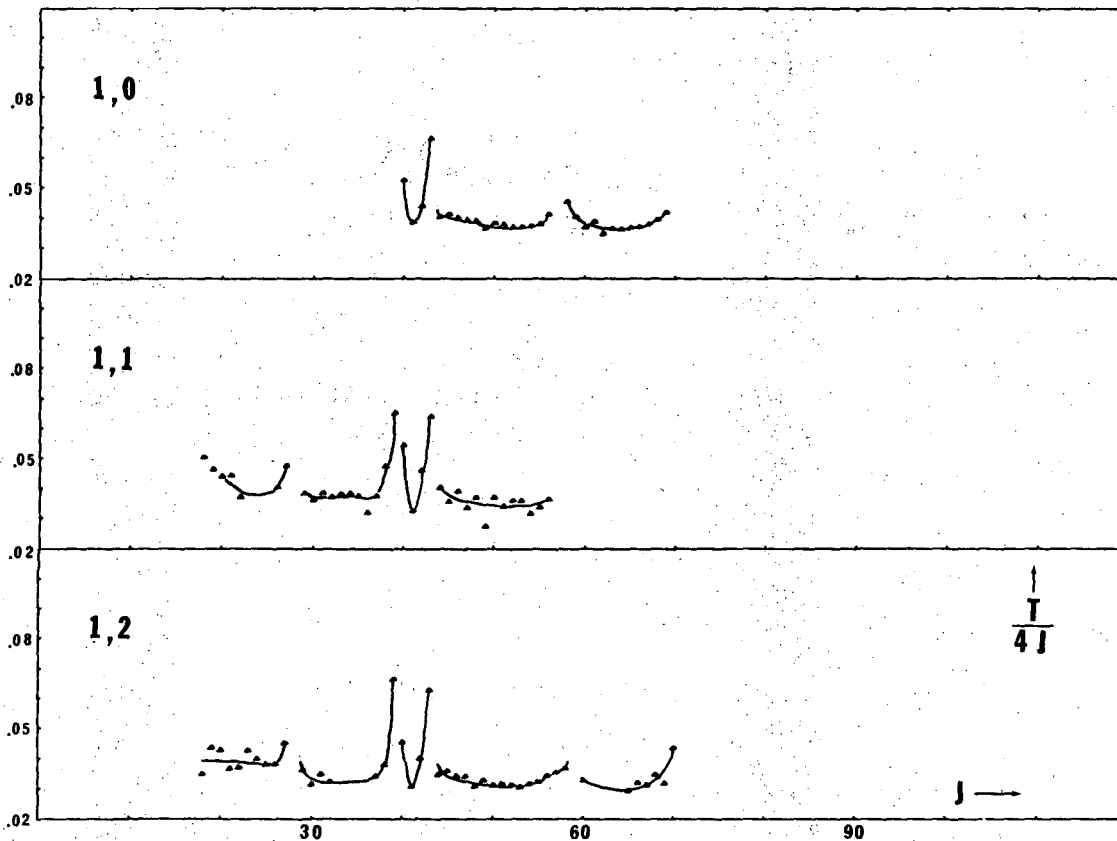
Table 6, continued. Term Values of the Perturbing States at  $J=0$  for  $\text{CaO}^{16}$

Z	12165	Q	12735	Y	12325	X	12430
Z + 1	12660	Q + 1	13235	Y + 1	12820	X + 1	12885
Z + 2	13155	Q + 2	13710	Y + 2	(13295)	X + 2	13345
Z + 3	13680	Q + 3	14210	Y + 3	13780	X + 3	13850
Z + 4	14155			Y + 4	14250	X + 4	14340
Z + 5	(14590)					X + 5	14800
Z + 6	15125	B	12113			X + 6	(15280)
Z + 7	15635	B + 1	12690			X + 7	15765
						X + 8	16220



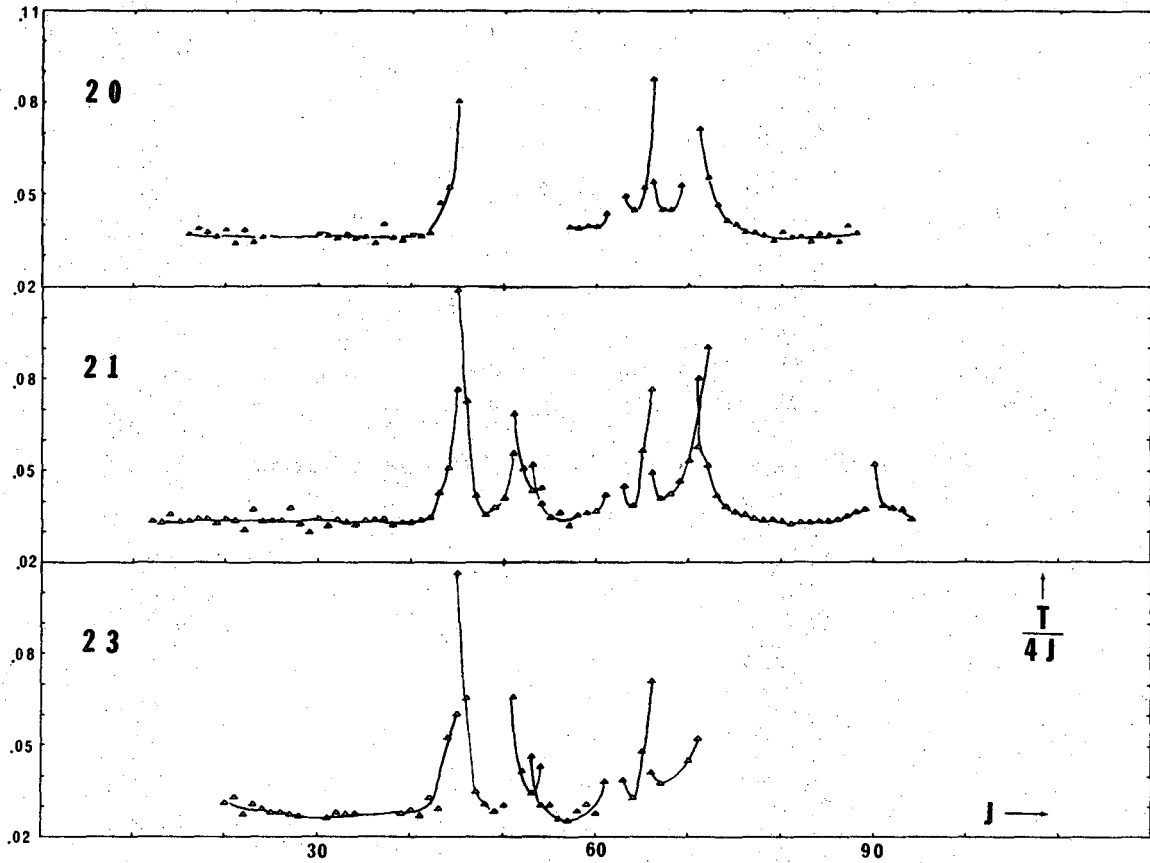
XBL 706-1176

Fig. 8.  $T/4J = [R(J-2) - R(J-1) + P(J) - P(J+1)]/4J$  plotted vs  $J$  for the  $(0,0)$  and  $(0,1)$  bands.



XBL 706-1175

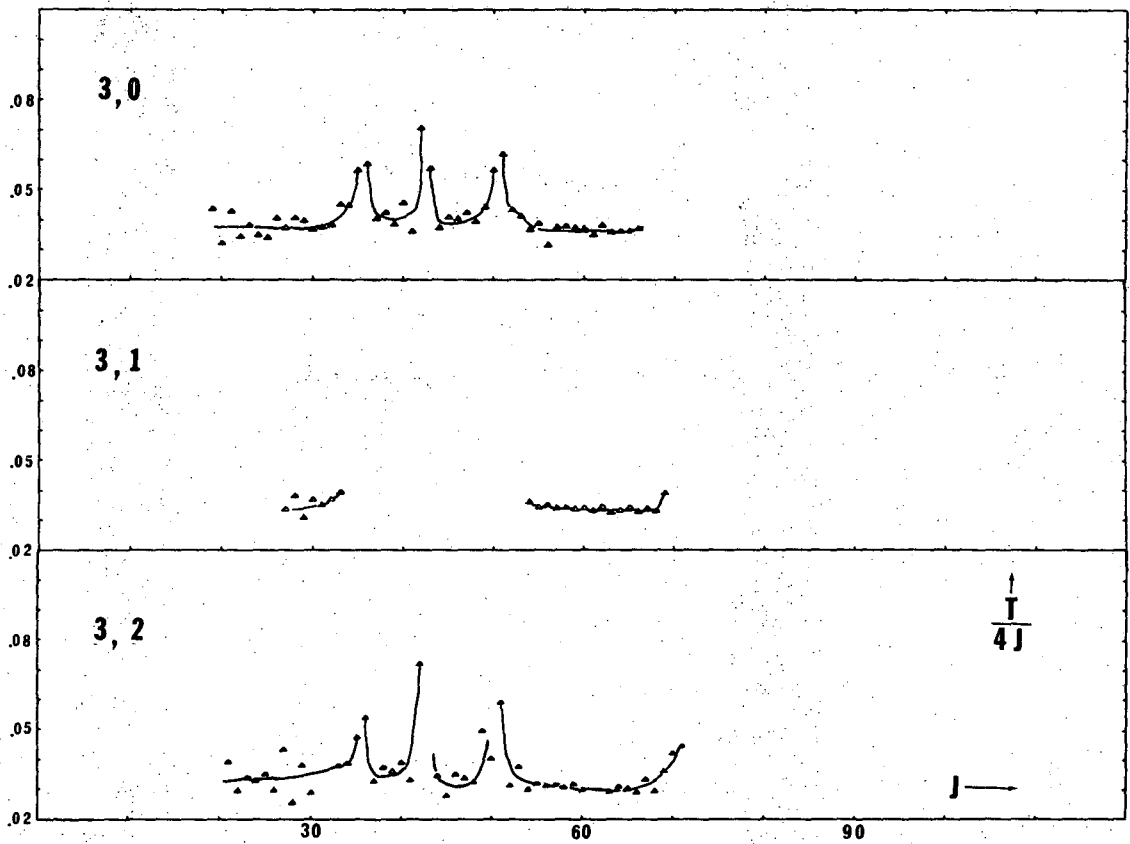
Fig. 9.  $T/4J$  plotted against  $J$  for the (1,0), (1,1), and (1,2) bands.



XBL 706-1174

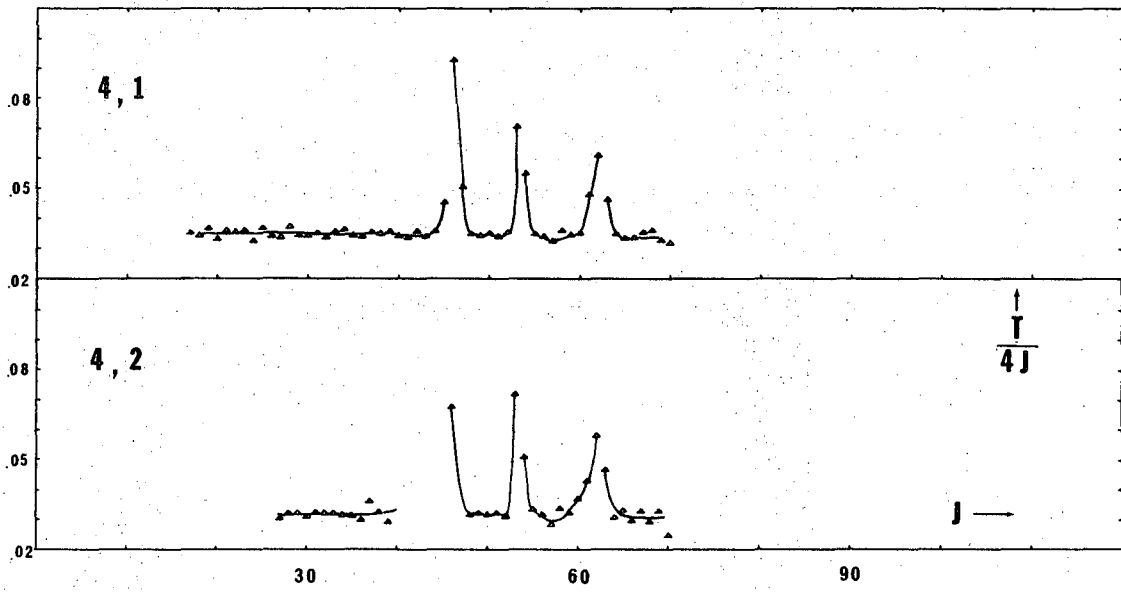
Fig. 10.  $T/4J$  plotted against  $J$  for the (2,0), (2,1), and (2,3) bands. The blank spot in the (2,0) plot is due to atomic lines which blotted out the CaO spectra.





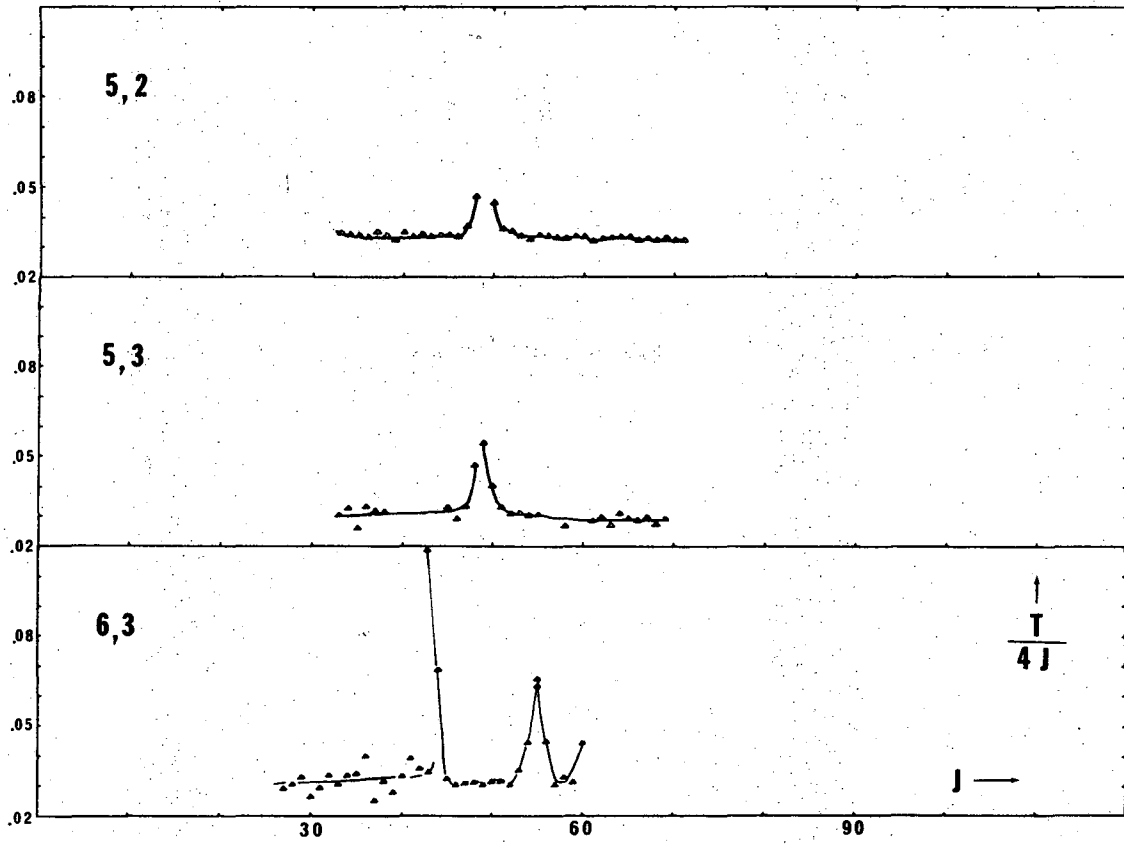
XBL 706-1171

Fig. 11.  $T/4J$  plotted vs  $J$  for the (3,0), (3,1), and (3,2) bands.



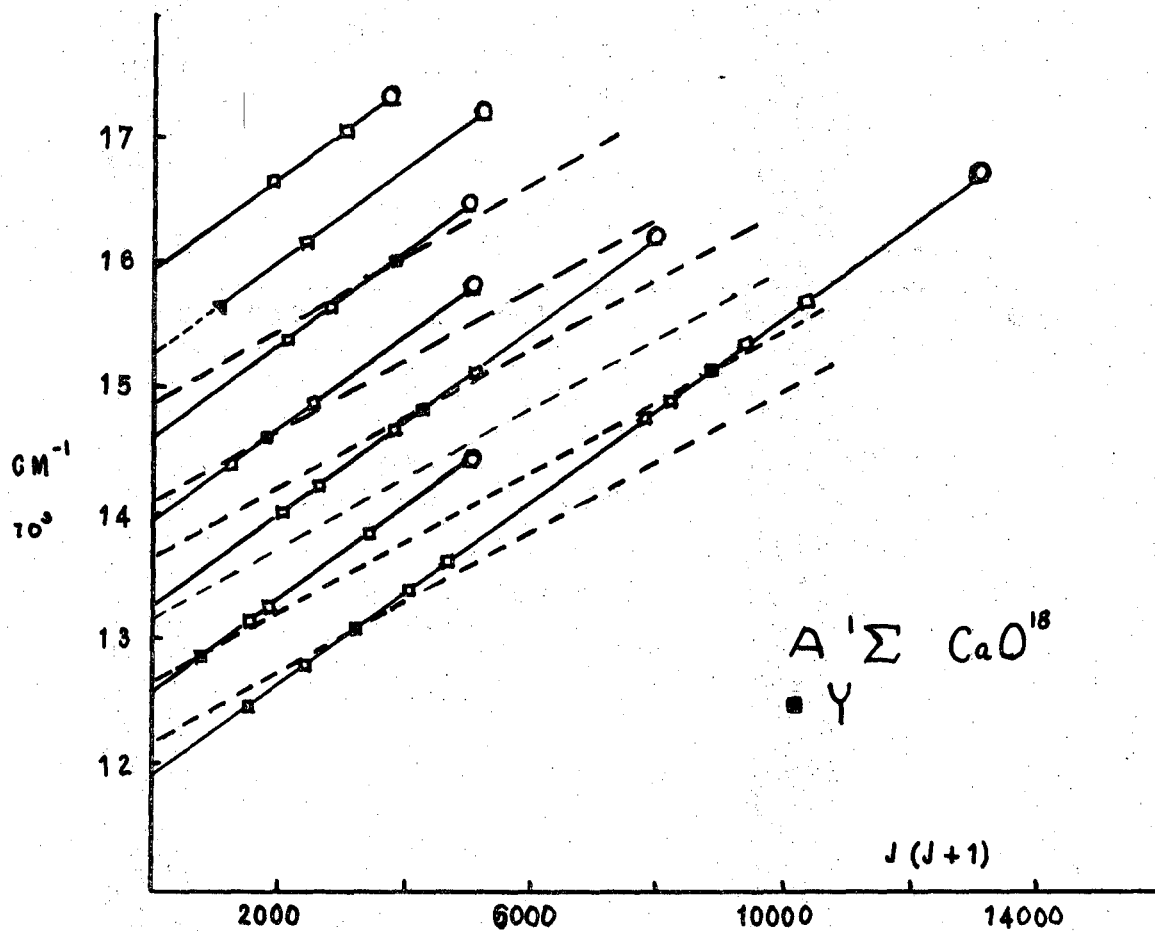
XBL 706-1173

Fig. 12.  $T/4J$  plotted against  $J$  for the (4,1) and (4,2) bands.



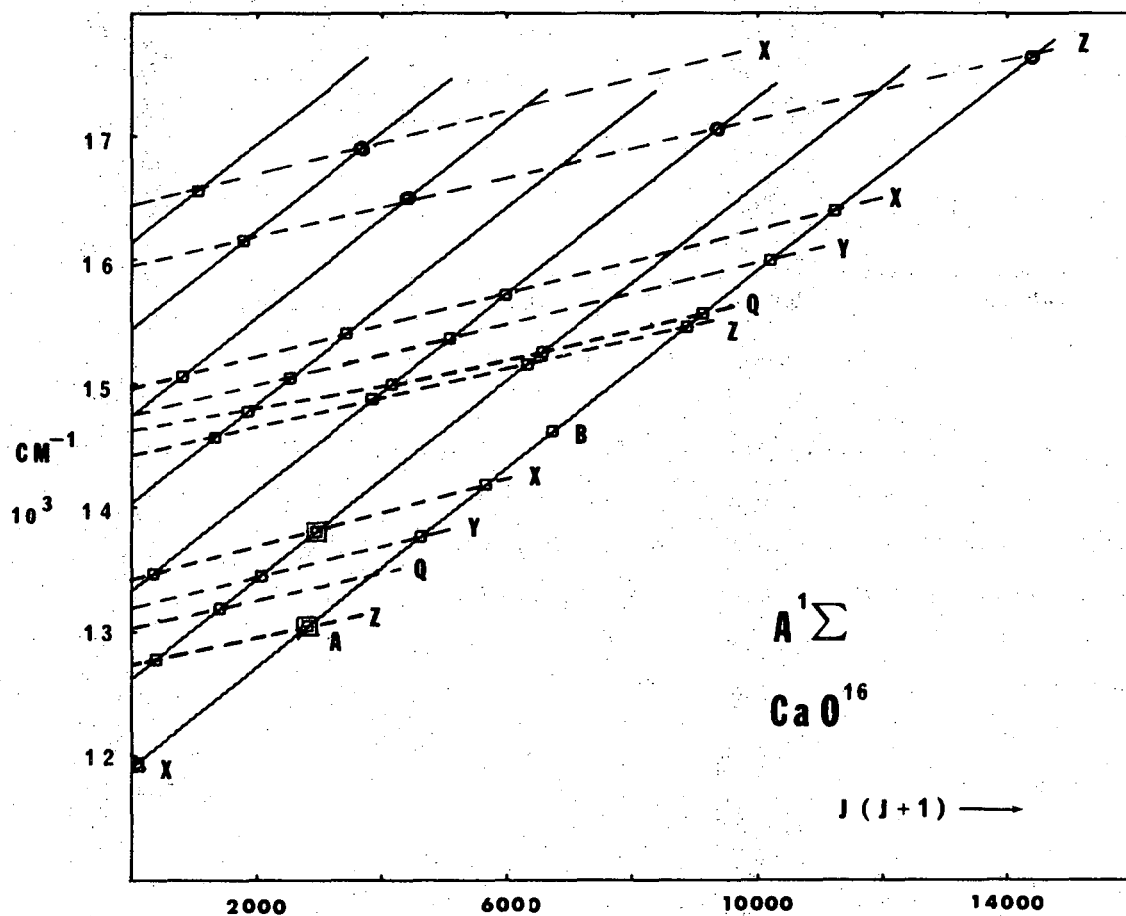
XBL 706-4172

Fig. 13.  $T/4J$  plotted against  $J$  for the (5,2), (5,3), and (6,3) bands.



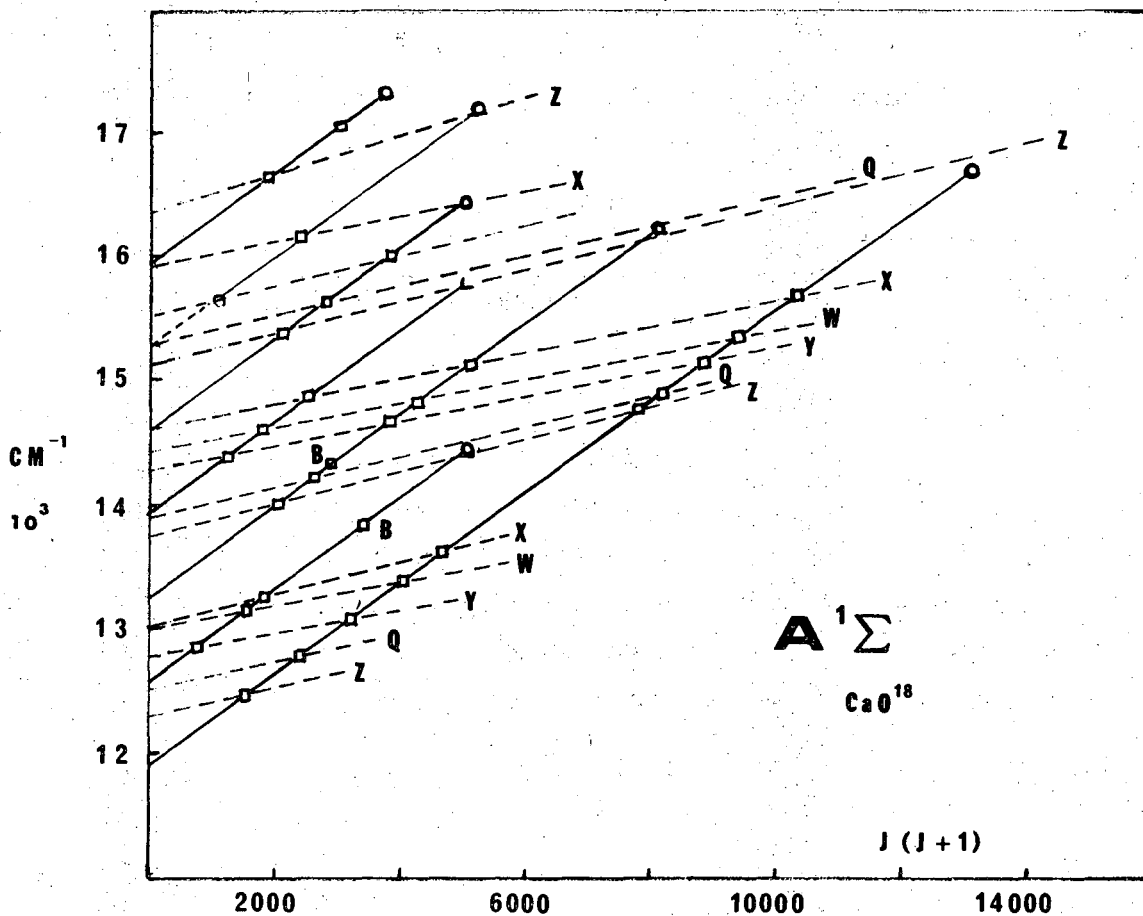
XBL 706-1162

Fig. 14. Plot of energy vs  $J(J+1)$ . The solid lines represent the first seven vibrational levels of the  $A'\Sigma$  state of  $CaO^{18}$  and the squares show the positions of the perturbations. The dashed lines indicate some vibrational levels of the  $Y^{18}$  perturbing state.



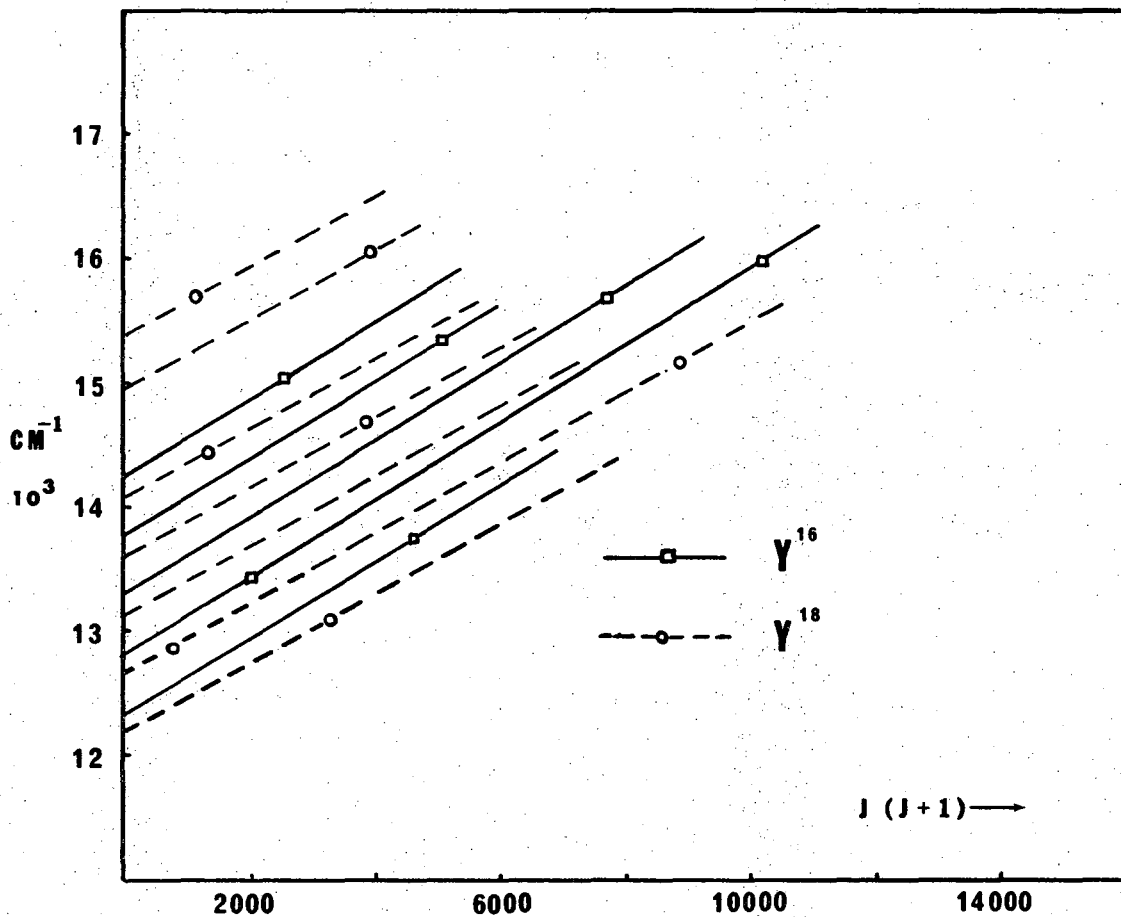
XBL 706-1164

Fig. 15. Plot of energy vs  $J(J+1)$ . The solid lines represent the vibrational levels of the  $A^1\Sigma$  state of  $\text{CaO}^{16}$ , the squares indicate perturbations, and the dashed lines connect perturbations arising from the same perturbing state. The zero of energy has been taken as the bottom of the  $X^1\Sigma$  potential curve.



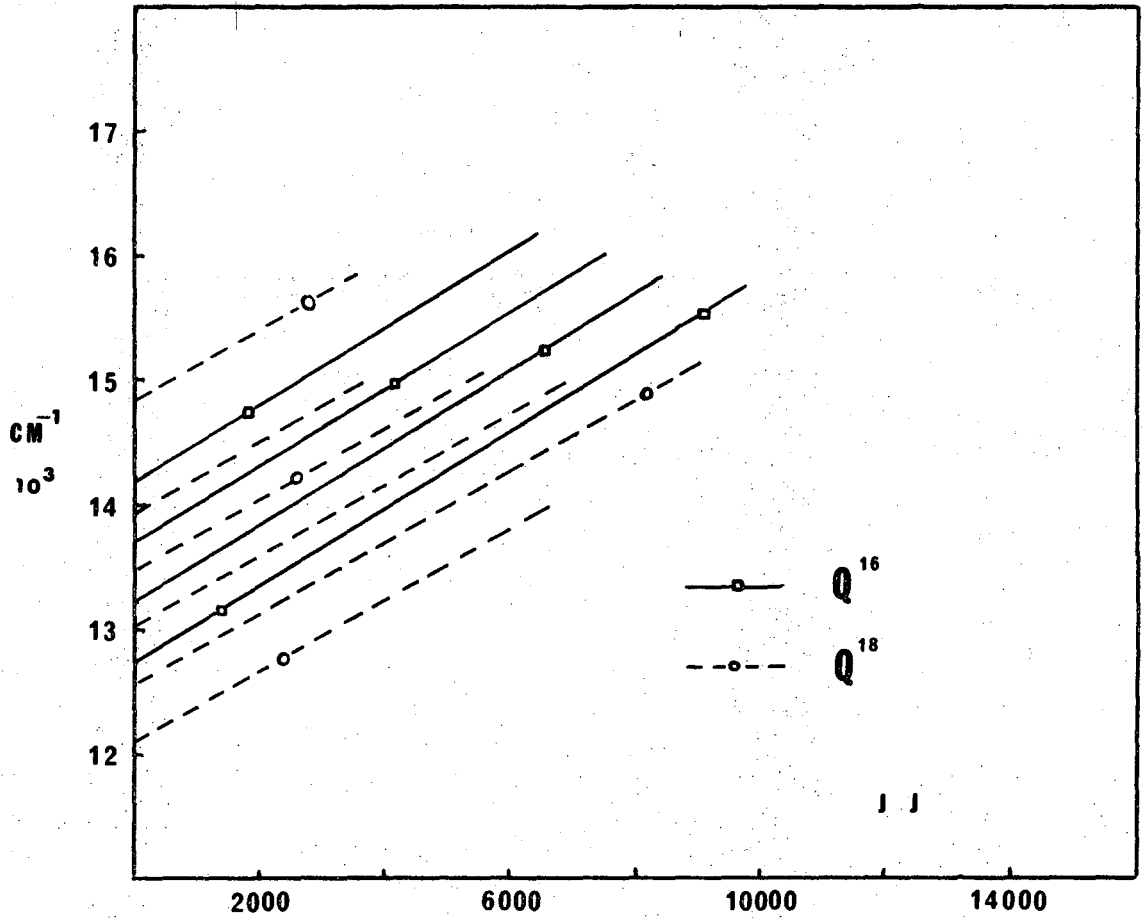
XBL 706-1167

Fig. 16. Plot of energy vs  $J(J+1)$ . The solid lines show the vibrational levels of the  $A^1\Sigma$  state of  $\text{CaO}^{18}$ , the squares indicate perturbations, and the dashed lines connect perturbations arising from the same perturbing state. The circles indicate the end of the analysis. The zero of energy is the bottom of the  $X^1\Sigma$  potential curve.



XBL 706-1169

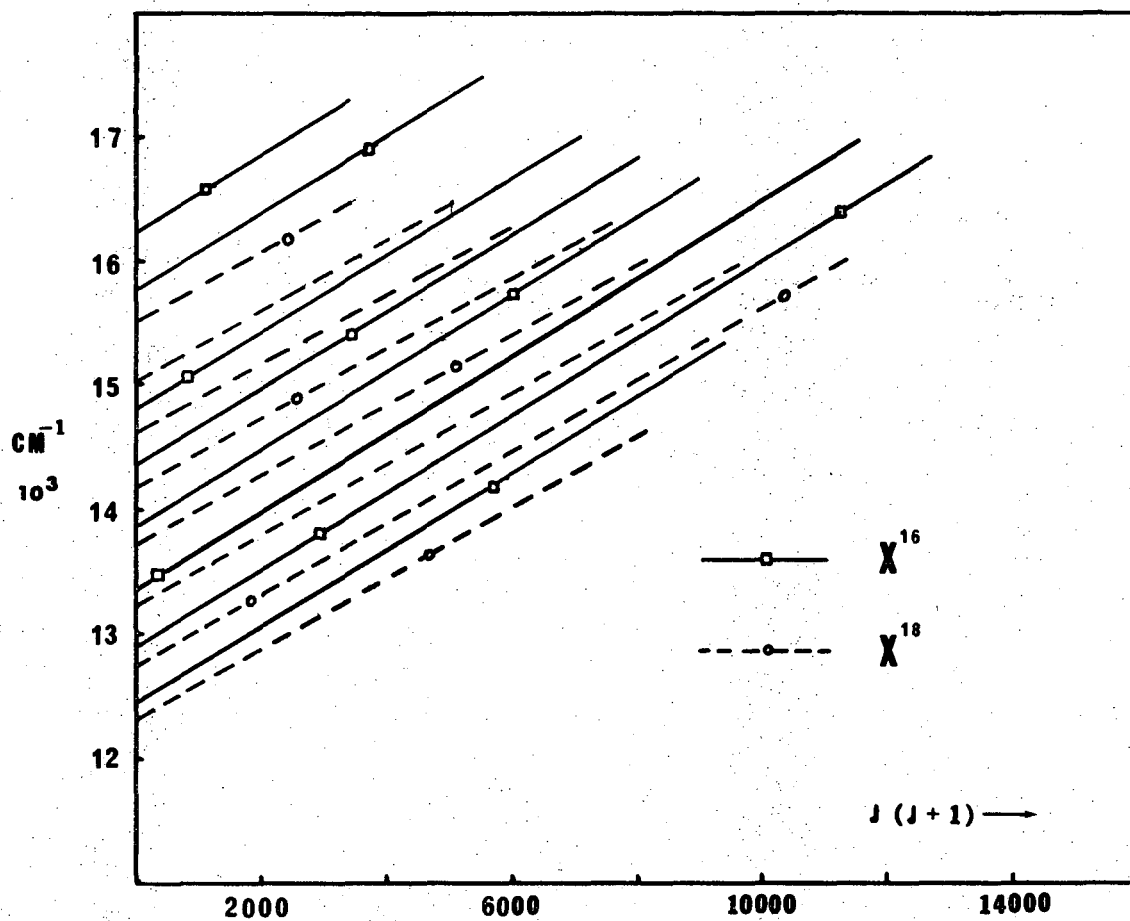
Fig. 17. Plot of energy vs  $J(J+1)$  showing the vibrational levels of the  $Y^{16}$  and  $Y^{18}$  perturbing states.



XBL 706-1166

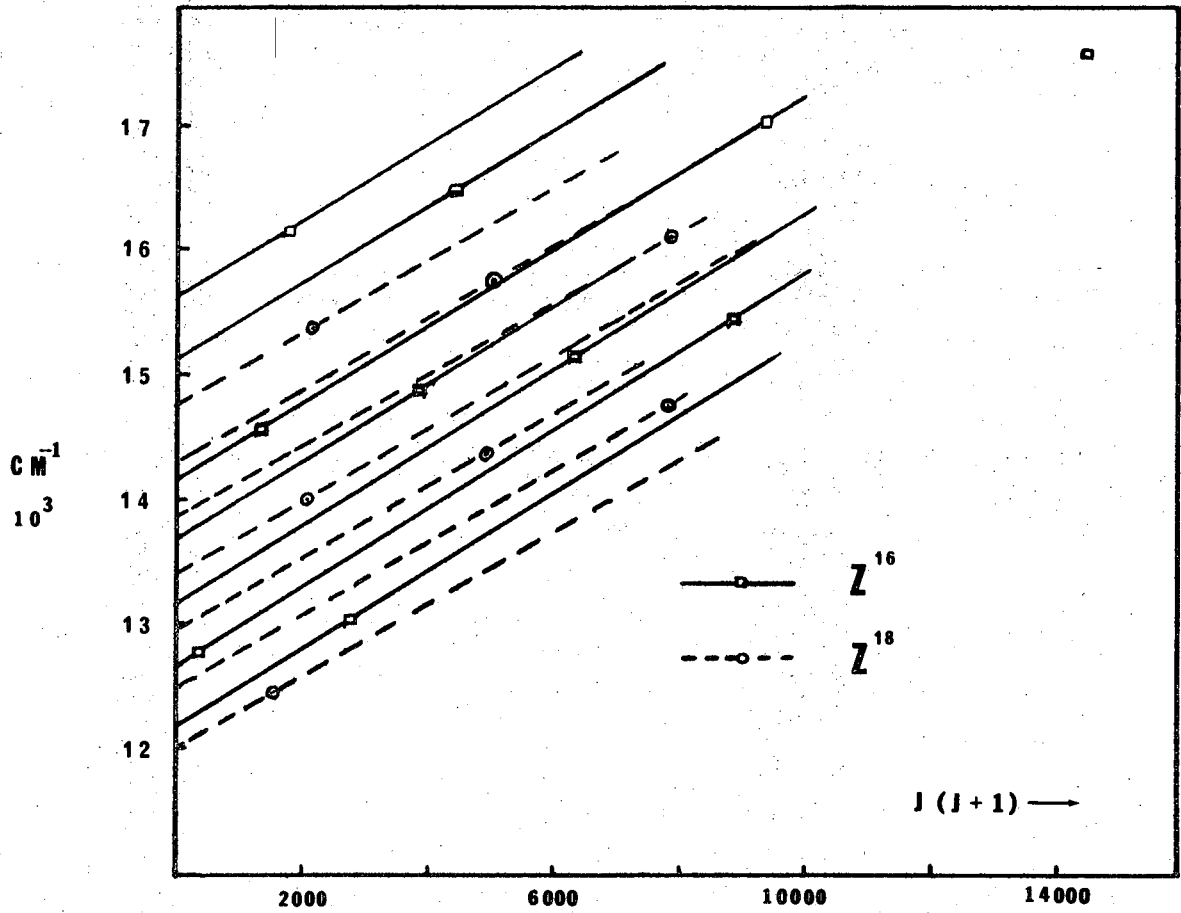
Fig. 18. Plot of energy vs  $J(J+1)$  showing the vibrational levels of the  $Q^{16}$  and  $Q^{18}$  perturbing states.





XBL 706-1165

Fig. 19. Plot of energy vs  $J(J+1)$  showing the vibrational levels of the  $X^{16}$  and  $X^{18}$  perturbing states.



XBL 706-1168

Fig. 20. Plot of energy vs  $J(J+1)$  showing the vibrational levels of the  $Z^{16}$  and  $Z^{18}$  perturbing states.

#### IV. CORRELATION OF THE PERTURBING STATES OF $\text{CaO}^{16}$ AND $\text{CaO}^{18}$

Hultin and Lagerqvist found six perturbing states in  $\text{CaO}^{16}$ , four called X, Y, Q and Z, having  $B_v \sim 0.33$  and  $\omega_e \sim 500$  and two, called A and B with  $B_v \sim 0.38$  and  $\omega_e \sim 600$ . In  $\text{CaO}^{18}$  six perturbing states have also been found. However five of them have  $B_v$  values of 0.30 (comparable to 0.33 in  $\text{CaO}^{16}$ ) and only one has a  $B_v$  value of .35 (comparable to 0.38 in  $\text{CaO}^{16}$ ). The  $A^{16}$  state is indicated by only one overlapped perturbation near a region where a Q perturbation is expected but not observed. It is possible then that the  $B_v$  value estimated for A is incorrect and that the set of  $Z^{16}$  perturbations are really due to two perturbing states with  $B_v \sim 0.33$ . It is even possible that the  $A^{16}$  perturbation is really due to the missing (Q-1) level since other states predicted in this region could shift it without interacting with  $A^1\Sigma$

(i.e. nine points of perturbation are possible between  $^3\Pi$  and  $^3\Sigma$  components in case (a),  $^1\Delta$  is probably present but invisible to a  $^1\Sigma$  state, etc. See Kovacs (1969) for a listing of possible interactions.) In this case the  $X^{16}$  or  $Y^{16}$  state may be due to two sets of perturbing levels.

First the two B-states,  $B^{16}$  and  $B^{18}$ , are correlated on the basis of their  $B_v$ -values. Using the  $X^1\Sigma$  constants given in Hultin and Lagerqvist (1950), the first thirty levels of that state were calculated for  $\text{CaO}^{16}$  and  $\text{CaO}^{18}$  and compared to the B state. The results were encouraging and so the constants found in Brewer and Hauge (1968) (which are based on higher experimental values and therefore should be better in the region of interest) were also tried. The comparison is shown in Table 7. There is good agreement between the experimental and

and calculated values of  $B_v$  found at the same energy. Since B is the only perturbing state with  $B_v$  and  $\Delta G$  values in this range, it is probably the  $X^1\Sigma$  state. Since the four vibrational levels found correlate to  $V = 18, 19$  in  $\text{CaO}^{16}$  and  $V = 20, 21$  in  $\text{CaO}^{18}$ , the isotopic shift cannot be directly calculated. Extrapolated values for  $V^{18} = 18, 19$  and  $V^{16} = 21$  give isotopic shifts quite close to the calculated ones and a vibrational numbering which is only off by one quantum number. The  $V^{18} = 20$  level appears to be perturbed.

The  $X^{18}, Y^{18}, Z^{18}, Q^{18}, W^{18}$ , and  $X^{16}, Y^{16}, Z^{16}, Q^{16}$  states will now be considered. The energy levels of  $\text{CaO}^{18}$  will be lower in energy than the corresponding levels in  $\text{CaO}^{16}$ . See Fig. 17 for example. If one compares the  $Y^{16}$  and  $Y^{18}$  electronic states, it is possible for  $(Y^{16} + 3)$  to have the same vibrational quantum number as  $(Y^{18})$ ,  $(Y^{18} + 1)$ , or  $(Y^{18} + 2)$ . In the following discussion, only the first two sets of levels lower in energy will be considered (i.e.,  $(Y^{16} + 1) \rightarrow (Y^{18})$ ,  $(Y^{16} + 2) \rightarrow (Y^{18} + 1)$ ,  $(Y^{16} + 3) \rightarrow (Y^{18} + 2)$ , etc. and  $(Y^{16} + 1) \rightarrow (Y^{18} + 1)$ ,  $(Y^{16} + 2) \rightarrow (Y^{18} + 2)$ ,  $(Y^{16} + 3) \rightarrow (Y^{18} + 3)$ , etc.). The sets at lower energies (i.e.  $(Y^{16} + 2) \rightarrow (Y^{18})$  ..... or  $(Y^{16} + 3) \rightarrow (Y^{18})$  ... etc.) can also form possible combinations, however (since the isotopic shifts would be larger in this case) they would put the origins of the perturbing states at least  $8000 \text{ cm}^{-1}$  below  $X^1\Sigma$  state. It is more important to check if these states are above or near  $X^1\Sigma$  in order to determine the ground state of  $\text{CaO}$ . Also the larger the shifts, the harder it is to extrapolate to a meaningful  $v$ -value. It is important although to remember that lower origins are possible.

Since we have five  $\text{CaO}^{18}$  states, four  $\text{CaO}^{16}$  states, and two

possibilities for each combination, there are forty ways to correlate the nine states. The comparison of  $Y^{16}$  with the next lowest set of  $Y^{18}$  levels will be called ( $Y^{16}Y^{18}$ ); the comparison with the second lowest set ( $Y^{16}Y^{18}_d$ ). The shifts calculated for all forty combinations are listed in Table A-1.

Equation (1) shows the relationship between  $v$ ,  $\omega_e x_e$ ,  $\omega_e$  and the energy shifts. If the shifts are plotted vs  $v$ , the curve should intersect the x-axis at  $v = -\frac{1}{2}$ . At low  $v$  the slope is  $\sim (\omega_e/(1-\rho))$ ; at higher  $v$ , the slope decreases in response to the  $\omega_e x_e$  terms. The vibrational quantum numbers for any of the forty combinations mentioned can be obtained by plotting the shifts vs a relative  $v$  and extrapolating to zero. Figure 24 shows sample plots of the shift vs  $v$  for various values of  $\omega_e x_e$  and  $\omega_e$ . Similar plots were used as aids in extrapolating the experimental values. The plots for all the  $Y^{18}$  combinations are shown in Fig. 21.

Of the 40 combinations plotted, 28 were rejected. Table A-2 shows the comparisons. One of three reasons is given for rejecting a correlation.

(1)  $v_p$  too high. Same discussion as above applies here. These combinations are possible, but correlations giving states above  $X^1\Sigma$  should be considered first.

(2) Scattered. Trends in energy away from the calculated shape of the curve (Fig. 24) were used as criteria, rather than one or two points being out of line. For example, an increase in slope at higher  $v$ -values (concave) would not be acceptable.

(3)  $\omega_e x_e$  (a-b).  $\omega_e$  and  $\omega_e x_e$  values can be obtained from the shift vs  $v$ -plot and also from the energy separations of the vibrational

levels and the v-quantum numbers. If the values from these two methods do not agree, that correlation is rejected.

An example can best clarify this method. Consider the ( $Q^{16} Y^{18}$ ) correlation. Various combinations of  $\omega_e$  and  $\omega_e x_e$  can fit the points. The lowest possible  $\omega_e$  ( $\omega_e x_e = 0$ ) value from the shift vs v plot can be obtained from the slope divided by  $(1-\rho)$ . (A higher  $\omega_e$  is possible since  $\omega_e x_e$  can decrease the slope, however a lower one is not for the same reason.  $\omega_e x_e$  would only decrease the slope further.) In this case  $\omega_e = 675$ . The highest  $\omega_e x_e$  which could be used is under ten. The quantum number for the  $Q^{16}$  level is  $v = 2$ . The difference between the  $v = 2$  and  $v = 3$  levels of  $Q^{16}$  is calculated from these constants as follows:

$$\begin{aligned} G(3.2) &= \omega_e(3.5) - \omega_e x_e(3.5)^2 - \omega_2(2.5) + \omega_e x_e(2.5)^2 \\ &= \omega_e - 6 \omega_e x_e = 675 - 6(10) = 615 \end{aligned}$$

The difference between the ( $Q^{16}$ ) and ( $Q^{16}+1$ ) levels is 500 so this correlation is wrong.  $\omega_e x_e$  would have to be 29 instead of 10 in order for  $\omega_e$  to equal 675. A higher  $\omega_e$  value would make  $G(3-2)$  still larger without substantially increasing the needed  $\omega_e x_e$  value. The comment for this correlation in Table A-2 is  $\omega_e x_e(10-29)$  where 10 and 29 are the  $\omega_e x_e$  values needed for the two methods.

Table 8(a) shows the 12 possible correlations left. If it is assumed that all the  $CaO^{18}$  states are used just once, then the ( $X^{16} X^{18} d$ ) correlation is correct. The  $Q^{16}$  state has a small matrix element in comparison to the  $X^{16}$ ,  $Y^{16}$ , and  $Z^{16}$  states. It is unlikely to be correlated to more than one  $CaO^{18}$  state.  $Y^{18}$  can be combined with either  $Y^{16}$  or  $Q^{16}$ . The  $Y^{18}$  perturbations are much stronger than

those of  $Q^{16}$  so the  $(Y^{18}Y^{16})$  correlation appears to be the correct one. The  $Q^{16}$  and  $Z^{16}$  states both go to  $Q^{18}$  and  $Z^{18}$ . This is reasonable since the  $Q$  and  $Z$  perturbations are very close to each other in both isotopes. The  $Z$  perturbations are much stronger in both cases, which indicates combinations of  $(Q^{16}Q^{18}d)$  and  $(Z^{16}Z^{18}d)$ . At this point all the  $CaO^{16}$  states and all the  $CaO^{18}$  states except  $W^{18}$  have been used. The three possible combinations using  $W^{18}$  are shown in Table 8(b) by dashed lines. Either  $(X^{16}W^{18}d)$  or  $(Y^{16}W^{18}d)$  would put  $W^{18}$  below  $X^{18}\Sigma$  along with  $Q^{18}$ ,  $Z^{18}$  and  $X^{18}$ . The  $(Y^{16}W)$  correlation would put  $W^{18}$  at  $\sim 11080 \text{ cm}^{-1}$ . The two possibilities for  $W^{18}$  are shown as dashed lines in Fig. 22. Among the states predicted to be in this region:  $^3\Pi$ ,  $^3\Sigma^-$ ,  $^1\Pi$ ,  $^1\Delta$ , the following states or substates can perturb a  $^1\Sigma^+$ :  $^3\Pi_1$ ,  $^3\Pi_0$ ,  $^1\Pi$ ,  $^3\Sigma_{J+1}^-$ ,  $^3\Sigma_{J-1}^-$ . Assuming Hund's case (a) the five states should be grouped as two, two, one, since four of them are predicted to be substates of triplet electronic states. If  $W$  and  $Y$  are components of a triplet, the splitting would be on the order of  $3000 \text{ cm}^{-1}$ . This seems too large. (The doublet splitting in  $AsO$ , a much heavier molecule, is  $1025 \text{ cm}^{-1}$ . The splitting here would not be expected to be larger.) If  $(Y^{16}W^{18})$  is not true, then  $W$  would be found at approximately  $-2500 \text{ cm}^{-1}$  relative to  $X^{18}\Sigma$ . A summary of the perturbing states and their constants is found in Table 9 for the best correlations.

If any of the above assumptions are wrong, other sets of correlations become possible. The assumptions are:

(1) There is a one to one correlation between the states perturbing  $A^{18}\Sigma$  in  $CaO^{16}$  and  $CaO^{18}$ .

(2) The perturbing states are  $X^{18}\Sigma$ ,  $^1\Pi$ ,  $^3\Pi_0$ ,  $^3\Pi_1$ ,  $^3\Sigma_{J+1}$ ,

and  ${}^3\Sigma^-_{J-1}$ . These states are predicted to be low-lying by analogy to the isoelectronic  $C_2$  states (Brewer, 1962), and are able to perturb a  ${}^1\Sigma^+$  (Kovacs, 1969). A recent paper (Carlson, et al., 1970) suggests a low-lying  ${}^3\Sigma^+$  state. The predicted  ${}^1\Delta$  also would not perturb a  ${}^1\Sigma$ . Perturbations between a  ${}^3\Sigma^+$  and a  ${}^1\Sigma^+$  state are predicted to be very weak (Kovacs, 1969) and so it would be difficult to find an indication of  ${}^3\Sigma^+$  in this study. Also six perturbing states and substates are predicted considering just  ${}^3\Pi$ ,  ${}^3\Sigma$ ,  ${}^1\Pi$ , and  $X^1\Sigma$  perturbing states and six are found. If the  ${}^3\Sigma^+$  state is included, one of the above states must be discredited, which would make it difficult to account for all of the sets of perturbations found. Two sets of perturbations are expected from both the  ${}^3\Pi$  and the  ${}^3\Sigma$  states, the  $X^1\Sigma$  state is well assigned to the B-perturbing state, and the  ${}^1\Pi$  state has low-lying counterparts in  $C_2$ , BeO, and MgO as well as coming from the same molecular orbital configuration as the  ${}^3\Pi$  state. So it would be hard to re-assign just one of the perturbing sets of perturbations to a  ${}^3\Sigma^+$ . The two weak sets, B and Q, are easily correlated with  $X^1\Sigma$  and  ${}^3\Pi_1$ . The perturbation at  $v' = 1, J = 57.9$ , which is assigned to the  $B^{18}$  state, is out of line however from the other B perturbations and might be due to a low  ${}^3\Sigma^+$  state.

(3) The origin of the perturbing states is not below  $8000 \text{ cm}^{-1}$ . It is possible that this assumption is false and that lower origins exist. However since there are too many correlations giving lower values to be able to pick out a consistent set and because of the difficulty in extrapolating larger shifts, it is not possible to come to any definite conclusions.



(4) The  $\omega_e x_e$  and the scattering criteria are assumed to be correct. There are at least three perturbing states below  $X^1\Sigma$  if they are true.

(5) The splitting between  $^3\Pi_0$  and  $^3\Pi_1$  is less than  $1000 \text{ cm}^{-1}$ . This is based on a comparison of splittings found in other molecules (i.e. AsO, PO).

(6) The size of a perturbation will not change drastically with a change of isotope, i.e.  $Q^{16} \rightarrow Q^{18}$ .

All the assumptions appear to be reasonable. Also a supporting piece of evidence for the assignment in Table 9 is found in a low-temperature matrix isolation study of CaO (Wang, 1969). Bands were found starting at  $20,367 \text{ cm}^{-1}$  and identified as CaO by their isotope shift ( $\text{CaO}^{18} - \text{CaO}^{16}$ ). The transition does not correspond to any known singlet transition and therefore indicates the possibility of a low-lying triplet state. It has been included in Fig. 23.

Also the splittings between states coming from the same molecular orbital configuration can be compared. For the ten-electron molecules ( $\text{N}_2$ , AlCl, etc.) the splittings between the  $^3\Pi$  and  $^1\Pi$  states from the  $X^4\Sigma\Pi^4\Pi^4$  configuration are between  $6000 - 16000 \text{ cm}^{-1}$  for a wide range of molecular weights (Brewer, 1962). For the eight electron molecules the splitting between the  $^1\Pi$  and  $^3\Pi$  states of the  $^2X^2\Sigma\Pi^3$  configuration is  $12000 \text{ cm}^{-1}$  for CaO and  $7600 \text{ cm}^{-1}$  for  $\text{C}_2$ . This fits in quite well with our expectations from the ten-electron molecule case.

Table 7. Comparison of the B state and  $X^1\Sigma$

B State				$X^1\Sigma$ Calculated				
	$\nu$	$G(\nu)_{-1}$ cm	$\Delta G$	$B\nu$	$\nu$	$G(\nu)_{-1}$ cm	$\Delta G$	$B\nu$
$\text{CaO}^{16}$	B	12113	581	.381	18	12039	580	.382
	B + 1	12694			19	12619		
$\text{CaO}^{18}$	B	12650	672	~.35	20	12716	575	.348
	B + 1	13322			21	13268		

Table 8. Correlations Between the Perturbing States of  $\text{CaO}^{18}$  and  $\text{CaO}^{16}$

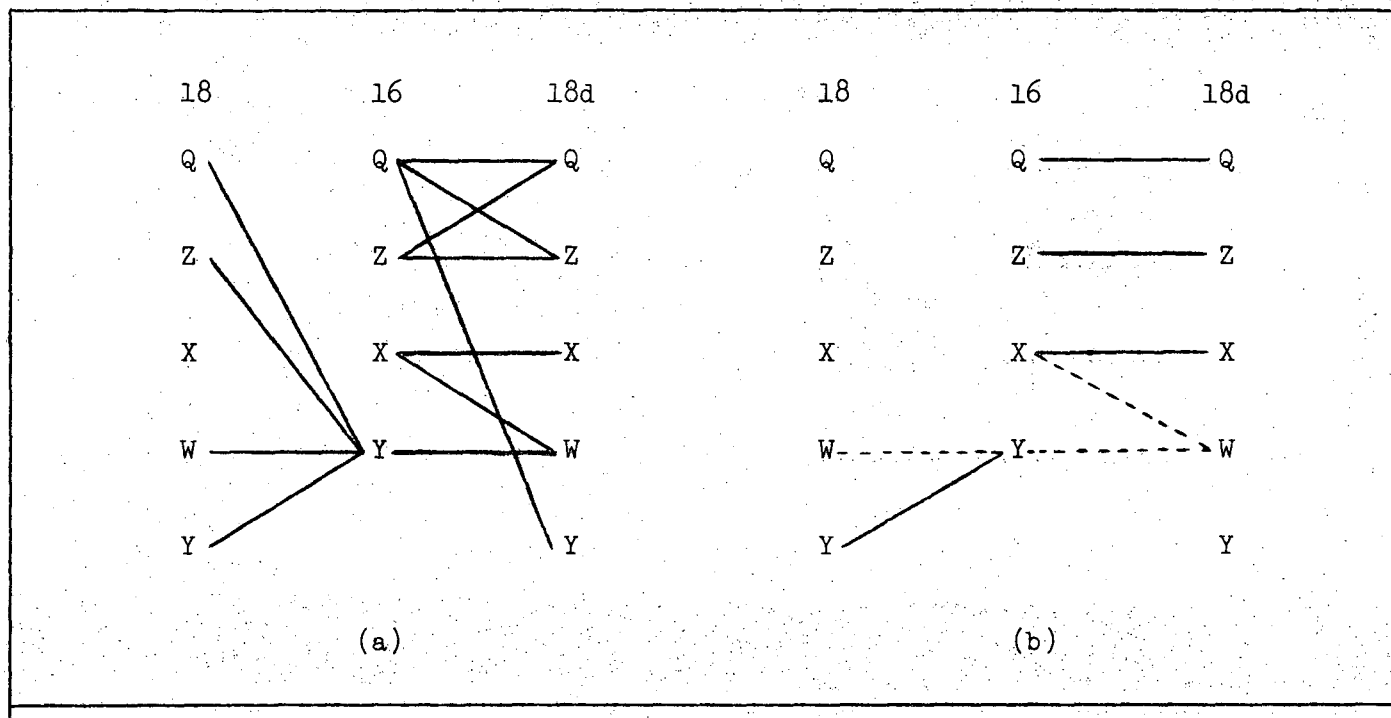
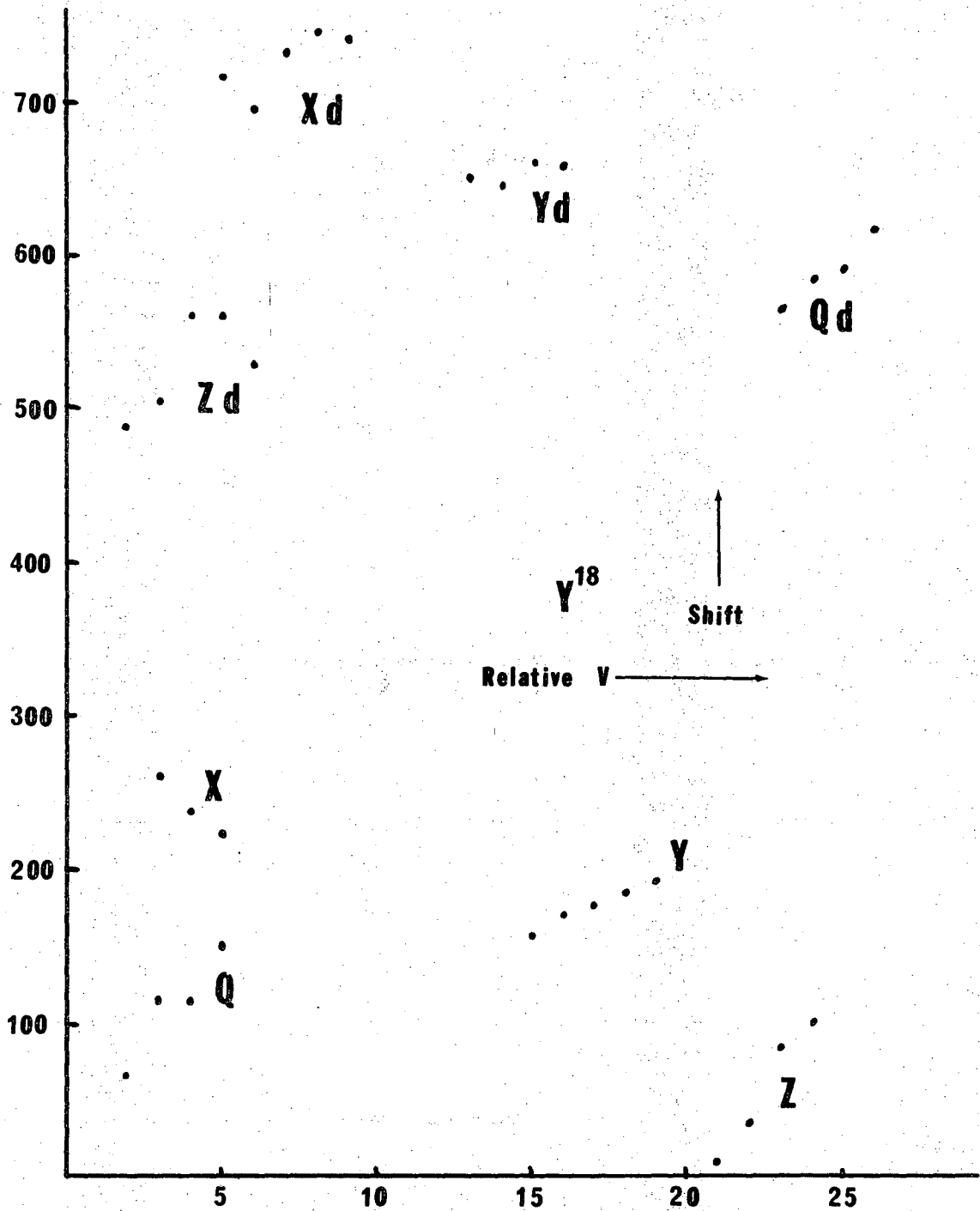


Table 9. Summary of Constants

State	$T_e$	$\omega_e$	$\omega_e x_e$	$B_e$	$\alpha_e$	$D(\times 10^{-6})$	$r_e \times 10^8$ cm
$A^1\Sigma$	11554.8	716	1.6	.4063	.0014	.54	1.906
$Y(^1\Pi?)$	8080	490	~1.5	~.31			
$X^1\Sigma$	0	732.1	4.81	.4444	.0033	.658	1.822
$\left. \begin{array}{l} X \\ W \\ Z \\ Q \end{array} \right\} \begin{array}{l} 3\Pi \\ 3\Sigma \end{array} ?$	~3000	< 730					

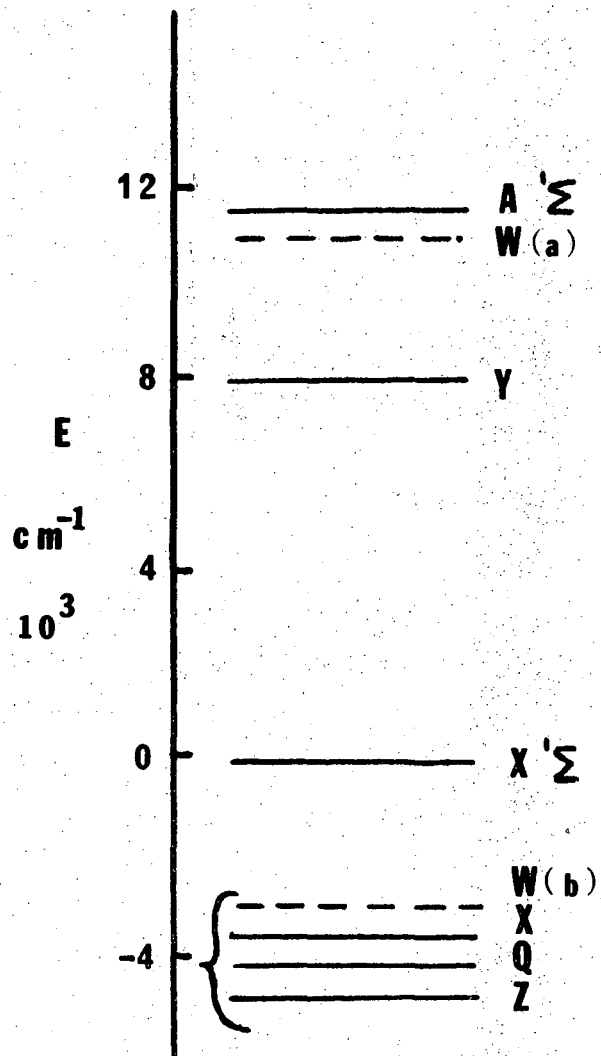
Table 10. Predicted and Observed Transitions in CaO, 3500 - 12,000 Å

Transition	cm <sup>-1</sup>	Å	Reference
A <sup>1</sup> Σ - X <sup>1</sup> Σ	11554.8	8660	Hultin and Lagerqvist, 1950
B <sup>1</sup> Π - <sup>1</sup> Π	17909	5580	
B <sup>1</sup> Π - <sup>1</sup> Δ	~22000	~8300	
B <sup>1</sup> Π - A <sup>1</sup> Σ	24434	4100	
B <sup>1</sup> Π - X <sup>1</sup> Σ	25989	3848	Lagerqvist, 1954
C <sup>1</sup> Σ - <sup>1</sup> Π	20776	4810	
C <sup>1</sup> Σ - X <sup>1</sup> Σ	28855	3465	Lagerqvist, 1954
<sup>3</sup> Π - <sup>3</sup> Π or <sup>3</sup> Σ	~21000	4760	Wang, 1969



XBL 706-1170

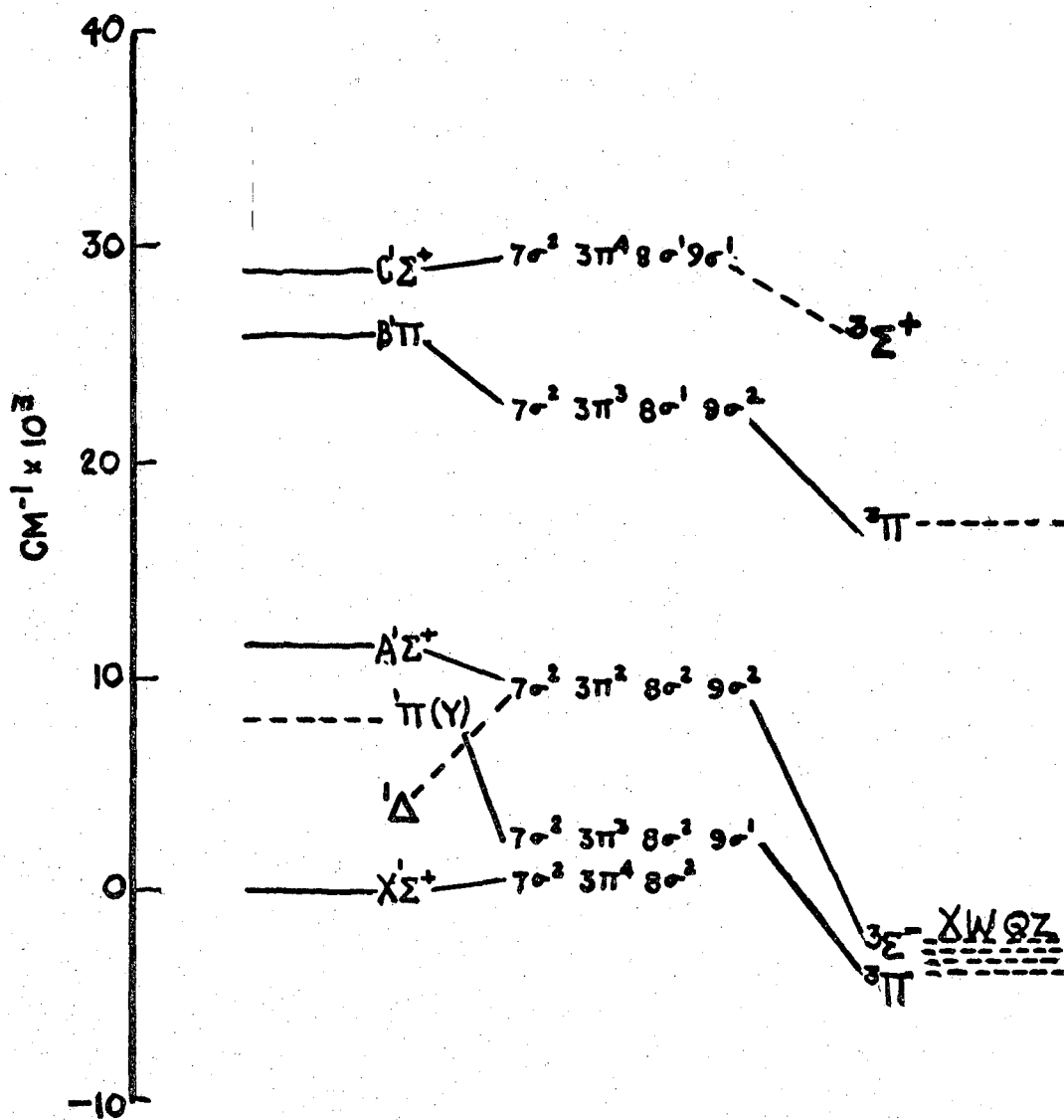
Fig. 21. Plot of the shift vs a relative vibrational numbering for all the correlations involving  $Y^{18}$ .



XBL 707-1377

Fig. 22. Relative energy scale for the perturbed and perturbing states.

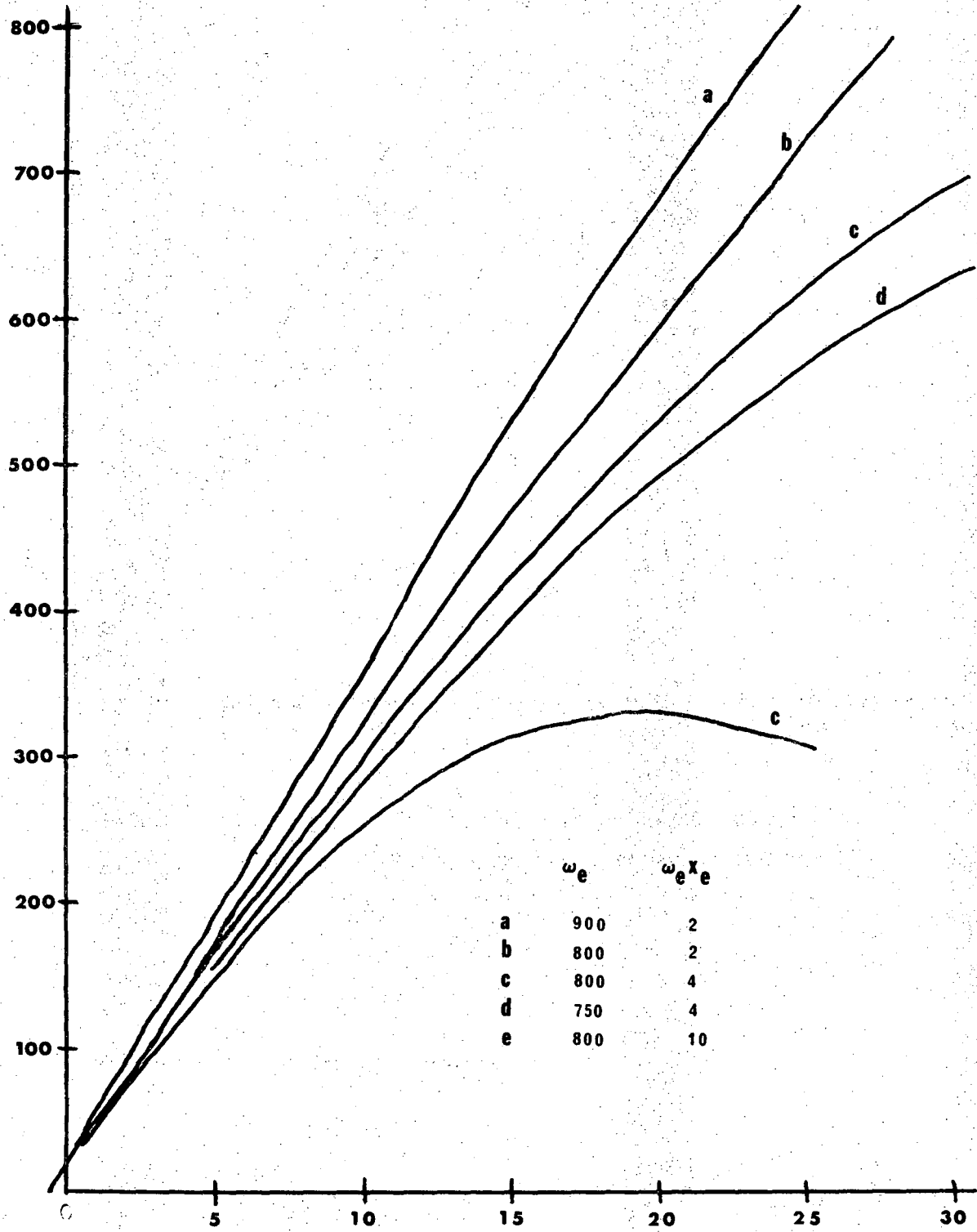
### ENERGY LEVELS OF CaO



XBL 707-1374

Fig. 23. Low-lying energy levels of CaO.





XBL 707-1375

Fig. 24. Calculated plots of the vibrational isotopic shift vs the vibrational quantum number  $V$  for several combinations of  $\omega_e$  and  $\omega_e x_e$ .

## V. CONCLUSION

The above comparison of  $\text{CaO}^{16}$  and  $\text{CaO}^{18}$  perturbations gives a good qualitative description of some of the low-lying electronic states of  $\text{CaO}$  and shows that the  $X^1\Sigma$  is not the ground state. It is hard to determine exact origins for X, Q, Z, and W because of the long extrapolations involved. The value given for all four is  $-3000 \text{ cm}^{-1} \pm 2000 \text{ cm}^{-1}$ . The Y state has a much shorter extrapolation and is found to be at  $8080 \pm 500 \text{ cm}^{-1}$ . Since the lowest  $^1\Sigma^+$  state in  $\text{C}_2$ ,  $\text{BeO}$ , and  $\text{MgO}$  has the largest  $\omega_e$  value, the  $\omega_e$  value for the X, Q, Z, Y, and W states is expected to be below 730.

The B state has been assigned to  $X^1\Sigma$ . However it is difficult to assign W, X, Q, Z and Y to specific states. Y should be a  $^1\Pi$  since it stands by itself and the other possible singlet,  $^1\Delta$ , cannot perturb a  $^1\Sigma$ . Hultin and Lagerqvist (1950) indicate that X may be the  $^3\Pi_0$  substate since its matrix element is independent of J. The Q perturbations are small and could be due to a  $^3\Pi_1 - ^1\Sigma^+$  interaction which has a small matrix element. That leaves W and Z to be assigned to  $^3\Sigma_{J+1}$ , and  $^3\Sigma_{J-1}$ .

It would be useful to determine the spectroscopic constants and origins of these states more accurately since the low-lying states of a molecule are needed for thermochemical calculations. Further experiments might include searching for calculated transitions (Table 10). For example, the  $B^1\Pi - Y$  transition is predicted to be at  $\sim 5580 \text{ \AA}$ , quite close to a strong, unanalyzed system at  $5555 \text{ \AA}$ . Another possibility, the molecular beam electric resonance technique used to measure the rotational constants of the ground state of  $\text{BaO}$  (Wharton and Klemperer, 1963), is probably not practical for  $\text{CaO}$  because of the difficulty of

obtaining a CaO beam. Matrix fluorescence experiments could give the vibrational constants of the lower state of the transition found by Wang (1969). Electron spin resonance might also be done in a matrix to determine which is the lowest state,  $^3\Pi$  or  $^3\Sigma$  (Kasai, 1968). Also the perturbations of another isotopic molecule, such as  $\text{Ca}^{44}\text{O}^{16}$ , could be analyzed to confirm the correlations made in this paper.

APPENDIX A

COMPARISON OF  $\text{CaO}^{16}$  AND  $\text{CaO}^{18}$

Table A-1. Shifts Between the Perturbing Vibrational Levels of  $\text{CaO}^{18}$  and  $\text{CaO}^{16}$

$Z^{16}$	-5	490	360	855	65	560	390	885	155	650
	10	505	425	950	95	590	435	960	180	675
	35	560	470	945	120	645	490	965	210	735
	85	560	450	885	195	670	510	940	275	750
	90	530	430	965	215	650	485	1020	275	710
			520				605	1115	290	825
		625				690		370	880	
		435						435		
$Q^{16}$	85	565	5	435	170	635	15	465	255	725
	115	585	25	505	200	670	45	515	290	755
	115	590	5	500	225	675	65	520	305	765
	150	615	50	505	270	725	105	565	330	805
$Y^{16}$	155	650	25	520	225	720	55	550	315	810
	170	645	90	565	255	730	100	575	340	815
	175	660	85	570	260	745	105	590	350	835
	185	655	75	545	295	765	135	605	375	845
	190		90		310		145		370	
$X^{16}$	260	715	130	585	330	785	160	615	420	875
	235	695	155	615	320	780	165	625	405	865
	225	730	135	640	310	815	155	660	400	905
	245	745	145	635	365	855	205	695	445	935
		740	180	640	400	860	235	695	460	
			195	675			280	778	500	
			270	755			340			
			285	740						
	$Y^{18}$	$Y^{18}_d$	$X^{18}$	$X^{18}_d$	$Q^{18}$	$Q^{18}_d$	$W^{18}$	$W^{18}_d$	$Z^{18}$	$Z^{18}_d$

Table A-2. Comparison of Perturbing States:  $\text{CaO}^{16}$ ,  $\text{CaO}^{18}$

	$X^{16}$	$Y^{16}$	$Q^{16}$	$Z^{16}$
$Y^{18}$	scattered	maybe	wexe (10-29)	wexe (3-177)
$Y^{18}_d$	Vp too high	Vp too high	maybe	scattering
$X^{18}$	scattered (concave)	scattered	scattered	scattered
$X^{18}_d$	maybe	scattered	scattered	Vp too high
$Q^{18}$	scattered	maybe	wexe (29-5)	wexe(1-100)
$Q^{18}_d$	Vp too high	scattered (concave)	maybe	maybe
$W^{18}$	scattered	maybe	wexe (10-125)	wexe(2-29)
$W^{18}_d$	maybe	maybe	wexe(1,15)	Vp too high
$Z^{18}$	scattered	maybe	wexe(6,30)	wexe(2-50)
$Z^{18}_d$	Vp too high	Vp too high	maybe	maybe

APPENDIX B

This appendix contains the listings for the computer programs used to analyze the data. They were written for operation on the CDC computers at the Lawrence Radiation Laboratory at Berkeley. The program language is CDC's Chippewa Fortran which is nearly identical to Fortran IV.

1. STAND

Program STAND uses the measured spectral standard lines to calculate the wavelength and energy ( $\text{cm}^{-1}$ ) for all the measured lines. Both the standard Th-lines and the CaO molecular lines were measured and recorded one to a card by a semi-automatic comparator (lent by Dr. John Phillips, University of California at Berkeley, Astronomy Department). Each card contained the relative position of the line, its relative intensity, and a code number indicating the type of line (standard, atomic, molecular, etc.)

The data deck consists of:

(a) TOY (I) indicates whether the measured line lies between 0-100 mm, 100-200 mm, or 200-300 mm on the measuring scale. The first data card reads -J1 with a 3A1 format.

(b) N, NLAST, and NU (format 3I5) where

N = order of fit +1

NU = number of standard lines

NLAST = the final value of N

(c) ETOL (format 8F10.5) is the tolerable error in calculating standard lines,

(d) SHIFT (format F10.2) relates the standard lines to the unknown lines. It is usually zero.

(e) Assigned standard line values YY(I) (format F10.3).

(f) Deck of measured lines, with all the standard lines first in the same order as their assigned values in (e).

(g) Blank card.

When N equals NLAST, one card is punched for each measured line with its wavelength, energy ( $\text{cm}^{-1}$ ), relative intensity.

This program was written by David Green and Joel Tellinghuisen.



```
PROGRAM STAND (INPUT,OUTPUT,PUNCH)
C STAND TAKES MEASURED SPECTRAL STANDARD LINES AND CALCULATES
C WAVELENGTH AND ENERGY (CM(-1)) FOR ALL MEASURED LINES
  DIMENSION TOY(3),BOY(1000),X(1000),Y(1000),STR (1000)
  DIMENSION AA(10,10),YINV(1000), YY(200), B(10),DE(200)
  DIMENSION INCA(1000)
  DIMENSION COM(200), VW(1000)
  DIMENSION XW(200),YYW(200)
  READ 800,TOY(1),TOY(2),TOY(3)
800  FORMAT (3A1)
801  READ1, N,NLAST,NU
  1  FORMAT (3I5)
  PUN=0.0
  NSUB=N-NLAST
  IF (NSUB.EQ.0) PUN=1.0
  IF (NU.EQ.0) GO TO 850
  NU1 = NU + 1
C N=ORDER OF FIT +1,NU=NO. OF STANDARD LINES,NTOT=TOTAL NO. OF LINES
C NLAST IS THE FINAL VALUE OF N
C ETOL IS THE TOLERABLE ERROR IN CALCULATION OF STANDARD LINES
  READ 41, ETOL
  41  FORMAT(8F10.5)
  READ 855, SHIFT
855  FORMAT (F10.2)
  2  FORMAT (F10.1,F5.0)
  89  FORMAT (40F2.0)
  235  FORMAT (F10.1)
C YY ARE THE STANDARD WAVE-LENGTHS
  READ 40, (YY(I),I=1,NU)
  40  FORMAT (F10.3)
  I=1
803  READ 42, INCA(I),BOY(I),X(I),STR(I)
  42  FORMAT(I6,5X,A1,F6.3,F6.1)
  PET =X(I)
  I=I+1
  IF(PET.NE.0.0) GO TO 803
  NTOT=I-2
  IF(BOY(1).EQ.TOY(3)) BET=200.
  IF(BOY(1).EQ.TOY(2)) BET=100.0
  IF (BOY(1) .EQ.TOY(1)) BET=0.0
  DO 804 I=1,NTOT
  IF (BOY(I) .EQ.TOY(1)) ADD=0.0
  IF(BOY(I).EQ.TOY(2)) ADD=100.0
  IF(BOY(I).EQ.TOY(3)) ADD=200.
  X(I)= X(I)+ADD
  DET=X(I)-BET
  IF(DET.GT.100.) X(I)=X(I)-100.
  BET=X(I)
804  CONTINUE
  DO 856 I = 1, NU
856  X(I)=X(I)+SHIFT
  1030  NW = NU
  200  NERR=0
  DO 53 I=1,NU
  XW(I) = X(I)
  53  YYW(I) = YY(I)
  103  N1 = N+1
```

```
      N2 = 2*N
DO 5  NF = 2,N2
      F10 = SUMXN(NW,(NF-2),XW,YYW,2)
DO 6  I=1,N
DO 7  J=1,N
      IF ((I+J).EQ.NF) 17,7
17    AA(I,J) = F10
      7 CONTINUE
      6 CONTINUE
      5 CONTINUE
DO 11 I = 1,N
      J = I-1
11    AA(I,N1) = SUMXN(NW,J,XW,YYW,1)
      CALL SOLVE(N,AA,B)
      3 FORMAT(8E15.6)
      PRINT 83
83    FORMAT (1H1,3X*COEFFICIENTS OF POLYNOMIAL*//)
      PRINT 3, (B(I),I=1,N)
      NM=N-1
      PRINT 71,NM
71    FORMAT ( //3X*POLYNOMIAL ORDER IS*I3//3X*STANDARD LINES*//)
      PRINT 19
19    FORMAT (//2X*MEASURED*4X*LAMBDA*4X*LAMBDA*2X*ERROR IN*6X*WAVE*/2X
1*POSITION*6X*TRUE*5X*CALC.*4X*LAMBDA*3X*NUMBERS*//)
DO 12 J = 1,NTOT
      Y(J) = YFUN(N,B,X(J))
12    YINV(J)=1.E4/Y(J)
C    WAVE CONVERTS ANGSTROMS IN AIR TO WAVE NOS. IN VACUUM
      CALL WAVE(NTOT,YINV,VW)
DO 13 J=1,NW
      Y(J) = YFUN(N,B,XW(J))
13    YINV(J) = 1.E4/Y(J)
      CALL WAVE(NW,YINV,VW)
DO 70 I=1,NW
      DE(I) = YYW(I) - Y(I)
700 PRINT 20, (XW(I),YYW(I),Y(I),DE(I),VW(I), I=1,NW)
200  FORMAT (F10.3,3F10.3,F10.2)
      GO TO 701
      OMEGA = 0.0
      SN = NW
      C=N
C    OMEGA TELLS THE GOODNESS OF FIT...THE SMALLER THE BETTER
DO 101 L=1,NW
      Q = (Y(L) - YYW(L))**2/(SN-C)
      OMEGA=OMEGA+Q
101  CONTINUE
      PRINT 102,OMEGA
102  FORMAT (//3X*OMEGA =*F10.5//)
C    THIS NEXT SECTION ELIMINATES ALL STANDARD LINES WHICH HAVE A
C    DIFFERENCE BETWEEN THE TRUE AND CALCULATED VALUES OF MORE THAN
C    ETOL ANGSTROMS
      L=1
      ERROR=ABS(DE(1))
DO 72 I=2,NW
      IF (ERROR.GE.ABS(DE(I))) GO TO 72
      ERROR=ABS(DE(I))
      L=I
```

```
72 CONTINUE
   IF (ERROR.GE.ETOL) GO TO 73
   GO TO 701
73  L1=L+1
   NERR=NERR+1
   IF (NERR.EQ.5) GO TO 555
   DO 74 J=L1,NW
   J1=J-1
      TEMPO = YYW(J)
      YYW(J1) = TEMPO
      TEMPO = XW(J)
      XW(J1)= TEMPO
74  CONTINUE
   NW = NW-1
   NS = NW-2
   IF (NLAST.EQ.NS) GO TO 525
   GO TO 103
555 PRINT 556
556 FORMAT (1H1,3X*THERE ARE MORE THAN 5 ERRORS*//)
   GO TO 701
525 PRINT 526
526 FORMAT (//3X*THERE ARE TOO FEW GOOD LINES*//)
701 PRINT 85
85  FORMAT ( //3X*OBSERVATIONS*//2X*MEASURED*4X*LAMBDA*6X*WAVE*3X
1*COMMENT*/2X*POSITION*5X*CALC.*3X*NUMBERS*//)
   PRINT 86, (X(I),Y(I),VW(I),INCA(I),STR(I), I=NU1,NTOT)
86  FORMAT(2F10.3,F10.2,I10,F6.1)
   IF(PUN.EQ.0.0) GO TO 880
   PUNCH 871, (VW(I),Y(I),STR(I),INCA(I),X(I), I=1,NTOT)
871 FORMAT(10X,3F10.2,I10,10X,F10.3)
880 CONTINUE
   N=N+1
566 IF (N.LE.NLAST) GO TO 1030
   GO TO 801
850 CONTINUE
END
FUNCTION SUMXN(NT,N,X,Y,JJ)
DIMENSION X(1000),Y(1000)
   S=0.0
   IF (JJ.EQ.1) 1,3
1 DO 2 I=1,NT
2   S = S + Y(I)*X(I)**N
   GO TO 20
3 DO 4 I=1,NT
4   S = S + X(I)**N
20 SUMXN = S
RETURN
END
SUBROUTINE SOLVE(N,A,R)
DIMENSION A(10,10),B(10)
   N1 = N+1
DO 3 I=1,N
   ATEM = A(I,I)
DO 4 J=1,N1
4   A(I,J) = A(I,J)/ATEM
DO 5 K=1,N
   IF (K-I) 51,5,51
```

```
51     BTEM = A(K,I)
      DO 6 J=1,N1
6       A(K,J) = A(K,J) - BTEM*A(I,J)
5     CONTINUE
3     CONTINUE
      DO 93 I=1,N
93     B(I) = A(I,N1)
      RETURN
      END
      FUNCTION YFUN(N,B,Z)
      DIMENSION B(10)
          T = B(1)
      DO 1 I=2,N
          T = T + B(I)*Z**(I-1)
1     CONTINUE
      YFUN = T
      RETURN
      END
      SUBROUTINE WAVE(NTOT,YINV,VW)
      DIMENSION VW(1000),YINV(1000)
      DO 150 K=1,NTOT
          TE=0.
          T=YINV(K)
C       P IS THE REFRACTIVE INDEX OF WET AIR AT THIS WAVE-LENGTH
151     P=((6432.8+2949810./((146.-T*T)+25540./((41.-T*T))*1.E-8))+1.
          T=YINV(K)/P
          IF ((ABS(TE-T)).LT.1.E-6) GO TO 152
          TE=T
          GO TO 151
152     VW(K)=T*1.E4
150     CONTINUE
      RETURN
      END
```

2. STNPLOT uses the cards punched by program STAND to plot the measured lines on a graph of energy ( $\text{cm}^{-1}$ ) vs relative intensity. The end of the deck is signaled by a card with 88 in columns 49 and 50. The dispersion in  $\text{cm}^{-1}$  per inch is given on the next card (format 8F10.5). See Figure (B-1) for a sample plot.

The program was written by Joel Tellinghuisen.

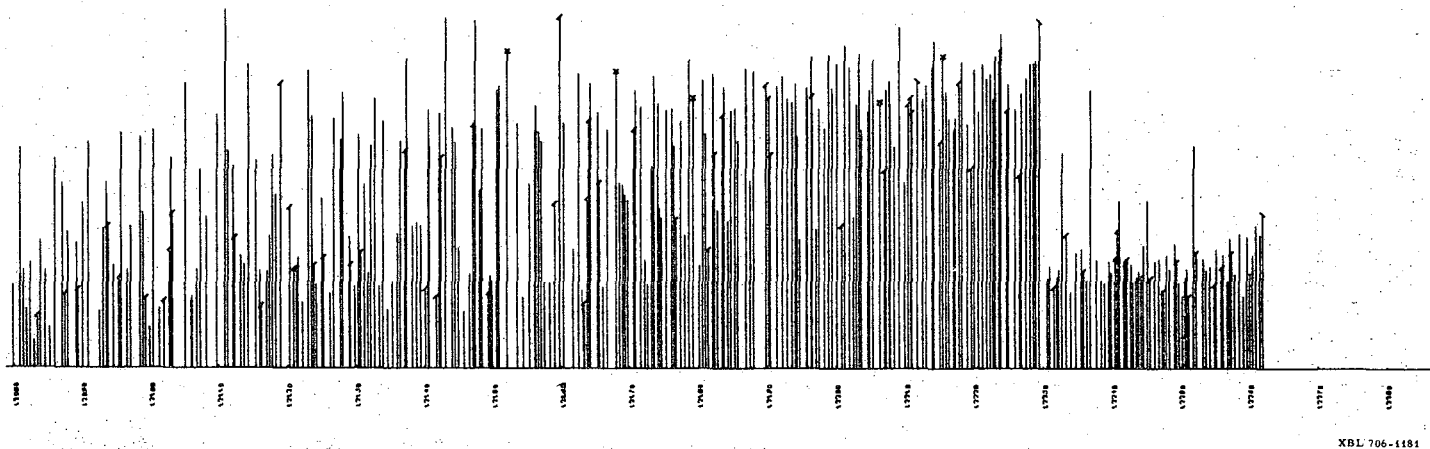


Fig. B-1. Sample plot of energy ( $\text{cm}^{-1}$ ) vs relative intensity from the program STN PLOT. Lines with bars slanting to the left ( ) indicate overlapped lines, bars slanting to the right ( ) red-degraded heads, and crosses ( ) two lines too close to be resolved.

```
PROGRAM STNPLOT(INPUT,OUTPUT,TAPE98,PLOT,TAPE99=PLOT)
DIMENSION VW(1000),Y(1000),STR(1000),INCA(1000)
C THE FOLLOWING CODE HAS BEEN USED FOR INCA.
C 0 AND 1 . . . ATOMIC LINES
C 2 . . . RED-DEGRADED BAND HEAD
C 3 . . . VIOLET-DEGRADED BAND HEAD
C 4 . . . SPIKE MEASURED ON CENTER
C INTEGERS 5 THRU 0 RESULT IN NO SYMBOLS ON PLOTTED LINES.
1 FORMAT(8F10.5)
2 FORMAT(10X,3F10.2,I10)
3 FORMAT(/////20X,*INPUT DATA*///)
4 FORMAT(///*PLOT DISPERSION = *F5.0,* CM-1 PER INCH*///)
501 CONTINUE
DO 11 I=1,1000
READ 2, VW(I),Y(I),STR(I),INCA(I)
IF (INCA(I).EQ.88) GO TO 12
11 CONTINUE
12 NTOT = I-1
PRINT 3
PRINT 2, (VW(I),Y(I),STR(I),INCA(I),I=1,NTOT)
READ 1, DISP
PRINT 4, DISP
CALL GRAPHX(VW,STR,INCA,NTOT,DISP)
READ 500, ISTOP
500 FORMAT (I5)
IF (ISTOP.NE.0) GO TO 501
CALL CCEND
END
SUBROUTINE GRAPHX(X,Y,IND,NT,DISP)
COMMON/CCPOOL/XL,XH,YL,YH,CXL,CXH,CYL,CYH
DIMENSION X(500),Y(500),IND(500),XP(3),YP(3)
XMIN = FMIN(NT,X) $ XMAX = FMAX(NT,X)
IA = XMIN/100. - 1
IB = XMAX/100. + 1
XL = 100.*IA $ XH = 100.*IB
DELTX = (XH-XL)/DISP*100.
CXL = 100. $ CXH = DELTX + 100.
YA = FMIN(NT,Y)
YL = 0.0 $ YH = 120. -YA
CYL = 300. $ CYH = 900.
GL = DELTX/100. + .1
NXL = GL
CALL CCGRID(1,NXL,6HNOLBLS,1,6)
CALL CCLBL(NXL,1)
DO 11 I=1,NT
XP(1) = X(I) $ XP(2) = X(I)
YP(1) = 105. -Y(I) $ YP(2) = 0.0
NSYM = 0
IF (IND(I).EQ.1) NSYM = 8
IF (IND(I).EQ.2) NSYM = 4
IF (IND(I).EQ.3) NSYM = 5
IF (IND(I).EQ.4) NSYM = 2
CALL CCPLT(XP,YP,2,4HJOIN,NSYM,5)
11 CONTINUE
CALL CCNEXT
RETURN
END
```

```
FUNCTION FMIN(N,X)
DIMENSION X(100)
  A = X(1)
DO 10 I=1,N
  IF (X(I).LT.A) A = X(I)
10 CONTINUE
FMIN = A
RETURN
END
FUNCTION FMAX(N,X)
DIMENSION X(100)
  B = X(1)
DO 11 I=1,N
  IF (X(I).GT.B) B = X(I)
11 CONTINUE
FMAX = B
RETURN
END
SUBROUTINE CCLBL(NX1,NY1)
COMMON/CCPOOL/XMIN,XMAX,YMIN,YMAX,CCXMIN,CCXMAX,CCYMIN,CCYMAX
COMMON/CCFACT/FACTOR
ISZERO=0
XD=XMAX-XMIN      $YD=YMAX-YMIN
CCXD=CCXMAX-CCXMIN  $CCYD=CCYMAX-CCYMIN
XI=XD/FLOAT(NX1)   $YI=YD/FLOAT(NY1)
KSIZE=1           $KORIENT=1
C LABEL FROM RIGHT TO LEFT ALONG THE X-AXIS.
DO 2 NX=ISZERO,NX1
  CCX=CCXMAX-CCXD*FLOAT(NX)/FLOAT(NX1)
  X=(CCX-CCXMIN)*XD/CCXD+XMIN
C SET X TO A TRUE ZERO IF X=0. TO WITHIN MACHINE ACCURACY.
  IF(ABS(X/XI).LT.1.0E-6)X=0.
  WRITE(98,28)X
2 CALL CCLTR(CCX+6.*FLOAT(KSIZE)/FACTOR,
* CCYMIN-70.*FLOAT(KSIZE)/FACTOR,KORIENT,KSIZE)
  KSIZE=1           $KORIENT=0
C LABEL UPWARD ALONG THE Y-AXIS.
DO 3 NY=ISZERO,NY1
  CCY=CCYMIN+CCYD*FLOAT(NY)/FLOAT(NY1)
  Y=(CCY-CCYMIN)*YD/CCYD+YMIN
C SET Y TO A TRUE ZERO IF Y=0. TO WITHIN MACHINE ACCURACY.
  IF(ABS(Y/YI).LT.1.0E-6)Y=0.
  WRITE(98,27)Y
3 CALL CCLTR(CCXMIN-70.*FLOAT(KSIZE)/FACTOR,CCY,KORIENT,KSIZE)
27 FORMAT(E10.2)
28 FORMAT(F7.0)
RETURN
END
```

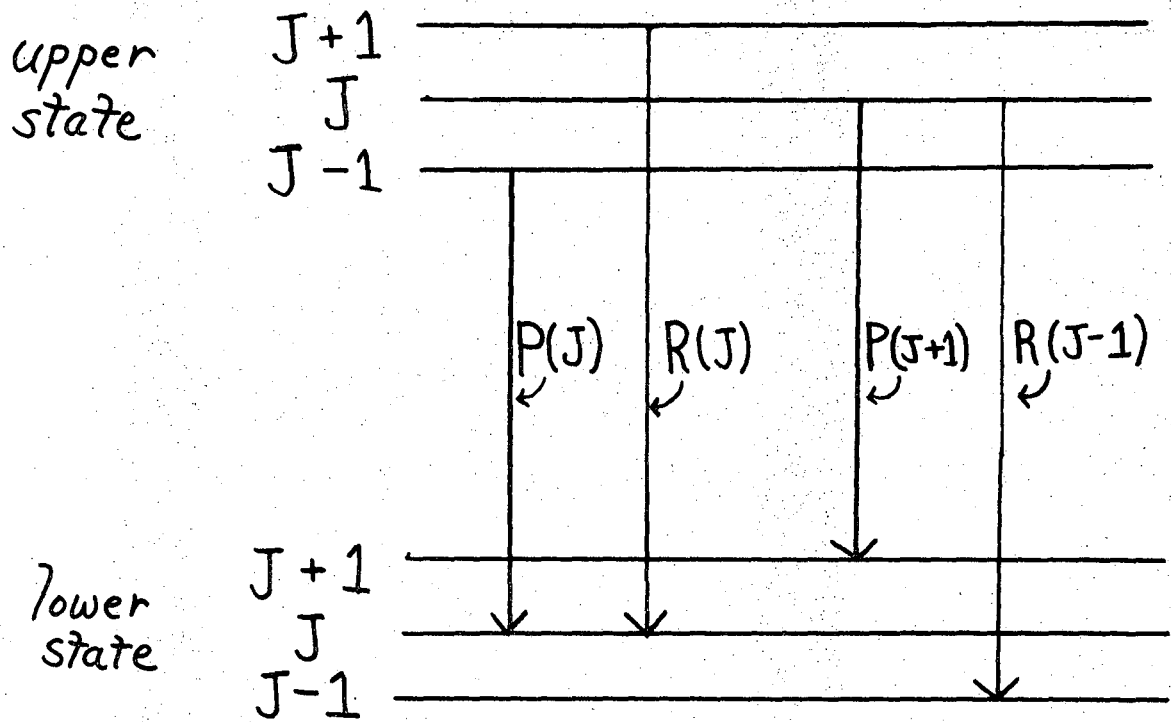


3. NOSORT calculates the combination differences,  $\Delta_2 F''(J)$ , for  $\text{CaO}^{18}$  from the spectroscopic constants of  $\text{CaO}^{16}$  and  $\rho$ . As illustrated in Figure B-2

$$\Delta_2 F''(J) = R(J-1) - P(J+1) = F_v''(J+1) - F_v''(J-1)$$

where  $F_v''(J)$  is the energy of the J-rotational level of the lower vibrational state. Thus the energy difference between one line in the R-branch and one line in the P-branch is known. The energy of R(J-1) is calculated and every line in the region [SCAN + R(J-1)] to [R(J-1) - SCAN] is assumed to be a possible candidate for R(J-1). The combination difference  $\Delta_2 F''(J)$  (IERR) is added to the possible R(J-1) lines and the program searches for P(J+1). If a pair of lines with the proper energy difference is found, a relative energy for the  $F_v'(J)$  level (called EAVE) is calculated using the energies of P(J+1) and R(J-1) plus the spectroscopic constants of the lower vibrational state. All the EAVE's found for all the J values considered (JSTR < J < JEND) are plotted on a scale of relative energy vs J(J+1) (see Figure B-3). The quantity SL\*J\*(J+1) was subtracted from EAVE so that the plot would be horizontal and graph paper not wasted. The numbers plotted in each case represent the relative intensities of the P-line, the A's indicate the calculated energy of P(J+1), and the circled numbers indicate combinations which have been assigned to the (0,0) band. Notice the perturbation at J 38.

A similar program is described in Kopp, et al., 1965.



XBL 707-1376

Fig. B-2. Plot illustrating the equations

$$\Delta_2'' F(J) = R(J-1) - P(J+1) = F_V''(J+1) - F_V''(J-1)$$

$$\Delta_2' F(J) = R(J) - P(J) = F_V'(J+1) - F_V'(J-1)$$



Fig. B-3. Sample plot of the program NOSORT. The coordinates are energy vs  $J(J+1)$ . Each number represents a possible assignment of  $P(J+1)$  and  $R(J-1)$ , the A's indicate the calculated energy of the  $J$  rotational level and the circled numbers show the combinations which have been assigned to the (0,0) band.

```
PROGRAM NOSORT(INPUT,OUTPUT,TAPE98,PLOT,TAPE99=PLOT)
DIMENSION S(800),DEN(800),X(2500),Y(2500),SYM(2500),
1  FV1(125),FV2(125),DIFF(125),R(125)
INTEGER SYM
SL=.3669
DISP=200.
I=1
3  READ 120,S(I),DEN(I)
120  FORMAT (12X,F10.2,13X,F5.2)
IF (S(I).EQ.0.0) GO TO 10
I=I+1
GO TO 3
10  ISPECT=I-1
READ 14,TE1,OE1,OEXE1,OEYE1,BE1,AE1,DE1,BEE1,HE1,GE1,GEE1
READ 14,TE2,OE2,OEXE2,OEYE2,BE2,AE2,DE2,BEE2,HE2,GE2,GEE2
14  FORMAT (8F10.2)
RHO = .959415
OE1=RHO*OE1
OEXE1=RHO**2*OEXE1
OEYE1=OEYE1*RHO**3
BE1=BE1*RHO**2
AE1=AE1*RHO**3
DE1=DE1*RHO**4
BEE1=BEE1*RHO**5
HE1=HE1*RHO**6
GE1=GE1*RHO**7
OE2=RHO*OE2
OEXE2=RHO**2*OEXE2
OEYE2=OEYE2*RHO**3
BE2=BE2*RHO**2
AE2=AE2*RHO**3
DE2=DE2*RHO**4
BEE2=BEE2*RHO**5
HE2=HE2*RHO**6
GE2=GE2*RHO**7
PRINT 999,TE1,TE2,OE1,OE2,OEXE1,OEXE2,OEYE1,OEYE2,BE1,BE2,
1AE1,AE2,DE1,DE2,BEE1,BEE2,HE1,HE2,GE1,GE2,GEE1,GEE2
999  FORMAT (//3X*STATE 1*25X*STATE 2*///3X*TE=*F12.3,17X*TE=*F12.3//3X
1*OE=*F12.3,17X*OE=*F12.3//3X*OEXE=*F10.4,17X*OEXE=*F10.4//3X
2*OEYE=*F10.4,17X*OEYE=*F10.4//3X*BE=*F12.7,17X*BE=*F12.7//3X
3*AE=*F12.8,17X*AE=*F12.8//3X*DE=*F12.4,17X*DE=*F12.4//3X*BEE=*
4E11.4,17X*BEE=*E11.4//3X*HE=*E12.4,17X*HE=*E12.4//3X*GE=*E12.4,
517X*GE=*E12.4//3X*GEE=*E11.4,17X*GEE=*E11.4//)
100  READ 14,ERR
IF(ERR.EQ.0.0) GO TO 1000
READ 14,SCAN
30  READ 2, V1,V2
2  FORMAT (3F10.5)
31  READ 701 ,JSTR,JEND
701  FORMAT (2I10)
PRINT 41,V2,V1
41  FORMAT (1H1*DATA FOR V',V''* 2F5.1)
PRINT 787, SL
787  FORMAT(2X*SL=*F10.5)
C=V1+.5
D=V2+.5
V00=TE2-TE1+OE2*D-D**2*(OEXE2-D*OEYE2)-OE1*C+C**2*(OEXE1-C*OEYE1)
```

```
1 +7.2525
  BV1= BE1-AE1*C
  DV1=DE1-BFE1*C
  HV1=HE1-GE1*C
  RV2= BF2-AE2*D
  DV2= DE2-BFE2*D
  HV2=HE2-GE2*D
  DO 20 J = JSTR , JEND
  A=J
  F=A+1.0
  FV1(J)=RV1*A*F-DV1*(A*F)**2
  FV2(J)=RV2*A*F-DV2*(A*F)**2
20 CONTINUE
  JAZZ = JEND -1
  DO 35 J = JSTR,JAZZ
  R(J)= V00+FV2(J+1) -FV1(J)
35 CONTINUE
  JSTOP=JEND-2
  DO 5 I =JSTR,JSTOP
  J1=I+1
  J2=I+2
5  DIFF(J1)=FV1(J2)-FV1(I)
  PRINT 6
6  FORMAT (2H1 *J*7X*D|IFF*9X*TRUF*9X*P LINE*7X*INT P *7X*R LINE*7X*
1  INT R*7X*ENERGY*5X*E-DIFF*)
  NO=0
  JO= JSTR+1
  DO 7 I=JO,JSTOP
  NO=NO+1
  IF(NO.GT.2500) GO TO 29
  SYM(NO)=1HA
  X(NO)=I*(I+1)
  Y(NO)=FV2(I)-SL*X(NO)
  PRINT114,I,DIFF(I),FV2(I)
114 FORMAT(2X,I5,3X,F10.2,3X,F10.2)
  PRINT 19,X(NO),Y(NO)
  SC1=R(I-1)+SCAN
  SC2=R(I-1)-SCAN
  DO 8 IN=I,ISPECT
  IF (S(IN).LE.SC1) GO TO 11
8  CONTINUE
11 JSCAN1= IN
  DO 9 IT=IN,ISPECT
  IF (S(IT).LE.SC2) GO TO 13
9  CONTINUE
13 JSCAN2= IT
  DO 12 J= JSCAN1,JSCAN2
  E1=S(J)-DIFF(I)+ERR
  E2=E1-2.*ERR
  DO 15 N = J,ISPECT
  IF(S(N).LT.E1) GO TO 101
  GO TO 15
101 IF(S(N).LT.E2) GO TO 12
  NO=NO+1
  IF (NO.GT.2500) GO TO 29
  EP=S(N)-V00+FV1(I+1)
  ER=S(J)-V00+FV1(I-1)
  X(NO)=I*(I+1)
  EAVE=(ER+EP)/2.0
```

```
EDIFF=EAVE- FV2(I)
Y(NO)=EAVE-SL*X(NO)
NDEN=(DEN(N)+5.0)*.1
SYM(NO)=10-NDEN
SYM(NO)=SYM(NO)+33B
SYM(NO)=LEFT(SYM(NO),54)
PRINT 19 ,S(N),DEN(N),S(J),DEN(J),EAVE,EDIFF,Y(NO)
19 FORMAT (33X,7(3X,F10.2))
15 CONTINUE
12 CONTINUE
7 CONTINUE
GO TO 40
29 NO=NO-1
40 CALL GRAPH(X,Y,SYM,NO,DISP)
GO TO 100
1000 CONTINUE
CALL CCEND
END
SUBROUTINE GRAPH( X,Y,SYM,NT,DISP)
COMMON/CCPOOL/XL,XH,YL,YH,CXL,CXH,CYL,CYH
DIMENSION X(3750),Y(3750),SYM(3750)
XMIN = FMIN(NT,X) $ XMAX = FMAX(NT,X)
IA = XMIN/100. - 1
IB = XMAX/100. + 1
XL = 100.*IA $ XH = 100.*IB
DELTX = (XH-XL)/DISP*100.
CXL = 100. $ CXH = DELTX + 100.
YMIN=FMIN(NT,Y) $ YMAX=FMAX(NT,Y)
IA=YMIN-2.0
IB=YMAX+2.0
YL=IA
YH=IB
CYL=200. $ CYH= 900.
GL = DELTX/100. + .1
NXL = GL
NYL=10
CALL CCGRID (NXL,6HLABELS,NYL)
DO 11 I=1, NT
YP= (Y(I)-YL)*(CYH-CYL)/( YH-YL)+CYL
XP=(X(I)-XL)*(CXH-CXL)/(XH-XL)+CXL
CALL CCLTR(XP,YP,0,1,SYM(I),1)
11 CONTINUE
CALL CCNEXT
RETURN
END
FUNCTION FMIN(N,X)
DIMENSION X(100)
A = X(1)
DO 10 I=1,N
IF (X(I).LT.A) A = X(I)
10 CONTINUE
FMIN = A
RETURN
END
FUNCTION FMAX(N,X)
DIMENSION X(100)
B = X(1)
DO 11 I=1,N
IF (X(I).GT.B) B = X(I)
11 CONTINUE
FMAX = B
RETURN
END
```

4. BOTH is basically the same program as NOSORT only after an R(J-1) and P(J+1) is found to satisfy the lower state combination difference, a P(J-1) must also be found to satisfy the upper state combination difference for (J-1). The upper state differences (DI) are read in by statement 38.

```
PROGRAM BOTH (INPUT,OUTPUT,TAPE98,PLOT,TAPE99=PLOT)
DIMENSION S(800),DEN(800),X(2500),Y(2500),SYM(2500),
1 FV1(125),FV2(125),DIFF(125),R(125)
DIMENSION DIF(125)
INTEGER SYM
SL=.3655
DISP=200.
I=1
3 READ 120,S(I),DEN(I)
12 FORMAT (12X,F10.2,13X,F5.2)
IF (S(I).EQ.0.0) GO TO 10
I=I+1
GO TO 3
10 ISPECT=I-1
READ 14,TE1,OE1,OEXE1,OYE1,BE1,AE1,DE1,BEE1,HE1,GE1,GEE1
READ 14,TE2,OE2,OEXE2,OYE2,BE2,AE2,DE2,BEE2,HE2,GE2,GEE2
14 FORMAT (8F10.2)
RHO = .959415
OE1=RHO*OE1
OEXE1=RHO**2*OEXE1
OYE1=OYE1*RHO**3
BE1=BE1*RHO**2
AE1=AE1*RHO**3
DE1=DE1*RHO**4
BEE1=BE1*RHO**5
HE1=HE1*RHO**6
GE1=GE1*RHO**7
OE2=RHO*OE2
OEXE2=RHO**2*OEXE2
OYE2=OYE2*RHO**3
BE2=BE2*RHO**2
AE2=AE2*RHO**3
DE2=DE2*RHO**4
BEE2=BEE2*RHO**5
HE2=HE2*RHO**6
GE2=GE2*RHO**7
PRINT 999,TE1,TE2,OE1,OE2,OEXE1,OEXE2,OYE1,OYE2,BE1,BE2,
1AE1,AE2,DE1,DE2,BEE1,BEE2,HE1,HE2,GE1,GE2,GEF1,GEF2
999 FORMAT (//3X*STATE 1*25X*STATE 2*///3X*TE=*F12.3,17X*TE=*F12.3//3X
1*OE=*F12.3,17X*OE=*F12.3//3X*OEXE=*F10.4,17X*OEXE=*F10.4//3X
2*OYE=*F10.4,17X*OYE=*F10.4//3X*BE=*F12.7,17X*BE=*F12.7//3X
3*AE=*F12.8,17X*AE=*F12.8//3X*DE=*E12.4,17X*DE=*E12.4//3X*BEE=*
4E11.4,17X*BEE=*E11.4//3X*HE=*E12.4,17X*HE=*E12.4//3X*GE=*F12.4,
517X*GE=*E12.4//3X*GEE=*E11.4,17X*GEE=*E11.4//)
100 READ 14,ERR
IF(ERR.EQ.0.0) GO TO 1000
READ 14,FRR2
READ 14,SCAN
30 READ 2, V1,V2
2 FORMAT (3F10.5)
31 READ 701 ,JSTR,JEND
701 FORMAT (2I10)
PRINT 41,V2,V1
41 FORMAT (1H1*DATA FOR V1,V2** 2F5.1)
PRINT 752,ERR,ERR2
752 FORMAT (1X,2F10.3)
PRINT 787, SL
787 FORMAT (2X*SL=*F10.5)
C=V1+.5
D=V2+.5
```



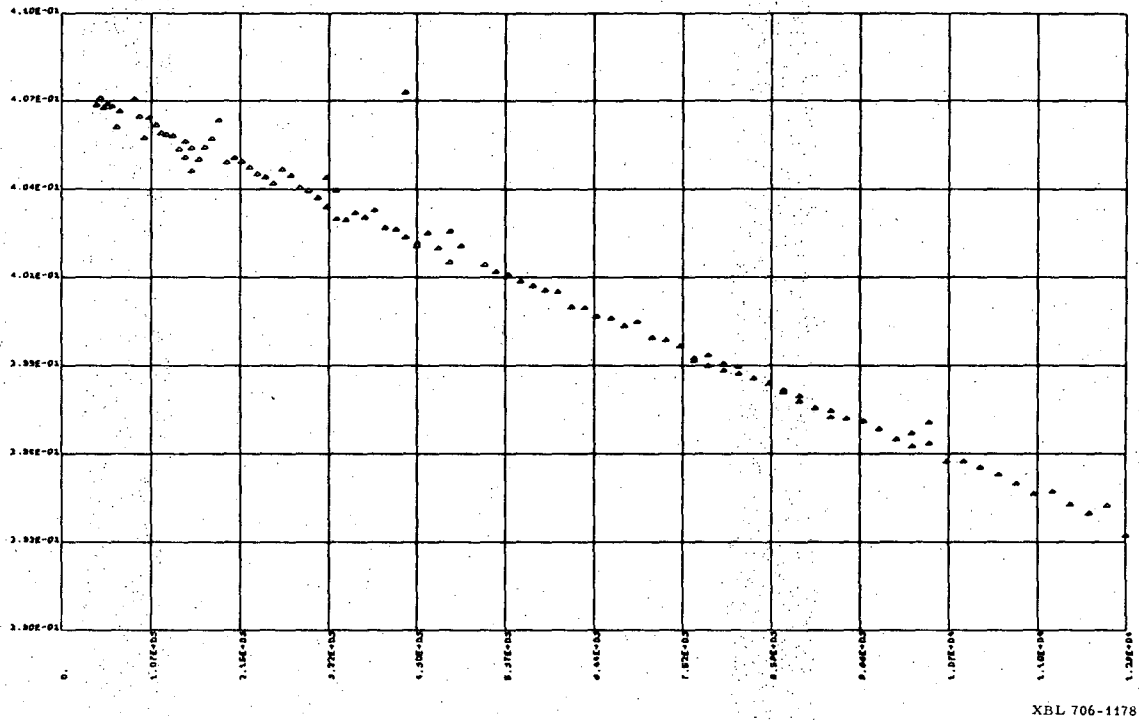
```
V00=TE2-TE1+OE2*D-D**2*(OFXE2-D*OEYE2)-OF1*C+C**2*(OFXE1-C*OEYE1)
1 +7.2525
  BV1= BE1-AE1*C
  DV1=DE1+BEE1*C
  HV1=HE1-GE1*C
  BV2= BE2-AE2*D
  DV2= DE2-BEE2*D
  HV2=HE2-GE2*D
DO 20 J = JSTR , JEND
  A=J
  F=A+1.0
  FV1(J)=BV1*A*F-DV1*(A*F)**2
  FV2(J)=BV2*A*F-DV2*(A*F)**2
20 CONTINUE
  JAZZ = JEND -1
DO 35 J = JSTR,JAZZ
  R(J)= V00+FV2(J+1) -FV1(J)
35 CONTINUE
  JSTOP=JEND-2
  DO 5 I=JSTR,JSTOP
    J1=I+1
    J2=I+2
5    DIFF(J1)=FV1(J2)-FV1(I)
    NO=0
42    NA=0
    JAP=0
38    READ37,JA,DI
37    FORMAT (I5,F10.5)
    TOP=JA+DI
    IF(TOP.EQ.0.0) GO TO 39
    NA=NA+1
    IF(NA.EQ.1) JO=JA+1
    DIF(JA)=DI
    JAP=JA
    GO TO 38
39    JSTOP=JAP+1
    IF(JAP.EQ.0) GO TO 1000
    PRINT 6
6    FORMAT (1X*J*25X*P(J+1)*7X*INT P*7X*R(J-1)* 7X*INT R*7X*ET-EC*
1 7X*DIF LOW*7X*DIF UP*7X*P(J-1)*)
    DO 7 I=JO,JSTOP
    NO=NO+1
    IF(NO.GT.2500) GO TO 29
    SYM(NO)=1HA
    X(NO)=I*(I+1)
    Y(NO)=FV2(I)-SL*X(NO)
    PRINT 114,I,DIFF(I),FV2(I),DIF( I-1)
114  FORMAT (2X,I5,3(3X,F10.2))
    PRINT 19,X(NO),Y(NO)
    SC1=R(I-1)+SCAN
    SC2=R(I-1)-SCAN
    DO 8 IN=1,ISPECT
    IF (S(IN).LE.SC1) GO TO 11
8    CONTINUE
11    JSCAN1= IN
    DO 9 IT=IN,ISPECT
    IF (S(IT).LE.SC2) GO TO 13
```

```
9      CONTINUE
13     JSCAN2= IT
       DO 12 J= JSCAN1,JSCAN2
       E1=S(J)-DIFF(I)+ERR
       E2=E1-2.0*ERR
       DO 15 N = J, ISPECT
       IF(S(N).LT.E1) GO TO 101
       GO TO 15
101    IF(S(N).LT.E2) GO TO 12
       E3=S(J)-DIF(I-1)+ERR2
       E4=E3-2.0*ERR2
       DO 16 NU=J, ISPECT
       IF (S(NU).LT.E3) GO TO 102
       GO TO 16
102    IF (S(NU).LT.E4) GO TO 15
       UP=S(J)-S(NU)
       BOT=S(J)-S(N)
       NO=NO+1
       IF (NO.GT.2500) GO TO 29
       EP=S(N)-V00+V1(I+1)
       ER=S(J)-V00+V1(I-1)
       X(NO)=I*(I+1)
       EAVE=(ER+EP)/2.0
       EDIFF=EAVE- FV2(I)
       Y(NO)=EAVE-SL*X(NO)
       NDEN=(DEN(N)+5.0)*.1
       SYM(NO)=10-NDEN
       SYM(NO)=SYM(NO)+33R
       SYM(NO)=LEFT(SYM(NO),54)
       PRINT 19,S(N),DEN(N),S(J),DEN(J),EDIFF,BOT, UP,S(NU)
19     FORMAT (20X,8(3X,F10.2))
16     CONTINUE
15     CONTINUE
12     CONTINUE
7      CONTINUE
       GO TO 42
1000   CONTINUE
       GO TO 40
29     NO=NO-1
40     CALL GRAPH(X,Y,SYM,NO,DISP)
       CALL CCFND
       END
       SUBROUTINE GRAP(I( X,Y,SYM,NT,DISP)
COMMON/CCPOOL/XL,XH,YL,YH,CXL,CXH,CYL,CYH
DIMENSION X(3750),Y(3750),SYM(3750)
       XMIN = FMIN(NT,X) $ XMAX = FMAX(NT,X)
       IA = XMIN/100. - 1
       IB = XMAX/100. + 1
       XL = 100.*IA $ XH = 100.*IB
       DELTX = (XH-XL)/DISP*100.
       CXL = 100. $ CXH = DELTX + 100.
       YMIN=FMIN(NT,Y) $ YMAX=FMAX(NT,Y)
       IA=YMIN-2.0
       IB=YMAX+2.0
       YL=IA
       YH=IB
       CYL=200. $CYH= 900.
       GL = DELTX/100. + .1
       NXL = GL
```

```
NYL=10
CALL CCGRID (NXL,6HLABELS,NYL)
DO 11 I=1, NT
YP= (Y(I)-YL)*(CYH-CYL)/(YH-YL)+CYL
XP=(X(I)-XL)*(CXH-CXL)/(XH-XL)+CXL
CALL CCLTR(XP,YP,0,1,SYM(I),1)
11 CONTINUE
CALL CCNEXT
RETURN
END
FUNCTION FMIN(N,X)
DIMENSION X(100)
A = X(1)
DO 10 I=1,N
IF (X(I).LT.A) A = X(I)
10 CONTINUE
FMIN = A
RETURN
END
FUNCTION FMAX(N,X)
DIMENSION X(100)
B = X(1)
DO 11 I=1,N
IF (X(I).GT.B) B = X(I)
11 CONTINUE
FMAX = B
RETURN
END
```

XBL 707-1442

5. TELL 1 calculates and plots  $\Delta_2 F(J)/4(J+\frac{1}{2})$  vs  $(J+\frac{1}{2})^2$  (see Eq. 3) for both the upper and lower state levels. Sample plots for the (0,0) band are shown in Figures B-4 and B-5. A sample data deck for the (4,2) band is also given. The first card has the vibrational numbering (4.0, 2.0), the next has the lowest and highest J-numbers for the R- and P-branches up to the first perturbation, then the assigned R and P lines are listed in order, the next set of J-numbers given, etc. The deck is ended by a blank card. Several data decks for different bands can be processed at once. A card with 100. in the first four columns signals the end of the input data.



XBL 706-1178

Fig. B-4. Plot of  $\Delta_2'' F(J)/4(J+\frac{1}{2})$  vs  $(J+\frac{1}{2})^2$  for the (0,0) band from program TELL 1. See Eq. 3.



```
PROGRAM TELL1 (INPUT,OUTPUT,TAPE98,PLOT,TAPE99=PLOT)
  DIMENSION XL(150),XH(150)
  DIMENSION JH(150),HDIFF(150),JL(150),BDIFF(150),P(150),R(150)
  DIMENSION BVH(150),BVL(150),D2L(150),D2H(150)
  G= 00 157
156  CONTINUE
    PRINT 378, VH,VL
378  FORMAT (1H1*VH,VL= *2F5.1)
101  IH=0
    IL=0
100  READ 1, JRL,JRH,APL,JPH
    1  FORMAT (4I5)
    D=JRL-JRH
    IF (D.EQ.0.0) GO TO 155
    DO 400I=1,150
    P(I)=0.0
    R(I)=0.0
400  CONTINUE
    READ 2,(R(I),I=JRL,JRH)
    READ 2,(P(I),I=JPL,JPH)
    2  FORMAT (12X,F10.2)
    JS=JRL
    IF (JPL.LT.JRL) JS=JPL
    JE=JRH
    IF (JPH.GT.JRH) JE=JPH
    PRINT 3,(J,P(J),R(J),J=JS,JE)
    3  FORMAT (1X,I5,5X,F10.2,5X,F10.2)
401  JO=JPL-2
    IF(JO.LE.1) GO TO 403
    IF(R(JO).EQ.0.0) GO TO 402
    IL=IL+1
    BDIFF(IL)=R(JO)-P(JPL)
    JL(IL)=JPL-1
    XL(IL)=(JL(IL)+.5)**2
    BVL(IL)=BDIFF(IL)/(4.0*(JL(IL)+.5))
    IF(IL.EQ.1)D2L(1)=0.0
    IF (IL.EQ.1 ) GO TO 402
    D2L(IL)=0.0
    JB=JL(IL)-JL(IL-1)
    IF(JB.NE.1) GO TO 402
    D2L(IL)=BDIFF(IL)-BDIFF(IL-1)
402  IF(R(JPL).EQ.0.0) GO TO 403
    IH=IH+1
    HDIFF(IH)=R(JPL)-P(JPL)
    JH(IH)=JPL
    XH(IH)=(JH(IH)+.5)**2
    BVH(IH)=HDIFF(IH)/(4.0*(JH(IH)+.5))
    IF(IH.EQ.1) D2H(1)=0.0
    IF(IH.EQ.1)GO TO 403
    D2H(IH)=0.0
    JB=JH(IH)-JH(IH-1)
    IF(JB.NE.1) GO TO 403
    D2H(IH)=HDIFF(IH)-HDIFF(IH-1)
403  JPL=JPL+1
    IF (JPL.LE.JPH) GO TO 401
    GO TO 100
155  CONTINUE
```

```
PRINT 181 ,VH,VL
181  FORMAT(1H1*LOWER STATE OF *2F5.1/1X*J*4X*C-DIFF*4X*2ND DIFF*
1 2X*BV*)
PRINT 17,(JL(I),BDIFF(I),D2L(I),BVL(I),I=1,IL)
IN=0
DO 19 J= 1,IL
IN=IN+1
BVL(IN)=BVL(J)
XL(IN)=XL(J)
19  IF(BVL(J).GT.0.8.OR.BVL(J).LT.0.1) IN=IN-1
IL=IN
CALL GRAPH ( XL,BVL,IL)
CALL LINE ( XL,BVL,IL)
PRINT 18 ,VH,VL
18  FORMAT(1H1*UPPER STATE OF *2F5.1/1X*J*4X*C-DIFF*4X*2ND DIFF*
1 2X*BV*)
PRINT 17,(JH(I),HDIFF(I),D2H(I),BVH(I),I=1,IH)
17  FORMAT (1X,I5,3(5X,F10.5))
IN=0
DO 20 J =1,IH
IN=IN+1
BVH(IN)=BVH(J)
XH(IN)=XH(J)
20  IF(BVH(J).GT.0.8.OR.BVH(J).LT.0.1) IN=IN-1
IH=IN
CALL GRAPH ( XH,BVH,IH)
CALL LINE ( XH,BVH,IH)
157 READ 5,VH,VL
5  FORMAT(2F10.2)
IF (VH.LT.99.0) GO TO 156
END
SUBROUTINE GRAPH (X,Y,NT)
COMMON/CCPOOL/XL,XH,YL,YH,CXL,CXH,CYL,CYH
DIMENSION ROUND(4)
DIMENSION X(150),Y(150)
XMIN=FMIN(NT,X) $ XMAX=FMAX(NT,X)
IB=XMAX+4.0
IA=0
XL=IA $ XH=IB
NXL=12
NYL=7
CXL=100. $CXH=1300.
CYL=200. $ CYH =900.
NROUND=4
ROUND(1)=1.0
ROUND(2)=2.0
ROUND(3)=2.5
ROUND(4)=5.0
CALL LINEUP (Y,NT,ROUND,NROUND,NYL,YL,YH)
CALL CCGRID (NXL,6HLABELS,NYL)
CALL CCLOT (X,Y,NT,6HNOJOIN,8,1)
CALL CCNEXT
RETURN
END
FUNCTION FMIN(N,X)
DIMENSION X(100)
A = X(1)
```



```
DO 10 I=1,N
  IF (X(I).LT.A) A = X(I)
10 CONTINUE
  FMIN = A
  RETURN
END
FUNCTION FMAX(N,X)
  DIMENSION X(100)
  B = X(1)
  DO 11 I=1,N
    IF (X(I).GT.B) B = X(I)
11 CONTINUE
  FMAX = B
  RETURN
END
SUBROUTINE LINE (X,Y,M)
  DIMENSION X(150),Y(150)
  IA=0
  3 CONTINUE
  SX=0.0
  SY=0.0
  SXY=0.0
  SX2=0.0
  DO 1J =1,M
    SX=SX+X(J)
    SY=SY+Y(J)
    SXY=SXY+X(J)*Y(J)
    SX2=SX2+X(J)**2
  1 CONTINUE
  R=M
  D=R*SX2-SX**2
  C1= (R*SXY-SX*SY)/D
  C2= (SX2*SY-SX*SXY)/D
  PRINT 2,C1,C2
  2 FORMAT (1X*LEAST SQUARES FIT OF LINE C1 X+C2=Y*/10X*C1=*
  1 E12.5/10X*C2=*E12.5)
  IF(IA.GT.0) GO TO 7
  TEST=.015
  J=0
  IA=1+IA
  DO 4I=1,M
    YT=C1*X(I)+C2
    DI= ABS(YT-Y(I))
    IF(DI.GT.TEST) GO TO 5
    J=J+1
    X(J)=X(I)
    Y(J)=Y(I)
  GO TO 4
  5 PRINT 6,X(I),Y(I),DI
  6 FORMAT (///40X,3F15.5)
  4 CONTINUE
  M=J
  GO TO 3
  7 CONTINUE
  RETURN
END
```

Sample Data Deck for the (4,2) Band

4.0 2.0  
25 45 24 47  
12884.59  
12883.85  
12882.81  
12881.56  
12880.43  
12879.20  
12877.87  
12876.63  
12875.14  
12873.78  
12872.41  
12870.31  
12868.66  
12867.14  
blank  
blank  
blank  
blank  
12854.33  
12848.56  
12849.45  
12847.29  
12844.76  
12842.25  
12839.63  
12836.99  
12834.41  
12831.72  
12828.84  
12825.97  
12822.86  
12819.96  
12816.83  
12813.80  
12810.47  
12807.09  
12803.94  
12800.59  
12797.04  
12793.57  
12789.92  
12786.29  
12781.49  
12774.71  
46 52 48 54  
12850.86  
12848.56  
12846.12  
12843.64  
12841.05  
12838.58  
12831.61  
12775.07  
12771.14

12767.13  
12763.17  
12759.05  
12754.92  
12746.49  
52 61 54 63  
12838.11  
12833.40  
12830.36  
12827.45  
12825.07  
12821.79  
12818.80  
12814.99  
12810.49  
12809.94  
12752.90  
12746.49  
12742.04  
12737.72  
12733.50  
12728.79  
12724.05  
12718.83  
12712.68  
12704.65  
61 69 63 71  
12811.56  
12806.05  
12802.93  
12799.37  
12796.15  
12792.46  
12789.05  
12784.81  
12782.58  
12712.01  
12705.57  
12700.63  
12693.44  
12690.66  
12685.36  
12680.61  
12675.58  
12670.68  
blank

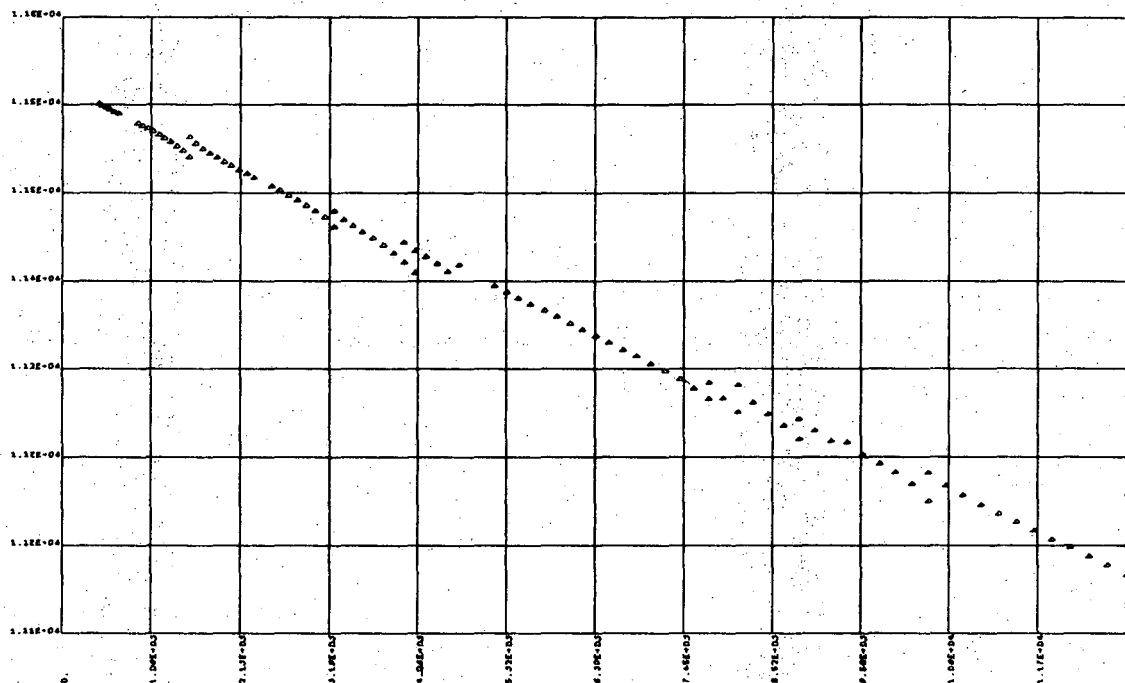
6. TELL 2 calculates and plots  $T/4J$  vs  $J$  (see Eq. 4). The same data deck setup used for TELL 1 can be used here. Sample plots are shown in Figs. 8-13.

```
PROGRAM TELL2(INPUT,OUTPUT,TAPE98,PLOT,TAPE99=PLOT)
DIMENSION R(150),P(150),X(150),T(150)
GO TO 157
156 CONTINUE
PRINT 378, VH,VL
378 FORMAT (1H1*VH,VL= *2F5.1)
IT=0
100 READ 1,JRL,JRH,JPL,JPH
1 FORMAT (4I5)
D=JRL-JRH
IF (D.EQ.0.0) GO TO 155
DO 3I=1,150
R(I)=0.0
P(I)=0.0
3 CONTINUE
READ 2, (R(I),I=JRL,JRH)
READ 2,(P(I),I=JPL,JPH)
2 FORMAT (12X,F10.2)
JTEST=JRH+1
J=JRL+2
4 IF(J.GT.JTEST) GO TO 100
IF(P(J+1).EQ.0.0.OR.P(J).EQ.0.0.OR.R(J-1).EQ.0.0.OR.R(J-2).EQ.0.0)
1 GO TO 5
A=J
IT=IT+1
T(IT)=(R(J-2)-R(J-1)+P(J)-P(J+1))/(4.0*A)
X(IT)=A
PRINT 6,X(IT),T(IT)
6 FORMAT(1X,2F10.5)
IF(T(IT).GT.0.1.OR.T(IT).LT.0.02) IT=IT-1
5 J=J+1
GO TO 4
155 CONTINUE
CALL GRAPH(X,T,IT)
157 READ 25,VH,VL
25 FORMAT (2F10.2)
IF (VH.LT.99.0) GO TO 156
CALL CCEND
END
SUBROUTINE GRAPH (X,Y,NT)
COMMON/CCPOOL/XL,XH,YL,YH,CXL,CXH,CYL,CYH
DIMENSION X(150),Y(150)
XMIN=FMIN(NT,X) $ XMAX=FMAX(NT,X)
IF(XMAX.LT.100.)GO TO 9
JA=XMAX/4.0+1.0
A=JA
NXL=JA
XH=JA*4
CXH=100.+100.*A
GO TO 10
9 CXH=2600.
XH=100.
NXL=25
10 XL=0.0
NYL=8
YL=.02
YH=.1
```

```
CXL=100.0
CYL=200.
CYH=900.
CALL CCGRID (NXL,6HLABELS,NYL)
CALL CCLOT (X,Y,NT,6HNOJOIN,8,1)
CALL CCNEXT
RETURN
END
FUNCTION FMIN(N,X)
DIMENSION X(100)
  A = X(1)
DO 10 I=1,N
  IF (X(I).LT.A) A = X(I)
10 CONTINUE
FMIN = A
RETURN
END
FUNCTION FMAX(N,X)
DIMENSION X(100)
  B = X(1)
DO 11 I=1,N
  IF (X(I).GT.B) B = X(I)
11 CONTINUE
FMAX = B
RETURN
END
```

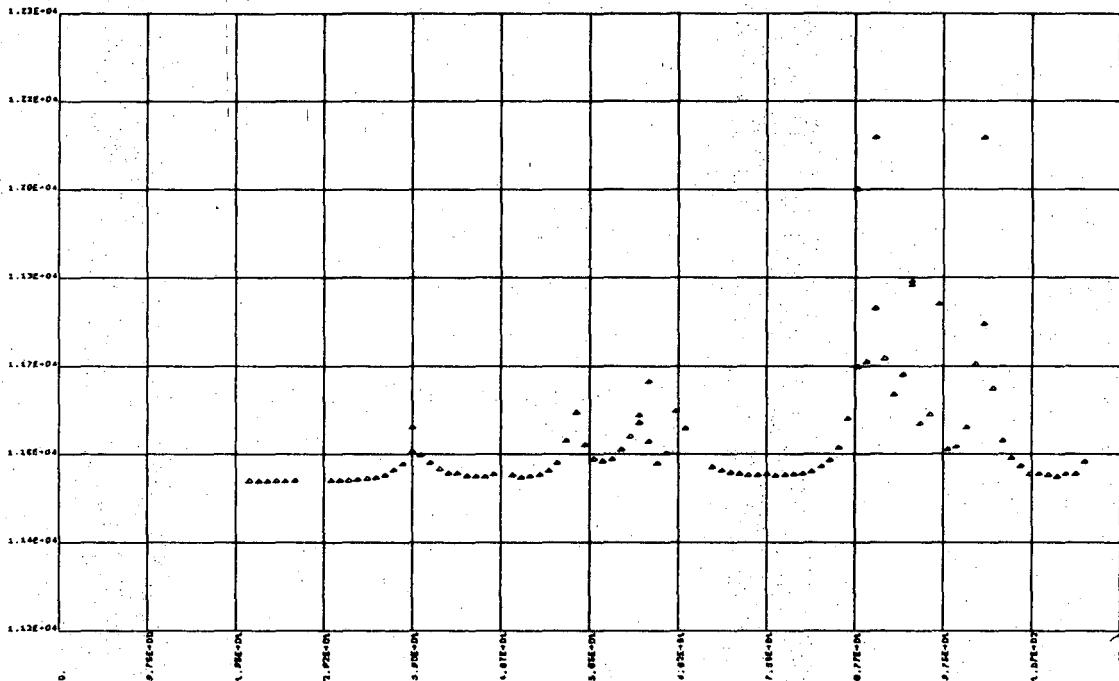
XBL 707-1395

7. ORIGIN calculates and plots  $[(R(J-1) + P(J))/2]$  vs  $J^2$  (see Eq. 6) and the left-hand side of Eq. 7 vs  $J$ . It uses the same data decks as TELL 1 only the second data card for each band has  $B_v''$  (format 10X, F10.2). Sample plots are given in Figs. B-6 and B-7.



XBL 706-1179

Fig. B-6. Plot of  $[(R(J-1) + P(J))/2]$  vs  $J^2$  for the (0,0) band from program ORIGIN. See Eq. 6.



XBL 706-1177

Fig. B-7. Plot of  $[B_V'' - \frac{1}{4}\{J(J+1)[P(J)+R(J-2)] - (J-1)[P(J+1) + R(J-1)]\}]$  vs J for the (0,0) band from program ORIGIN. See Eq. 7.



```
PROGRAM ORIGIN(INPUT,OUTPUT,TAPE98,PLOT,TAPE99=PLOT)
DIMENSION R(150),P(150),X(150),T(150)
DIMENSION V1(150),V2(150)
DIMENSION X1(150)
GO TO 157
156   CONTINUE
      PRINT 378,VH,VL
378   FORMAT (1H1*VH,VL=*2F5.1)
      READ 7,BV1,BV2
7     FORMAT(2F10.5)
      IT=0
100   READ 1,JRL,JRH,JPL,JPH
1     FORMAT (4I5)
      D=JRL-JRH
      IF (D.EQ.0.0) GO TO 155
      DO 3I=1,150
      R(I)=0.0
      P(I)=0.0
3     CONTINUE
      READ 2, (R(I),I=JRL,JRH)
      READ 2,(P(I),I=JPL,JPH)
2     FORMAT (12X,F10.2)
      JTEST=JRH+1
      J=JRL+2
4     IF (J.GT.JTEST) GO TO 100
      IF (P(J+1).EQ.0.0.OR.P(J).EQ.0.0.OR.R(J-1).EQ.0.0.OR.R(J-2).EQ.0.0)
1     GO TO 5
      A=J
      IT=IT+1
      V1(IT)=BV2+.25*((P(J)+R(J-2))*(A+1.0)-(P(J+1)+R(J-1))*(A-1.0))
      V2(IT)=(R(J-1)+P(J))/2.0
      X(IT)=A*A
      X1(IT)=A
      PRINT 8,A,V1(IT),V2(IT),X(IT)
8     FORMAT (1X,4(3X,F10.2))
      IF (V2(IT).GT.15000.0.OR.V2(IT).LT.10000.0) IT=IT-1
      IF (V1(IT).GT.15000.0.OR.V1(IT).LT.10000.0) IT=IT-1
5     J=J+1
      GO TO 4
155   CONTINUE
      CALL LINE(X,V2,IT)
      CALL GRAPH(X,V2,IT)
      CALL GRAPH(X1,V1,IT)
157   READ 25,VH,VL
25   FORMAT (2F10.2 )
      IF (VH.LT.99.0) GO TO 156
      CALL CCEND
      END
      SUBROUTINE GRAPH (X,Y,NT)
      COMMON/CCPOOL/XL,XH,YL,YH,CXL,CXH,CYL,CYH
      DIMENSION ROUND(4)
      DIMENSION X(150),Y(150)
      XMIN=FMIN(NT,X) $ XMAX=FMAX(NT,X)
      IA=XMIN-4.0
      IB=XMAX+4.0
      XH=IB
      XL=0.0
```

```
CXL=100.    $CXH=1300.
NXL=12
NYL=7
CYL=200.    $    CYH =900.
NO=NT+1
Y(NO)=FMAX(NT,Y) +25.
NROUND=4
ROUND(1)=1.0
ROUND(2)=2.0
ROUND(3)=2.5
ROUND(4)=5.0
  CALL LINEUP (Y,NO,ROUND,NROUND,NYL,YL,YH)
  PRINT 1, YL,YH
1  FORMAT (20X*YL,YH=* 2F15.5)
  YWHY=(YH-YL)/7.0
  PRINT 2,YWHY
2  FORMAT (20X*DIVISION=* F15.5)
  CALL CCGRID (NXL,6HLABELS,NYL)
  CALL CCPLOT (X,Y,NT,6HNOJOIN,8,1)
  CALL CCNEXT
  RETURN
  END
  FUNCTION FMIN(N,X)
  DIMENSION X(100)
    A = X(1)
  DO 10 I=1,N
    IF (X(I).LT.A) A = X(I)
10  CONTINUE
  FMIN = A
  RETURN
  END
  FUNCTION FMAX(N,X)
  DIMENSION X(100)
    B = X(1)
  DO 11 I=1,N
    IF (X(I).GT.B) B = X(I)
11  CONTINUE
  FMAX = B
  RETURN
  END
  SUBROUTINE LINE (X,Y,M)
  DIMENSION X(150),Y(150)
  IA=0
  3  CONTINUE
    SX=0.0
    SY=0.0
    SXY=0.0
    SX2=0.0
    DO 1J =1,M
      SX=SX+X(J)
      SY=SY+Y(J)
      SXY=SXY+X(J)*Y(J)
      SX2=SX2+X(J)**2
1  CONTINUE
    R=M
    D=R*SX2-SX**2
    C1= (R*SXY-SX*SY)/D
```

```
      C2= (SX2*SY-SX*SY)/D
      PRINT 2,C1,C2
2     FORMAT (1X*LEAST SQUARES FIT OF LINE C1 X+C2=Y*/10X*C1=*
1     F10.5/10X*C2=*F15.5)
      IF(IA.GT.0) GO TO 7
      TEST=25.
      J=0
      IA=1+IA
      DO 4I=1,M
      YT=C1*X(I)+C2
      DI= ABS(YT-Y(I))
      IF(DI.GT.TEST) GO TO 5
      J=J+1
      X(J)=X(I)
      Y(J)=Y(I)
      GO TO 4
5     PRINT 6,X(I),Y(I),DI
6     FORMAT (///40X,3F15.5)
4     CONTINUE
      M=J
      GO TO 3
7     CONTINUE
      RETURN
      END
```

XBL 707-1381

8. VIBDIF calculates and plots  $A/2$  vs  $J^2$  (see Eq. 10). The input data is two TELL 1-data decks of two bands having the same upper vibrational level.

```
PROGRAM VIBDIF (HNPOT,OUTPUT,TAPE98,PLOT,TAPE99=PLOT)
DIMENSION R(150),P(150),V(2,2), X(150),T(2,150),A(150)
PRINT 1
1  FORMAT (1H1,20X*(R(J-1)-P(J))/2 =V0+(B'-B''')J 2 =T*)
   DO 14 I=1,150
   T(1,I)=0.0
   T(2,I)=0.0
14  CONTINUE
   I=1
20  IF(I.GT.2) GO TO 21
   READ 10,V(I,1),V(I,2)
10  FORMAT (8F10.2)
   PRINT 11,V(I,1), V(I,2)
11  FORMAT (//*V', V''= * 2F10.2)
100 READ 12,JRL,JRH,JPL,JPH
12  FORMAT (4I5)
   D=JRL-JRH
   IF(D.EQ.0.0) GO TO 155
   DO 13 IK=1,150
   R(IK)=0.0
   P(IK)=0.0
13  CONTINUE
   READ 2,(R(IK),IK=JRL,JRH)
   READ 2,(P(IK),IK=JPL,JPH)
2   FORMAT (12X,F10.2)
   J=JPL
6   IF (J.GT.JPH) GO TO 100
4   IF(R(J-1).EQ.0.0.OR.P(J).EQ.0.0) GO TO 5
   T(I,J)=(R(J-1)+P(J))/2.0
   PRINT 15,J,T(I,J)
15  FORMAT (3X,I5,F15.5)
5   J=J+1
   GO TO 6
155 I=I+1
   GO TO 20
21  IT=0
   DO 16 J=1,150
   IF(T(1,J).EQ.0.0.OR.T(2,J).EQ.0.0) GO TO 16
   IT=IT+1
   IF (V(1,2).GT .V(2,2) )A(IT)=T(2,J)-T(1,J)
   IF (V(1,2).LT.V(2,2)) A(IT)=T(1,J)-T(2,J)
   H=J
   X(IT)=H*H
   PRINT 17,J,X(IT),A(IT)
17  FORMAT (3X,I5,2F15.5)
   IF( A(IT).GT.8000.0.OR.A(IT).LT.-10.) IT=IT-1
16  CONTINUE
   CALL LINE (X,A,IT,C1,C2)
   CALLGRAPH (X,A,IT)
   CALL CCEND
   END
SUBROUTINE GRAPH (X,Y,NT)
COMMON/CCPOOL/XL,XH,YL,YH,CXL,CXH,CYL,CYH
DIMENSION ROUND(4)
DIMENSION X(150),Y(150)
XMIN=FMIN(NT,X) $ XMAX=FMAX(NT,X)
IA=0
```

```
IB=XMAX+4.0
XL=IA $ XH=IB
CXL=100. $CXH=1300.
NXL=12
NYL=7
CYL=200. $ CYH =900.
NROUND=4
ROUND(1)=1.0
ROUND(2)=2.0
ROUND(3)=2.5
ROUND(4)=5.0
CALL LINEUP (Y,NT,ROUND,NROUND,NYL,YL,YH)
YH=YH+25.
CALL CCGRID (NXL,6HLABELS,NYL)
CALL CCLOT (X,Y,NT,6HNOJOIN,8,1)
CALL CCNEXT
RETURN
END
FUNCTION FMIN(N,X)
DIMENSION X(100)
A = X(1)
DO 10 I=1,N
IF (X(I).LT.A) A = X(I)
10 CONTINUE
FMIN = A
RETURN
END
FUNCTION FMAX(N,X)
DIMENSION X(100)
B = X(1)
DO 11 I=1,N
IF (X(I).GT.B) B = X(I)
11 CONTINUE
FMAX = B
RETURN
END
SUBROUTINE LINE (X,Y,M,C1,C2)
DIMENSION X(150),Y(150)
IA=0
3 CONTINUE
SX=0.0
SY=0.0
SXY=0.0
SX2=0.0
DO 1J =1,M
SX=SX+X(J)
SY=SY+Y(J)
SXY=SXY+X(J)*Y(J)
SX2=SX2+X(J)**2
1 CONTINUE
R=M
D=R*SX2-SX**2
C1= (R*SXY-SX*SY)/D
C2= (-SX2*SY-SX*SXY)/D
PRINT 2,C1,C2
2 FORMAT (1X*LEAST SQUARES FIT OF LINE C1 X+C2=Y*/10X*C1=*
1 F10.5/10X*C2=*F15.5)
```

```
IF(IA.GT.0) GO TO 7
TEST=10.
J=0
IA=1+IA
DO 4I=1,M
YT=C1*X(I)+C2
DI= ABS(YT-Y(I))
IF(DI.GT.TEST) GO TO 5
J=J+1
X(J)=X(I)
Y(J)=Y(I)
GO TO 4
5 PRINT 6,X(I),Y(I),DI
6 FORMAT (///40X,3F15.5)
4 CONTINUE
M=J
GO TO 3
7 CONTINUE
RETURN
END
```

XBL 707-1387

#### ACKNOWLEDGMENTS

I would like to thank Dr. Brewer for his patience, help, and friendship. His weekly group seminars were very profitable and he was never too busy to answer our questions. I would also like to thank Dr. S. Davis of the Physics Department and Dr. J. Phillips of the Astronomy Department for their generous contributions of both time and equipment.

The staff and shops of Lawrence Radiation Laboratory have spoiled me with their consistent friendly help.

It has been very pleasant to be part of Dr. Brewer's research group. I appreciated their help in the lab and enjoyed our miniature golf games and coffee breaks. In particular, I would like to mention Dr. Joel Tellinghuisen.

I would also like to thank my friends in Berkeley and my parents for their support and encouragement.

This work was done under the auspices of the U. S. Atomic Energy Commission.



REFERENCES

- Ballik and Ramsey, *Astrophys. J.*, 137, 61 (1963).
- Brewer, L., Proceedings of the Robert A. Welch Foundation Conferences on Chemical Research, 1962.
- Brewer and Hauge, *J. of Mol. Spect.*, 25 No. 3, 330 (1968).
- Carlson, Kaiser, Moser, Wahl, *J. of Chem. Phys.*, 52 No. 9, 4678 (1970).
- Gaydon, *Proc. Roy. Soc.*, 231, 437 (1955).
- Gerö, L., *Z. Physik*, 93, 669 (1935).
- Hauge, Ph. D. Thesis, University of California, Berkeley, UCRL-16338 (1965).
- Herzberg, G., *Spectra of Diatomic Molecules*, D. Van Nostrand, Ind. Ed., N. Y. (1950).
- Kasai, P., *J. of Chem. Phys.* 49, 4979 (1968).
- Kovacs, *Z. Physik.*, 106, 431 (1937).
- Kovacs, Rotational Structure in the Spectra of Diatomic Molecules, Adam-Hilger, London (1969).
- Hultin and Lagerqvist, *Arkiv Fysik*, Vol. 1-2, 471 (1950).
- Kopp, I., Aslund, N., Edvensson, G., Lindgren, B., *Arkiv for Fysik*, Band 30 nr 23, 321 (1965).
- Lagerqvist, *Arkiv for Fysik*, Band 8, nr 6, 83 (1954).
- Wang, J. L. F., Ph. D. Thesis, University of California, Berkeley, UCRL-19093 (1969).
- Wharton, L., and Klemperer, W., *J. of Chem. Phys.*, 38, No. 1, 2705 (1963).

LEGAL NOTICE

*This report was prepared as an account of Government sponsored work. Neither the United States, nor the Commission, nor any person acting on behalf of the Commission:*

- A. Makes any warranty or representation, expressed or implied, with respect to the accuracy, completeness, or usefulness of the information contained in this report, or that the use of any information, apparatus, method, or process disclosed in this report may not infringe privately owned rights; or*
- B. Assumes any liabilities with respect to the use of, or for damages resulting from the use of any information, apparatus, method, or process disclosed in this report.*

*As used in the above, "person acting on behalf of the Commission" includes any employee or contractor of the Commission, or employee of such contractor, to the extent that such employee or contractor of the Commission, or employee of such contractor prepares, disseminates, or provides access to, any information pursuant to his employment or contract with the Commission, or his employment with such contractor.*

TECHNICAL INFORMATION DIVISION  
LAWRENCE RADIATION LABORATORY  
UNIVERSITY OF CALIFORNIA  
BERKELEY, CALIFORNIA 94720